JYVÄSKYLÄ STUDIES IN COMPUTING
239

Konstantin Aleksandrov

Phase-Locked Loops with Active PI Filter: the Lock-In Range Computation

JYVÄSKYLÄN YLIOPISTO

JYVÄSKYLÄ STUDIES IN COMPUTING 239

Konstantin Aleksandrov

Phase-Locked Loops with Active PI Filter: the Lock-In Range Computation

Esitetään Jyväskylän yliopiston informaatioteknologian tiedekunnan suostumuksella
julkisesti tarkastettavaksi yliopiston Agora-rakennuksen Alfa-salissa
kesäkuun 17. päivänä 2016 kello 10.

Academic dissertation to be publicly discussed, by permission of
the Faculty of Information Technology of the University of Jyväskylä,
in building Agora, Alfa hall, on June 17, 2016 at 10 o'clock.

UNIVERSITY OF JYVÄSKYLÄ

JYVÄSKYLÄ 2016

Phase-Locked Loops with Active PI Filter: the Lock-In Range Computation

JYVÄSKYLÄ STUDIES IN COMPUTING 239

Konstantin Aleksandrov

Phase-Locked Loops with Active PI Filter: the Lock-In Range Computation

UNIVERSITY OF JYVÄSKYLÄ

JYVÄSKYLÄ 2016

Editors
Timo Männikkö
Department of Mathematical Information Technology, University of Jyväskylä
Pekka Olsbo, Ville Korkiakangas
Publishing Unit, University Library of Jyväskylä

URN:ISBN:978-951-39-6688-1
ISBN 978-951-39-6688-1 (PDF)

ISBN 978-951-39-6687-4 (nid.)
ISSN 1456-5390

Jyväskylä University Printing House, Jyväskylä 2016

ABSTRACT

Aleksandrov, Konstantin
Phase-locked loops with active PI filter: the lock-in range computation
Jyväskylä: University of Jyväskylä, 2016, 38 p.(+included articles)
(Jyväskylä Studies in Computing
ISSN 1456-5390; 239)
ISBN 978-951-39-6687-4 (nid.)
ISBN 978-951-39-6688-1 (PDF)
Finnish summary
Diss.

The present work is devoted to the study of the lock-in range of phase-locked loop (PLL). The PLL concept was originally described by H. de Bellescize in 1932. Nowadays various modifications of PLL are widely used in radio systems (e.g., AM/FM radio, software-defined radio), telecommunication systems (e.g., GSM, CDMA), global positioning systems (GPS), computer architectures, and other domains. PLL is of great current interest due to continued increase of its possible applications (optical PLLs, neuronal PLLs, and others).

PLL operating principle is to adjust the phase of a local (tunable) oscillator to the phase of a reference oscillator. The lock-in range concept, which was introduced in 1960's by IEEE Fellow F. M. Gardner, is used to describe fast synchronization of oscillators without cycle-slipping – the undesired growth of phase difference. However, in the second edition of the fundamental handbook "Phase-lock Techniques", which was published in 1979, F. M. Gardner remarked that the suggested definition of the lock-in range may lack rigor in general case. Despite this fact, the lock-in range is a useful concept and is used in many PLL applications. Thus, the problem of rigorous lock-in range definition, which was stated in 1979 by F. M. Gardner, and the lock-in range computation according to its rigorous definition have important applied relevance.

In the present work, the lock-in range of nonlinear PLL model is studied according to a recently suggested rigorous mathematical definition. We pay our attention to the nonlinear PLL model with active proportionally-integrating (PI) filter in the signal's phase space. The relation for the lock-in range computation is presented. For the case of sinusoidal characteristics of phase detector the analytical estimates of the lock-in range are derived. The estimates we have obtained improve the known estimates of the lock-in range of PLL with active PI filter. For the case of triangular characteristics of phase detector the exact formulae of the lock-in range are obtained. The numerical simulations performed are to confirm the adequacy of the obtained results.

Keywords: phase-locked loop, signal's phase space, active PI, lock-in range, cycle slipping

Author

Konstantin Aleksandrov
Department of Mathematical Information Technology,
University of Jyväskylä, Finland;
Faculty of Mathematics and Mechanics,
St. Petersburg State University

Supervisors

Professor Pekka Neittaanmäki
Department of Mathematical Information Technology,
University of Jyväskylä, Finland

Professor Nikolay V. Kuznetsov
Department of Mathematical Information Technology,
University of Jyväskylä, Finland;
Faculty of Mathematics and Mechanics,
St. Petersburg State University, Russia

Professor Gennady A. Leonov
Faculty of Mathematics and Mechanics,
St. Petersburg State University, Russia

Reviewers

Professor Vladimir Rasvan
Faculty of Automatics, Computers and Electronics,
University of Craiova, Romania

Professor Ivan Zelinka
Department of Computer Science,
VŠB – TUO, Czech Republic

Opponent

Professor Sergei Abramovich
School of Education and Professional Studies,
State University of New York at Potsdam, USA

ACKNOWLEDGEMENTS

This thesis has been completed in the Doctoral School of the Faculty of Information Technology, University of Jyväskylä.

I greatly appreciate the opportunity I have had to participate in the Educational and Research Double Degree Programme organized by the Department of Mathematical Information Technology (University of Jyväskylä) and the Department of Applied Cybernetics (Saint Petersburg State University).

This work was funded by the Scholarship of the President of Russia and Russian Science Foundation (14-21-00041).

I would like to express my sincere gratitude to my supervisors Prof. Pekka Neittaanmäki, Prof. Nikolay V. Kuznetsov, and Prof. Gennady A. Leonov for their guidance and continuous support.

I'm very grateful to Prof. Vladimir Rasvan (University of Craiova) and Prof. Ivan Zelinka (VŠB – Technical University of Ostrava) for their valuable comments.

I also would like to thank Prof. Timo Tiihonen for very important comments and remarks.

I also would like to thank Steve Legrand and Billy Braithwaite for English corrections, which taught me a lot and helped to improve all my writings.

I would like to express my deepest thanks to my beloved Anastasiia A. Parkhomenko for her faith in me and lightening my way.

Finally, I am eternally grateful to my parents Elena A. Aleksandrova and Dmitry A. Aleksandrov, who brought me up and gave me my life principles and views, and for whom I will be forever indebted.

LIST OF FIGURES

FIGURE 1 Structure of the work. 11
FIGURE 2 PLL model in the signal space. 13
FIGURE 3 The acquisition process of PLL. 14
FIGURE 4 PLL model in the signal's phase space. 15
FIGURE 5 Example of possible periodic trajectories. 18
FIGURE 6 Examples of the lock-in domain and the cycle slipping effect. ... 19
FIGURE 7 Examples of domain $D_{\text{lock}-\text{in}}((-|\tilde{\omega}|,|\tilde{\omega}|))$: the intersection of lock-in domains $D_{\text{lock}-\text{in}}(-|\tilde{\omega}|)$ (red area) and $D_{\text{lock}-\text{in}}(|\tilde{\omega}|)$ (green area) results in $D_{\text{lock}-\text{in}}((-|\tilde{\omega}|,|\tilde{\omega}|))$ (yellow area). 20
FIGURE 8 The domain $D_{\text{lock}-\text{in}}((-\omega_l,\omega_l))$ 22
FIGURE 9 Calculation of the lock-in frequency, ω_l, in the case of sinusoidal PD characteristic. 23
FIGURE 10 Comparison of numerical and analytical estimates of the lock-in frequency, ω_l, in the case of sinusoidal PD characteristic. 23
FIGURE 11 Diagrams for the lock-in frequency ω_l calculation in the case of triangular PD characteristic. 24

CONTENTS

ABSTRACT
ACKNOWLEDGEMENTS
LIST OF FIGURES
CONTENTS
LIST OF INCLUDED ARTICLES

1 INTRODUCTION AND THE STRUCTURE OF THE WORK 9
1.1 Introduction 9
1.2 Structure of the work 12
1.3 Included articles and author contribution 12

2 PROBLEM STATEMENT AND MAIN RESULTS 13
2.1 Mathematical model of PLL 13
2.2 The lock-in range of PLL with active PI filter 16
2.3 The lock-in range computation for the case of sinusoidal and triangular PD characteristic 22

3 CONCLUSIONS 26

YHTEENVETO (FINNISH SUMMARY) 27

REFERENCES 28

APPENDIX 1 NUMERICAL COMPUTATION OF THE LOCK-IN RANGE 36

INCLUDED ARTICLES

LIST OF INCLUDED ARTICLES

PI K. D. Aleksandrov, N. V. Kuznetsov, G. A. Leonov, M. V. Yuldashev, R. V. Yuldashev. The lock-in range of PLL-based circuits with proportionally-integrating filter and sinusoidal phase detector characteristic. *arXiv:1603.08401*, 2016.

PII K. D. Aleksandrov, N. V. Kuznetsov, G. A. Leonov, M. V. Yuldashev, R. V. Yuldashev. The lock-in range of classical PLL with impulse signals and proportionally-integrating filter. *arXiv:1603.09363*, 2016.

PIII G. A. Leonov, K. D. Aleksandrov. Frequency-domain criteria for the global stability of phase synchronization systems. *Doklady Mathematics, Vol. 92, No. 3, pp. 769 – 772*, 2015.

PIV K. D. Aleksandrov, N. V. Kuznetsov, G. A. Leonov, P. Neittaanmäki, S. M. Seledzhi. Pull-in range of the PLL-based circuits with proportionally-integrating filter. *IFAC-PapersOnLine, Vol. 48, No. 11, pp. 720 – 724*, 2015.

PV K. D. Aleksandrov, N. V. Kuznetsov, G. A. Leonov, P. Neittaanmäki, S. M. Seledzhi. Pull-in range of the classical PLL with impulse signals. *IFAC-PapersOnLine, Vol. 48, No. 1, pp. 562 – 567*, 2015.

PVI K. D. Aleksandrov, N. V. Kuznetsov, G. A. Leonov, S. M. Seledzhi. Best's conjecture on pull-in range of two-phase Costas loop. *IEEE 6th International Congress on Ultra Modern Telecommunications and Control Systems (ICUMT 2014), pp. 78 – 82*, 2014.

PVII G. A. Leonov, I. G. Burova, K. D. Aleksandrov. Visualization of four limit cycles of two-dimensional quadratic systems in the parameter space. *Differential Equations, Vol. 49, No. 13, pp. 1675 – 1703*, 2013.

1 INTRODUCTION AND THE STRUCTURE OF THE WORK

1.1 Introduction

The synchronization of two weakly coupled oscillators was originally described in "Horologium Oscillatorium" by Dutch physicist Christiaan Huygens: *"Two clocks so constructed from two hooks imbedded in the same wooden beam, the motions of each pendulum in opposite swings were so much in agreement that they never receded the least bit from each other <...>. For a long time I was amazed at this unexpected result, but after a careful examination finally found that the cause of this is due to the motion of the beam, even though this is hardly perceptible"* (Huygens, 1966). This is a classic example about the phase synchronization of oscillators. The wooden beam serves as a regulator, which provides the synchronization of the pendulums. Small motions of a beam in a system of this kind affect pendulums of clocks in such way that they have opposite phases in some time.

The phase-locked loop (PLL) was developed for synchronization of two oscillators as well: the reference oscillator and the local (tunable) oscillator. Originally the PLL was described by French engineer H. de Bellescize in 1932 (Bellescize, 1932, 1935). The PLL was used in synchrodyne (homodyne) receivers (see, e.g., (Tucker, 1954)) for a signal demodulation by tuning a local oscillator to the frequency of a reference oscillator. The synchrodyne receivers were developed as an alternative to superheterodyne receivers (Armstrong, 1921). However, the first wide use of PLLs is dated back to the 1940s for the horizontal-sweep synchronization in television receivers (Wendt and Fredentall, 1943; Gruen, 1953) and for the synchronization in color television (George, 1951; Richman, 1953, 1954). Applications of PLLs multiplied after the PLL principles were implemented in integrated circuits (Grebene and Camenzind, 1969).

Nowadays, various modifications of PLLs are being developed (see, e.g., (Costas, 1956, 1962; Hershey et al., 2002; Tretter, 2008)). These PLL-based circuits are widely used in radio systems (e.g., AM/FM radio, software-defined radio), wireless communication systems (e.g., GSM, CDMA), and global posi-

tioning systems (GPS) for carrier recovery, frequency tracking, demodulation, and frequency synthesis (see, e.g., (Viterbi, 1959; Blanchard, 1976; Johnson et al., 1984; Rosenkranz, 1985; Janc and Jasper, 1988; Meyr and Ascheid, 1990; Rapeli, 1992; Crawford, 1994; Mitola, 1995; Vankka, 1997; Ahola et al., 1999; Jorgensen, 1999; Egan, 2000; Ahola and Halonen, 2003; Kaplan and Hegarty, 2005)). In computer architecture PLL-based circuits are used for clock recovery, data synchronization, frequency synthesis, and others (Kung, 1988; Razavi, 1996; Kauraniemi and Vuori, 1997; Kim et al., 2003; Moon et al., 2005; Keliu and Sánchez-Sinencio, 2006). PLLs are also used in optical systems (DeLange, 1968; Lindgren, 1970; Kazovsky, 1985; Alexander, 1997; Chan, 2000; Lerber et al., 2009) and neuronal systems (Tokunaga and Mori, 1990; Wei-Ping and Chin-Kan, 1998; Hoppensteadt and Izhikevich, 2000; Ahissar, 2003).

A large amount of engineering literature is devoted to the study of PLL-based circuits and the various characteristics related to their stability (see, e.g. a rather comprehensive bibliography of pioneering works in (Lindsey and Tausworthe, 1973)). The first well-known books on the study of PLL are dated back to the 1960s (see e.g. (Gardner, 1966; Shakhgildyan and Lyakhovkin, 1966; Viterbi, 1966)). Nowadays, PLL analysis is an active research area (see (Kroupa, 2003; Gardner, 2005; Aaltonen et al., 2005; Banerjee, 2006; Rapinoja et al., 2006; Best, 2007; Kudrewicz and Wasowicz, 2007; Proakis and Salehi, 2008; Goldman, 2007; Saukoski et al., 2008; Speeti et al., 2009; Shakhtarin, 2012; Shalfeev and Matrosov, 2013)).

Proper operating of PLL is characterized by frequency range concepts such as pull-in range and lock-in range (Gardner, 1966; Shakhgildyan and Lyakhovkin, 1966; Viterbi, 1966). These concepts are widely used nowadays (see, e.g., (Kroupa, 2003; Gardner, 2005; Best, 2007)). Usually, in engineering literature, only non-strict definitions are given for the concepts; thus, in a handbook on synchronization and communications (Kihara et al., 2002) there is a remark *"to check these definitions carefully before using them"* was given.

The pull-in range corresponds to mistuning between the reference and local oscillators, where the PLL will synchronize for every initial state of its components (see, e.g., (Gruen, 1953; Gardner, 1966; Viterbi, 1966; Abramovich and Leonov, 1978)). However, that synchronization process may be slow. In order to consider the property of the PLL to synchronize in a short time, a lock-in range concept was introduced by F. M. Gardner (Gardner, 1966): "*If, for some reason, the frequency difference between input and VCO is less than the loop bandwidth, the loop will lock up almost instantaneously without slipping cycles. The maximum frequency difference for which this fast acquisition is possible is called the lock-in frequency*". However, due to nonlinear behavior of PLL the initial states of its components may affect the acquisition process and associated frequency ranges (see, e.g., (Kuznetsov et al., 2015; Best et al., 2015)). Thereby, in the Gardner's 2nd edition (Gardner, 1979), the following problem was stated: *"There is no natural way to define exactly any unique lock-in frequency"*(Gardner, 1979). Nevertheless, *"despite its vague reality, lock-in range is a useful concept"* (Gardner, 2005). Subsequently, a rigorous mathematical definition of the lock-in range was suggested in (Kuznetsov, 2016;

Kuznetsov et al., 2015; Leonov et al., 2015b) to overcome the stated problem.

In the present work, the lock-in range of PLL with active proportionally-integrating (PI) filter is studied. Application of phase plane analysis (see (Tricomi, 1933; Andronov et al., 1937)) allowed the author to obtain exact relation for the lock-in range computation for the sinusoidal and triangular characteristics of a phase detector. For the case of PLL with sinusoidal characteristic of phase detector, the analytical estimates for the lock-in range were obtained. These estimates improve the estimates given in (Gardner, 2005; Huque, 2011; Huque and Stensby, 2013). For the case of PLL with triangular characteristic of phase detector the exact formulae for the lock-in range computation were derived. The numerical simulations were performed to confirm the adequacy of the analytical results.

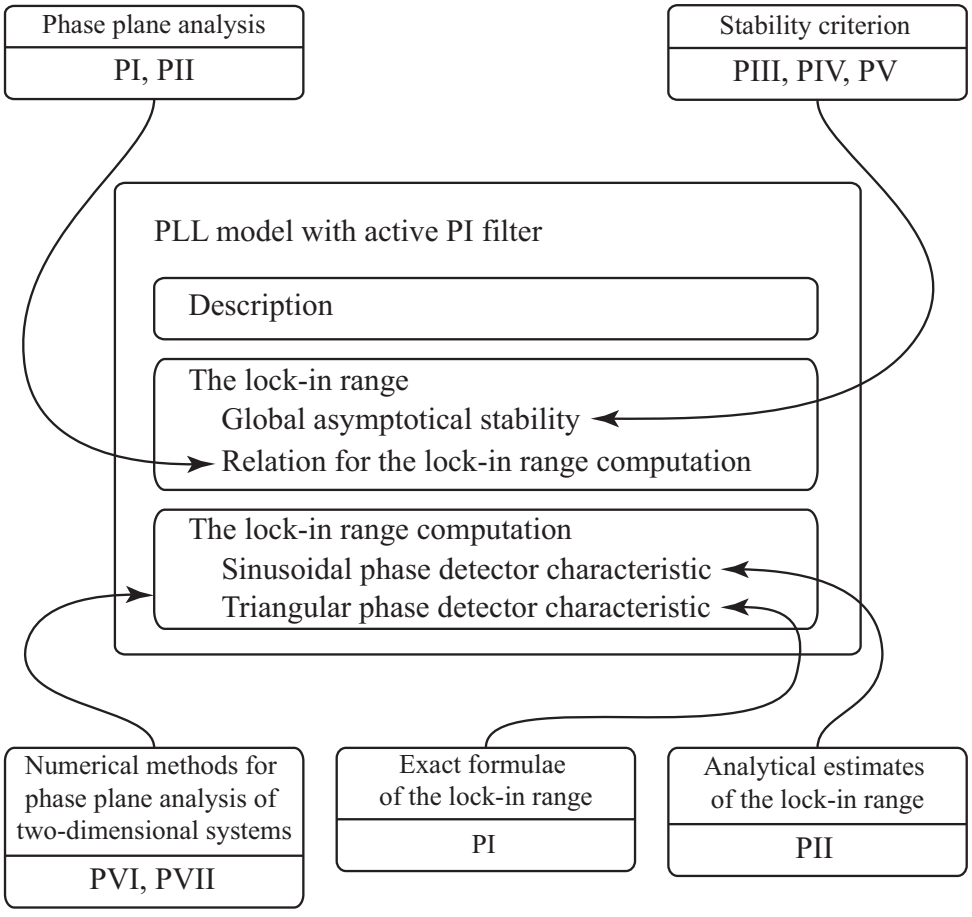

FIGURE 1 Structure of the work.

1.2 Structure of the work

The present work consists of an introduction and one chapter (see Figure 1). In the introduction an overview on the history of PLL and its applications is given. A number of classical works devoted to the PLL study are highlighted. The problem concerning the study of the lock-in range is outlined.

The first chapter of the present work consists of three sections. The first section is devoted to the description of PLL operating principles. The model of PLL in a signal's phase space is described, and the equations for PLL with active PI filter are derived. In the next section of the first chapter, a rigorous mathematical definition of the lock-in range of the considered PLL is given. For the case of sinusoidal and triangular characteristics of phase detector the relation for the lock-in range computation is derived. In the last section the analytical estimates for the lock-in range of PLL with sinusoidal and triangular characteristics are presented. The numerical diagrams which confirm the adequacy of the obtained analytical results are constructed.

Appendix 1 contains the programming code for constructing numerical diagrams from the first chapter.

1.3 Included articles and author contribution

The study of the lock-in range in the present work required the development and application of numerical methods of analysis (see (PVII; PVI)), development of global stability criteria (see (PV; PIV; PIII)), and development of analytical methods for the study of separatrices of saddle equilibria in two-dimensional systems (see (PII; PI)).

In (PVII; PVI), the author developed and applied numerical methods for the study of phase plane of two-dimensional systems. In (PV; PIV; PIII), the author proved the stability criterion and applied the criterion for the case of PLL with active PI filter. In (PI), for the case of sinusoidal characteristic of phase detector, the author derived analytical estimates of the lock-in range, which improve estimates from (Gardner, 2005; Huque, 2011; Huque and Stensby, 2013). In (PII), for the case of triangular characteristic of phase detector, the author obtained the exact formulae of the lock-in range.

The results of this work were presented at an IEEE Conference (6th International Congress on Ultra Modern Telecommunications and Control Systems, ICUMT-2014), at IFAC Conferences (8th Vienna International Conference on Mathematical Modeling, MATHMOD-2015, and 1st Conference on Modeling, Identification and Control of Nonlinear Systems, MICNON-2015); at the seminars of the Department of Applied Cybernetics (St. Petersburg State University), and at the seminars of the Department of Mathematical Information Technology (University of Jyväskylä).

2 PROBLEM STATEMENT AND MAIN RESULTS

Next, following to papers (PI; PII; PIII) and (Leonov et al., 2012, 2015b), the main content is presented.

2.1 Mathematical model of PLL

Consider a physical model of classical PLL in the signal space (see Figure 2). This model contains the following blocks: a reference oscillator (Input), a voltage-

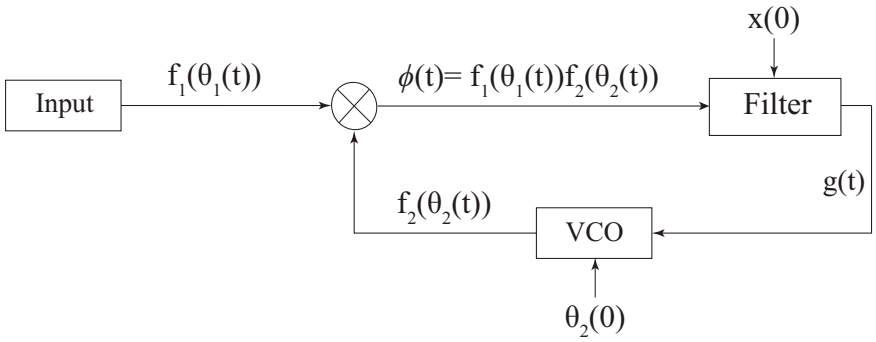

FIGURE 2 PLL model in the signal space.

controlled oscillator (VCO), a filter (Filter), and an analog multiplier as a phase detector (PD).

The signals $f_1(\theta_1(t))$ and $f_2(\theta_2(t))$ of Input and VCO (here $\theta_2(0)$ is the initial phase of VCO) enter the multiplier block. The resulting signal, $\phi(t)$, is filtered by a low-pass filter, Filter (here $x(0)$ is an initial state of Filter). The filtered signal $g(t)$ is used as a control signal for the VCO.

The main purpose of PLL is to adjust the phase $\theta_2(t)$ of VCO to the phase $\theta_1(t)$ of Input. This process is called an acquisition process. When the VCO phase is adjusted to the phase of Input, i.e. the difference between phases is constant,

VCO generates signal (voltage) of the same frequency as Input. This state of PLL is called locked state (see Figure 3).

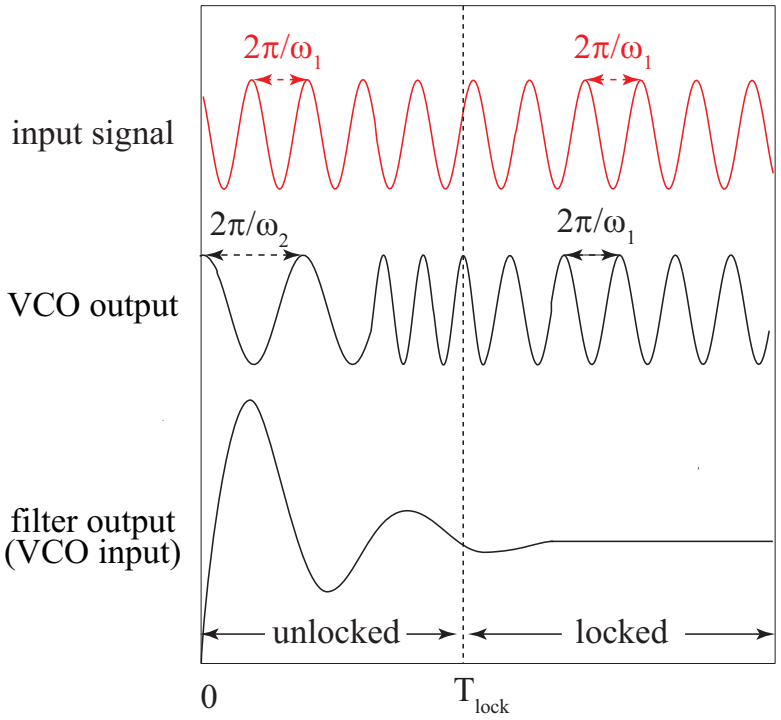

FIGURE 3 The acquisition process of PLL.

The PLL model in the signal space is difficult to study, since the equations describing the model are non-autonomous (see, e.g., (Abramovitch, 2002; Kudrewicz and Wasowicz, 2007; Leonov et al., 2015)). By contrast, the PLL model in the signal's phase space can be described by autonomous equations (Gardner, 1966; Shakhgildyan and Lyakhovkin, 1966; Viterbi, 1966), which simplifies the study of PLL-based circuits. The application of averaging methods (Mitropolsky and Bogolubov, 1961; Samoilenko and Petryshyn, 2004) allows one to reduce the model of PLL-based circuits in the signal space to the model in the signal's phase space (see, e.g., (Kuznetsov et al., 2009, 2011, 2012b,a, 2013; Kuznetsov, 2008; Kudryashova et al., 2014; Best et al., 2015; Leonov et al., 2015c,d; Kuznetsov et al., 2015)).

Consider now a model of classical PLL in the signal's phase space (see Figure 4). Input and VCO generate phases $\theta_1(t)$ and $\theta_2(t)$, respectively. These phases enter to the inputs of the PD. The output of the phase detector in the signal's phase space is called a phase detector characteristic and has the form

$$K_d\varphi(\theta_1(t)-\theta_2(t)). \tag{1}$$

The maximum absolute value of PD output $K_d > 0$ is called a phase detector gain (see, e.g., (Best, 2007; Goldman, 2007)). The periodic function, $\varphi(\theta_\Delta(t))$, depends

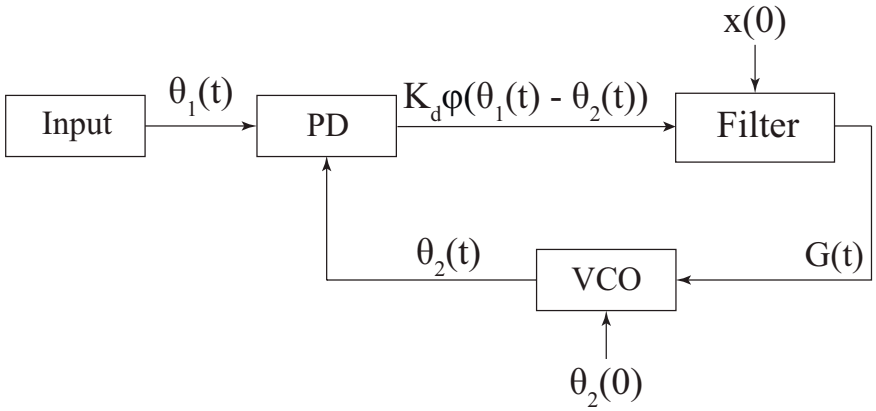

FIGURE 4 PLL model in the signal's phase space.

on phase difference $\theta_1(t) - \theta_2(t)$ (which is called a phase error and denoted by $\theta_\Delta(t)$). The PD characteristic depends on the design of PLL and the signal waveforms $f_1(\theta_1)$ of Input and $f_2(\theta_2)$ of VCO (see, e.g., (Kuznetsov et al., 2009; Leonov et al., 2011; Kuznetsov et al., 2011, 2012a; Leonov et al., 2015a)).

The output of PD is processed by Filter.The active PI filter with transfer function $W(s) = \frac{1+\tau_2 s}{\tau_1 s}$, $\tau_1 > 0$, $\tau_2 > 0$ is then considered. The filter can be described as (see, e.g., (Baker, 2011))

$$\begin{cases} \dot{x}(t) = K_d \varphi(\theta_\Delta(t)), \\ G(t) = \frac{1}{\tau_1} x(t) + \frac{\tau_2}{\tau_1} K_d \varphi(\theta_\Delta(t)), \end{cases} \tag{2}$$

where $x(t)$ is the filter state. The output of Filter $G(t)$ is used as a control signal for VCO:

$$\dot{\theta}_2(t) = \omega_2^{\text{free}} + K_v G(t), \tag{3}$$

where ω_2^{free} is the VCO free-running frequency and $K_v > 0$ is the VCO gain coefficient. The frequency of reference signal is usually assumed to be constant:

$$\dot{\theta}_1(t) \equiv \omega_1. \tag{4}$$

Relations (2), (3) and (4) result in an autonomous system of differential equations:

$$\begin{cases} \dot{x} = K_d \varphi(\theta_\Delta), \\ \dot{\theta}_\Delta = \omega_1 - \omega_2^{\text{free}} - \frac{K_v}{\tau_1} \left(x + \tau_2 K_d \varphi(\theta_\Delta) \right). \end{cases} \tag{5}$$

The difference between the reference frequency and the VCO free-running frequency is denoted as $\omega_\Delta^{\text{free}}$: $\omega_\Delta^{\text{free}} = \omega_1 - \omega_2^{\text{free}}$. By linear transformation $x \to K_d x$ we have

$$\begin{cases} \dot{x} = \varphi(\theta_\Delta), \\ \dot{\theta}_\Delta = \omega_\Delta^{\text{free}} - \frac{K_0}{\tau_1} \left(x + \tau_2 \varphi(\theta_\Delta) \right), \end{cases} \tag{6}$$

where $K_0 = K_v K_d$ is the loop gain. Relations (6) describe the nonlinear model of PLL with active PI filter in the signal's phase space.

If the PD characteristic is an odd function, relations (6) are not changed by transformation

$$\left(\omega_{\Delta}^{\text{free}}, x, \theta_{\Delta}\right) \to \left(-\omega_{\Delta}^{\text{free}}, -x, -\theta_{\Delta}\right).$$

This property allows one to use the concept of frequency deviation

$$\left|\omega_{\Delta}^{\text{free}}\right| = \left|\omega_1 - \omega_2^{\text{free}}\right|$$

and consider (6) with $\omega_{\Delta}^{\text{free}} \geq 0$ only.

For the most common PD characteristics (1) of classical PLL, function $\varphi(\theta_{\Delta})$ is a 2π-periodic piecewise smooth odd function (see, e.g., (Gardner, 1966; Shakhgildyan and Lyakhovkin, 1966; Gardner, 1966)). For such PD characteristic, the right side of (6) is 2π-periodic in θ_{Δ}, and we can consider locked states of (6) in a 2π-interval of θ_{Δ}, $\theta_{\Delta} \in (-\pi, \pi]$.

The case of a 2π-periodic piecewise smooth odd function $\varphi(\theta_{\Delta})$ is considered further.

2.2 The lock-in range of PLL with active PI filter

Consider the acquisition process of PLL with active PI filter in terms of (6). The locked states of PLL correspond to the *asymptotically stable* equilibria of (6) (see, e.g., (Leonov et al., 2015b)).

Definition 1 (e.g., (Lyapunov, 1892))**.** *The equilibrium* $\left(\theta_{eq}, x_{eq}\right)$ *of (6) is said to be asymptotically stable if for every* $\varepsilon > 0$ *there exists a* $\delta > 0$ *such that, if* $|| \left(\theta_{\Delta}(0), x(0)\right) - \left(\theta_{eq}, x_{eq}\right) || < \delta$*, then for every* $t \geq 0$ *we have* $|| \left(\theta_{\Delta}(t), x(t)\right) - \left(\theta_{eq}, x_{eq}\right) || < \varepsilon$*, and* $\lim\limits_{t \to +\infty} || \left(\theta_{\Delta}(t), x(t)\right) - \left(\theta_{eq}, x_{eq}\right) || = 0$.

Hence, in order to find the locked states of PLL, we need to perform two steps. The first step is to check if there exist any equilibrium of (6) and find all existing equilibria. The second step is to check asymptotic stability of those equilibria. For this purpose, the classical criteria of stability are used, e.g. the Routh-Hurwitz criterion (see, e.g., (Gopal, 2002; Gantmacher and Brenner, 2005)).

In order to study the locked states of PLL with active PI filter, consider the following property of (6). Linear transformation $x \to x + \frac{\tau_1 \omega_{\Delta}^{\text{free}}}{K_0}$ shifts each phase trajectory in the phase plane of (6) vertically:

$$\begin{cases} \dot{x} = \varphi(\theta_{\Delta}), \\ \dot{\theta}_{\Delta} = -\frac{K_0}{\tau_1}\left(x + \tau_2 \varphi(\theta_{\Delta})\right). \end{cases} \tag{7}$$

The equilibria $\left(\theta_{eq}, x_{eq}\right)$ of (7) can be found by equating the right side of (7) to zero:

$$\begin{cases} 0 = \varphi(\theta_{\Delta}), \\ 0 = -\frac{K_0}{\tau_1}\left(x + \tau_2 \varphi(\theta_{\Delta})\right). \end{cases} \tag{8}$$

For (8), the θ_Δ coordinates of equilibria are equal to zeros of $\varphi(\theta_\Delta)$ (if any), and the x coordinate is equal to zero. The phase trajectories of (7) coincide with phase trajectories of (6) for $\omega_\Delta^{\text{free}} = 0$. Thus, if the equilibria $\left(\theta_{eq}, x_{eq}\right)$ of (6) exist for $\omega_\Delta^{\text{free}} = 0$, they also exist for any arbitrary ω_Δ and are shifted vertically by $\frac{\tau_1 \omega_\Delta^{\text{free}}}{K_0}$, i.e.,

$$\left(\theta_{eq}\left(\omega_\Delta^{\text{free}}\right), x_{eq}\left(\omega_\Delta^{\text{free}}\right)\right) = \left(\theta_{eq}, \frac{\tau_1 \omega_\Delta^{\text{free}}}{K_0}\right). \tag{9}$$

The θ_Δ-coordinates of (9) are equal to zeros of $\varphi(\theta_\Delta)$ and do not depend on $\omega_\Delta^{\text{free}}$, while the x-coordinates of (9) coincide and depend on $\omega_\Delta^{\text{free}}$.

In interval $\theta_\Delta \in (-\pi, \pi]$, denote the asymptotically stable equilibria of (6) by $\left(\theta_{eq}^s, x_{eq}(\omega_\Delta^{\text{free}})\right)$ and the remaining equilibria by $\left(\theta_{eq}^u, x_{eq}(\omega_\Delta^{\text{free}})\right)$. If no asymptotically stable equilibrium exists, the PLL will never synchronize for any arbitrary initial loop state $(\theta_\Delta(0), x(0)) \notin \left(\theta_{eq}^u, x_{eq}(\omega_\Delta^{\text{free}})\right)$.

For the case of sinusoidal and triangular PD characteristics, the equilibria of (6) are given by (see (PI; PII))

$$\left(\theta_{eq}, x_{eq}\left(\omega_\Delta^{\text{free}}\right)\right) = \left(\pi k, \frac{\tau_1 \omega_\Delta^{\text{free}}}{K_0}\right), \ k \in \mathbb{Z}. \tag{10}$$

For any arbitrary $\omega_\Delta^{\text{free}}$, the equilibria

$$\left(\theta_{eq}^s + 2\pi k, x_{eq}\left(\omega_\Delta^{\text{free}}\right)\right) = \left(2\pi k, \frac{\omega_\Delta^{\text{free}} \tau_1}{K_0}\right), \ k \in \mathbb{Z}$$

are asymptotically stable, and the equilibria

$$\left(\theta_{eq}^u + 2\pi k, x_{eq}\left(\omega_\Delta^{\text{free}}\right)\right) = \left(\pi + 2\pi k, \frac{\omega_\Delta^{\text{free}} \tau_1}{K_0}\right), \ k \in \mathbb{Z} \tag{11}$$

are unstable (saddle) equilibria.

If the PLL model (6) with certain frequency difference, $\omega_\Delta^{\text{free}}$, synchronizes for each initial loop state, then the model is *globally asymptotically stable*:

Definition 2 (e.g., (Leonov and Kuznetsov, 2014))**.** *If for a certain frequency difference, $\omega_\Delta^{\text{free}}$, any solution of (6) tends to an equilibrium, then the system with such $\omega_\Delta^{\text{free}}$ is called globally asymptotically stable.*

In a number of works, the global asymptotic stability of the PLL model with active PI filter (6) for certain PD characteristics (e.g., with sinusoidal and triangular PD characteristics) is considered (see, e.g., (Gubar', 1961; Bakaev, 1963; Viterbi, 1966)). By methods of the phase plane analysis (Tricomi, 1933; Andronov et al., 1937), in (Viterbi, 1966) the global asymptotic stability of the PLL model with active PI filter (6) and sinusoidal PD characteristic for any arbitrary $\omega_\Delta^{\text{free}}$ is stated. However, to rigorously complete the proof given in (Viterbi, 1966), additional explanations are required, i.e., the absence of heteroclinic trajectory and limit cycles of the first kind (see Figure 5) are needed to be explained.

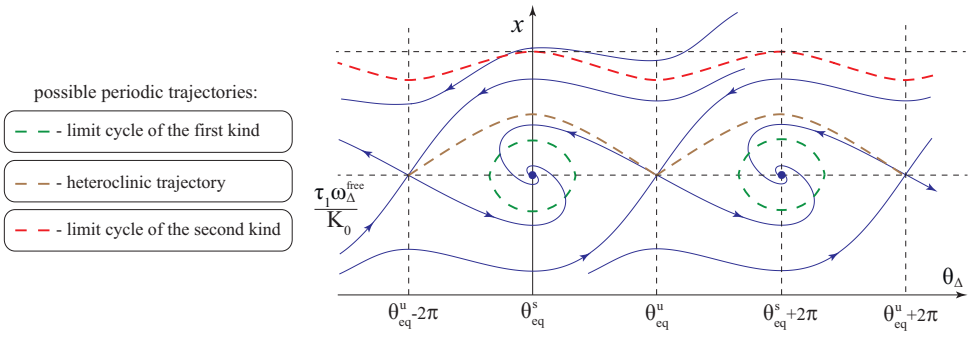

FIGURE 5 Example of possible periodic trajectories.

To overcome these difficulties, the methods of the Lyapunov functions construction (Lyapunov, 1892) can be applied (see, e.g., (Bakaev, 1963; Bakaev and Guzh, 1965; Gelig et al., 1978; Leonov and Kuznetsov, 2014)). For that purpose the modifications of classical stability criteria for cylindrical phase space are developed in (Gelig et al., 1978; Leonov and Kuznetsov, 2014). In (PIII), the global asymptotic stability of the PLL model with active PI filter (6) and 2π-periodic piecewise smooth function $\varphi(\theta_\Delta)$ such that

$$\begin{aligned}
&\int_0^{2\pi} \varphi(\theta_\Delta)d\theta_\Delta = 0;\\
&\forall\theta^0_\Delta \in (-\infty,+\infty) \quad \exists\delta>0:\\
&\int_{\theta^0_\Delta}^{\theta_\Delta} \varphi(\theta_\Delta)d\theta_\Delta \neq 0, \quad \forall\theta_\Delta \in \left(\theta^0_\Delta-\delta,\theta^0_\Delta\right)\cup\left(\theta^0_\Delta,\theta^0_\Delta+\delta\right);
\end{aligned} \tag{12}$$

is proved for any arbitrary $\omega_\Delta^{\text{free}}$ using Lyapunov function

$$V(x,\theta_\Delta) = \frac{K_0}{2\tau_1}\left(x-\frac{\tau_1\omega_\Delta^{\text{free}}}{K_0}\right)^2 + \int_0^{\theta_\Delta}\varphi(s)ds \geq 0;$$

$$\dot V(x,\theta_\Delta) = -\frac{K_0\tau_2}{\tau_1}\varphi^2(\theta_\Delta) < 0, \quad \forall\theta_\Delta \neq \{\theta_{eq}+2\pi k\}.$$

However, phase error θ_Δ may substantially increase during the acquisition process. In order to consider the synchronization of the PLL model without undesired growth of the phase error θ_Δ, a lock-in range concept was introduced in (Gardner, 1966): "*If, for some reason, the frequency difference between input and VCO is less than the loop bandwidth, the loop will lock up almost instantaneously without slipping cycles. The maximum frequency difference for which this fast acquisition is possible is called the lock-in frequency*".

It is said that cycle slipping occurs if (see, e.g., (Meyr, 1975; Ascheid and Meyr, 1982; Ershova and Leonov, 1983))

$$\limsup_{t\to+\infty}|\theta_\Delta(0)-\theta_\Delta(t)| \geq 2\pi.$$

For (6) with fixed $\omega_\Delta^{\text{free}}$, the domain of initial loop states for which the synchronization without cycle slipping occurs is called the lock-in domain, $D_{\text{lock-in}}(\omega_\Delta^{\text{free}})$ (see Figure 6).

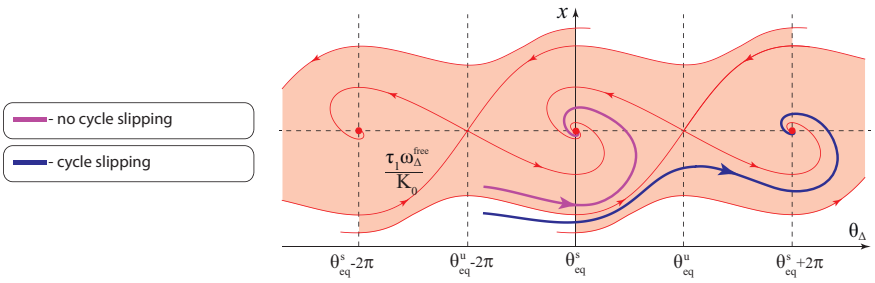

(a) Sinusoidal PD characteristic: $K_0 = 200$, $\tau_1 = 0.5$, $\tau_1 = 0.05$

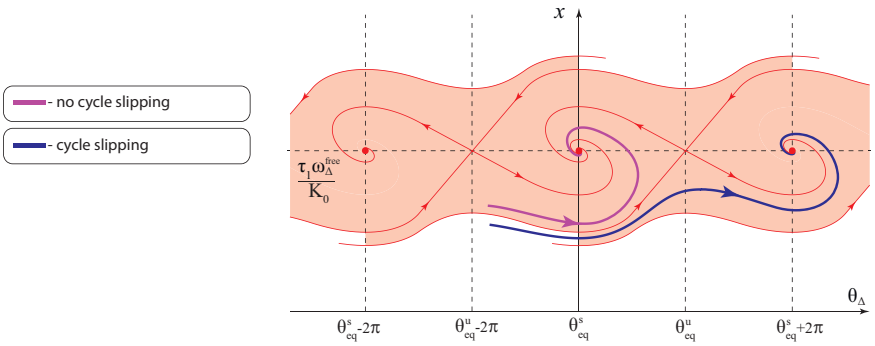

(b) Triangular PD characteristic: $K_0 = 200$, $\tau_1 = 0.5$, $\tau_1 = 0.05$

FIGURE 6 Examples of the lock-in domain and the cycle slipping effect.

However, in general, even for zero frequency difference ($\omega_\Delta^{\text{free}} = 0$) and a sufficiently large initial state of filter ($x(0)$), cycle slipping may take place (see, e.g., (Kuznetsov et al., 2015; Best et al., 2015; Kudryashova et al., 2014)). Thus, in 1979, F. M. Gardner wrote: *"There is no natural way to define exactly any unique lock-in frequency"* and *"despite its vague reality, lock-in range is a useful concept"* (Gardner, 1979). To overcome the stated problem, in (Kuznetsov et al., 2015; Leonov et al., 2015b) the rigorous mathematical definition of the lock-in range is suggested. For PLL with odd PD characteristics, the definition of the lock-in range is as follows:

Definition 3 (e.g., (Leonov et al., 2015b)). *The lock-in range of model (6) is a maximal range $[0, \omega_l)$ such that for each frequency deviation $|\omega_\Delta^{\text{free}}| \in [0, \omega_l)$ the model (6) is globally asymptotically stable and the following domain*

$$D_{\text{lock-in}}((-\omega_l, \omega_l)) = \bigcap_{|\omega_\Delta^{\text{free}}|<\omega_l} D_{\text{lock-in}}(\omega_\Delta^{\text{free}})$$

contains all corresponding locked states of (6).

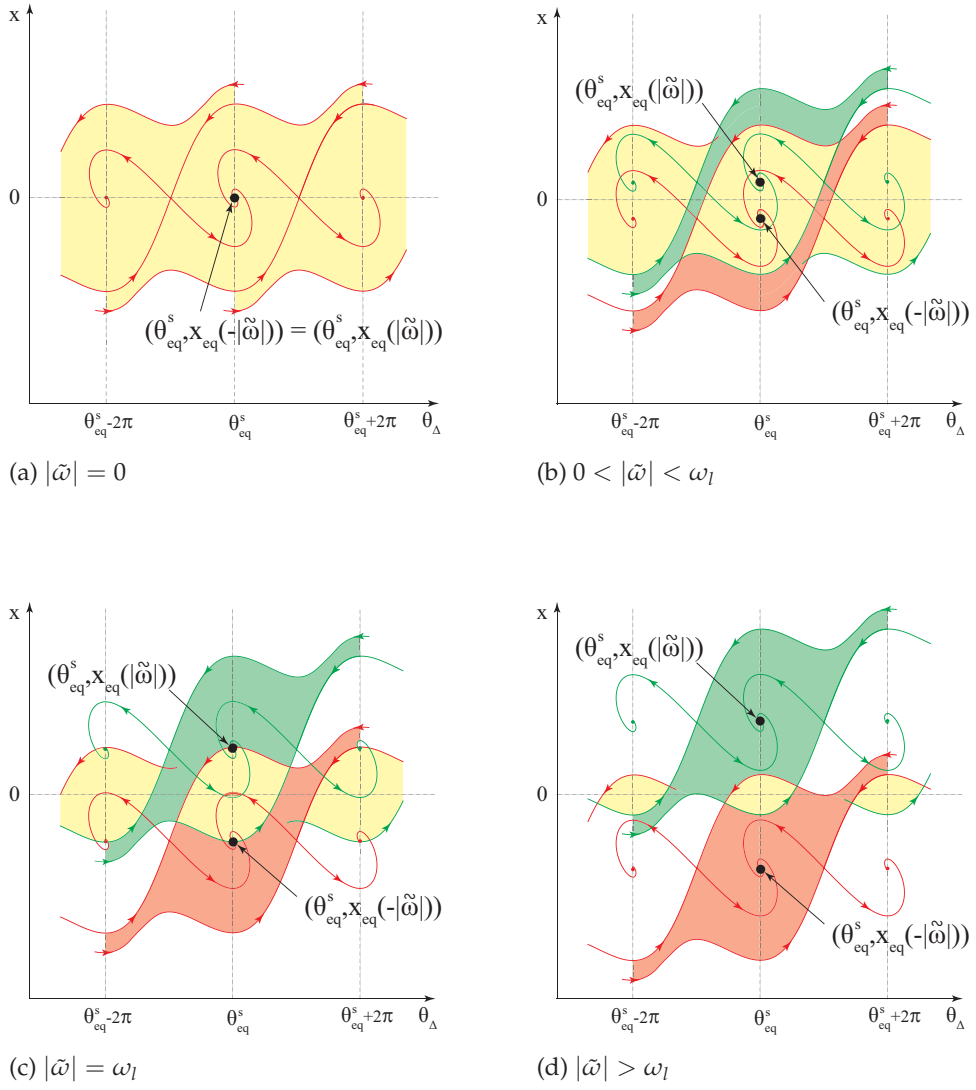

(a) $|\tilde{\omega}| = 0$

(b) $0 < |\tilde{\omega}| < \omega_l$

(c) $|\tilde{\omega}| = \omega_l$

(d) $|\tilde{\omega}| > \omega_l$

FIGURE 7 Examples of domain $D_{\text{lock-in}}((-|\tilde{\omega}|,|\tilde{\omega}|))$: the intersection of lock-in domains $D_{\text{lock-in}}(-|\tilde{\omega}|)$ (red area) and $D_{\text{lock-in}}(|\tilde{\omega}|)$ (green area) results in $D_{\text{lock-in}}((-|\tilde{\omega}|,|\tilde{\omega}|))$ (yellow area).

Definition 3 implies that if the PLL is in a locked state, then after an abrupt change of $\omega_\Delta^{\text{free}}$ within a lock-in range $[0, \omega_l)$ the corresponding acquisition process of PLL leads, if it is not interrupted, to a new locked state without cycle slipping (Kuznetsov et al., 2015).

Recall that the phase trajectories in the phase plane of (6) are shifted vertically by linear transformation $x \to x + \frac{\tau_1 \omega_\Delta^{\text{free}}}{K_0}$, and the equilibria $\left(\theta_{eq}, x_{eq}\left(\omega_\Delta^{\text{free}}\right)\right)$ of (6) are described by (9). Thus, to find the lock-in range of (6) (under the assumption of global asymptotic stability of (6)) we need to find the maximal frequency deviation, $|\tilde{\omega}| = \omega_l$ (where ω_l is called a lock-in frequency), such that the vertical intervals

$$\theta_\Delta = \theta_{eq}^s, \ -\frac{\tau_1 |\tilde{\omega}|}{K_0} < x < \frac{\tau_1 |\tilde{\omega}|}{K_0}$$

are contained in $D_{\text{lock-in}}\left((-|\tilde{\omega}|, |\tilde{\omega}|)\right)$ (see Figure 7).

For the most common PD characteristics, function $\varphi(\theta_\Delta)$ has two zeros in interval $\theta_\Delta \in (-\pi, \pi]$, and the one corresponding equilibrium, $\left(\theta_{eq}^s, x_{eq}(\omega_\Delta^{\text{free}})\right)$, is asymptotically stable, while the another one is unstable (see, e.g., (Kuznetsov et al., 2011; Leonov et al., 2012)). Consider the steps for finding the lock-in frequency ω_l of (6). First, let frequency deviation $|\tilde{\omega}| = 0$ (see Figure 7a). For this case, the symmetric locked states of (6), $\left(\theta_{eq}^s, x_{eq}(|\tilde{\omega}|)\right)$ and $\left(\theta_{eq}^s, x_{eq}(-|\tilde{\omega}|)\right)$, coincide and are inside $D_{\text{lock-in}}(0)$. Slowly increase $|\tilde{\omega}|$ (see Figure 7b) until the symmetric locked states of (6) reach the border of $D_{\text{lock-in}}\left((-|\tilde{\omega}|, |\tilde{\omega}|)\right)$ (see Figure 7c). A further increment of $|\tilde{\omega}|$ leads the symmetric locked states of (6) to be outside $D_{\text{lock-in}}\left((-|\tilde{\omega}|, |\tilde{\omega}|)\right)$ (see Figure 7d). Thus, ω_l that is desired corresponds to Figure 7c.

Let us derive the exact relation for the lock-in range computation in the case of sinusoidal and triangular characteristics of the PLL model (6). Consider in detail the critical case from Figure 7c, which corresponds to lock-in frequency ω_l. The lock-in domain of (6) for a certain frequency difference, $\omega_\Delta^{\text{free}}$, is bounded by the separatrices of saddle equilibria (11) and vertical lines $\theta_\Delta = \theta_{eq}^s + 2\pi k$ (see Figure 6a). The $D_{\text{lock-in}}\left((-\omega_l, \omega_l)\right)$ of (6) is the intersection of the lock-in domains for $\omega_\Delta^{\text{free}} \in (-\omega_l, \omega_l)$. Thus, to compute the lock-in range of (6), we need to find $\omega_\Delta^{\text{free}} = \omega_l$ such that

$$x_{eq}(-\omega_\Delta^{\text{free}}) = Q(\theta_{eq}^s, \omega_\Delta^{\text{free}}), \tag{13}$$

where $Q(\theta_\Delta, \omega_\Delta^{\text{free}})$ is the separatrix of unstable saddle equilibrium $\left(\theta_{eq}^u, x_{eq}(\omega_\Delta^{\text{free}})\right)$ (see Figure 8).

Since the phase trajectories in the phase plane of (6) are shifted vertically by linear transformation $x \to x + \frac{\tau_1 \omega_\Delta^{\text{free}}}{K_0}$, we obtain an exact relation for lock-in frequency ω_l:

$$-\frac{\omega_l}{K_0/\tau_1} = \frac{\omega_l}{K_0/\tau_1} + Q(\theta_{eq}^s, 0) \ \Rightarrow \ \omega_l = -\frac{K_0 Q(\theta_{eq}^s, 0)}{2\tau_1}. \tag{14}$$

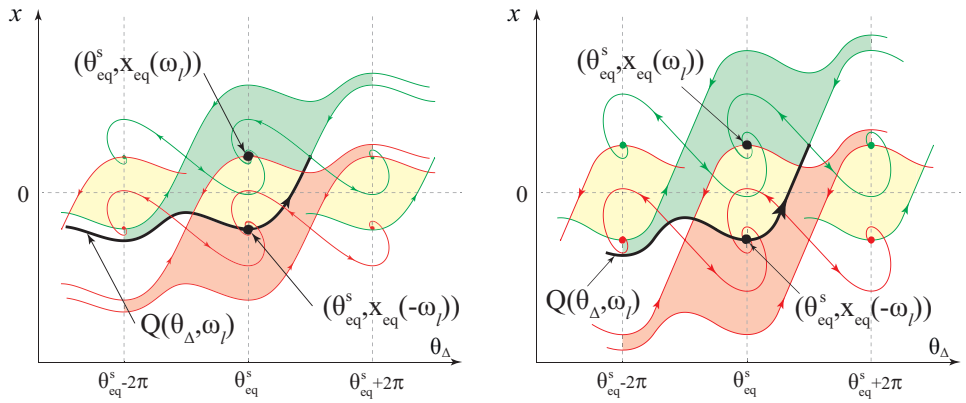

(a) Sinusoidal PD characteristic (b) Triangular PD characteristic

FIGURE 8 The domain $D_{\text{lock-in}}((-\omega_l, \omega_l))$.

2.3 The lock-in range computation for the case of sinusoidal and triangular PD characteristic

In the present section, the analytical estimates and numerical diagrams for the lock-in range computation, which are based on relation (14), are presented for the case of sinusoidal and triangular PD characteristics.

Consider the PLL with active PI filter and signals $f_1(\theta_1(t)) = \sin(\theta_1(t))$ and $f_2(\theta_2(t)) = \cos(\theta_2(t))$. For this case, the PD characteristic of the PLL model (6) is sinusoidal (see, e.g., (Leonov et al., 2012, 2015a)):

$$K_d = \frac{1}{2}, \qquad \varphi(\theta_\Delta) = \sin(\theta_\Delta). \tag{15}$$

Numerical simulations are used to compute the lock-in range of (6) using (14). The separatrix, $Q(\theta_\Delta, 0)$, is numerically integrated and the corresponding lock-in frequency, ω_l, is approximated. The obtained numerical results can be illustrated by diagram in Figure 9a.

Relations (6) depend on the value of two coefficients, $\frac{K_0}{\tau_1}$ and τ_2; thus, in Figure 9a we can plot a single curve for every fixed value of τ_2 and variables τ_1, K_0 by choosing the X-axis as $\frac{K_0}{\tau_1}$. The results of numerical simulations show that for sufficiently large $\frac{K_0}{\tau_1}$, the value of ω_l grows almost proportionally to $\frac{K_0}{\tau_1}$. Hence, in Figure 9a the Y-axis can be chosen as $\frac{\omega_\Delta^{\text{free}}\tau_1}{K_0}$ for the illustration of the obtained results.

To obtain lock-in frequency ω_l for fixed τ_1, τ_2, and K_0 using Figure 9a, we consider the curve corresponding to τ_2 that was chosen. Next, for the X-value equal to $\frac{K_0}{\tau_1}$ we get the Y-value of the curve. Finally, we multiply the Y-value by $\frac{K_0}{\tau_1}$ (see Figure 9b).

However, examples are known (see, e.g., (Best et al., 2015; Bianchi et al., 2015)) for which numerical simulation is a challenging task and may lead to

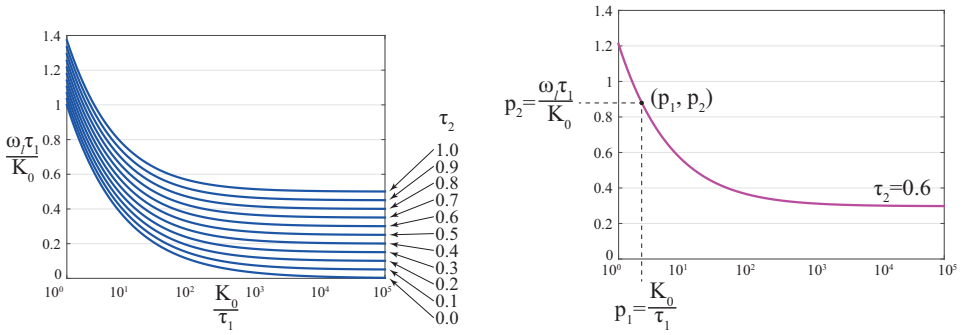

(a) Diagrams for the lock-in frequency ω_l calculation.

(b) The lock-in frequency calculation: $\omega_l = p_1 p_2$.

FIGURE 9 Calculation of the lock-in frequency, ω_l, in the case of sinusoidal PD characteristic.

wrong conclusion about synchronization due to possible existence of hidden oscillations (Leonov et al., 2011, 2012; Kuznetsov et al., 2013; Leonov and Kuznetsov, 2013; Kuznetsov et al., 2014; Leonov et al., 2015; Dudkowski et al., 2016). The analytical estimates

$$\omega_l = \frac{K_0\sqrt{K_0/\tau_1}}{\tau_1} + \frac{K_0^2\tau_2}{3\tau_1^2} + O\left((\tau_2/\tau_1)^2\right), \tag{16}$$

$$\omega_l = \frac{K_0\sqrt{K_0/\tau_1}}{\tau_1} + \frac{K_0^2\tau_2}{3\tau_1^2} + \frac{K_0^2\tau_2^2(5-6\ln 2)}{18\tau_1^2}\sqrt{K_0/\tau_1} + O\left((\tau_2/\tau_1)^3\right), \tag{17}$$

which are obtained in (PI) confirm the adequacy of the presented numerical results. In Figure 10, the numerical estimate (dashed curve) is compared with an-

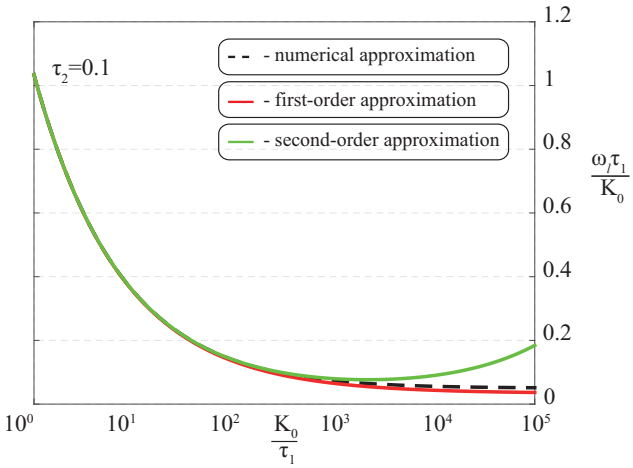

FIGURE 10 Comparison of numerical and analytical estimates of the lock-in frequency, ω_l, in the case of sinusoidal PD characteristic.

alytical estimates (16) (red curve) and (17) (green curve). The obtained estimates improve the estimates from (Gardner, 2005; Huque, 2011; Huque and Stensby, 2013) for $\frac{K_0}{\tau_1}$ being not large.

Consider now the PLL with active PI filter and impulse signals $f_1(\theta_1(t)) = \text{sign}\,[\sin(\theta_1(t))]$ and $f_2(\theta_2(t)) = \text{sign}\,[\cos(\theta_2(t))]$. For this case, the 2π-periodic PD characteristic of the PLL model (6) is triangular (see, e.g., (Leonov et al., 2011; Kuznetsov et al., 2011, 2015)):

$$K_d = 1, \qquad \varphi(\theta_\Delta) = \begin{cases} \frac{2}{\pi}\theta_\Delta, & \text{if } -\frac{\pi}{2} \le \theta_\Delta(t) \le \frac{\pi}{2}, \\ -\frac{2}{\pi}\theta_\Delta + 2, & \text{if } \frac{\pi}{2} \le \theta_\Delta(t) \le \frac{3\pi}{2}. \end{cases} \tag{18}$$

The numerical diagrams analogous to Figure 9a are obtained in Figure 11.

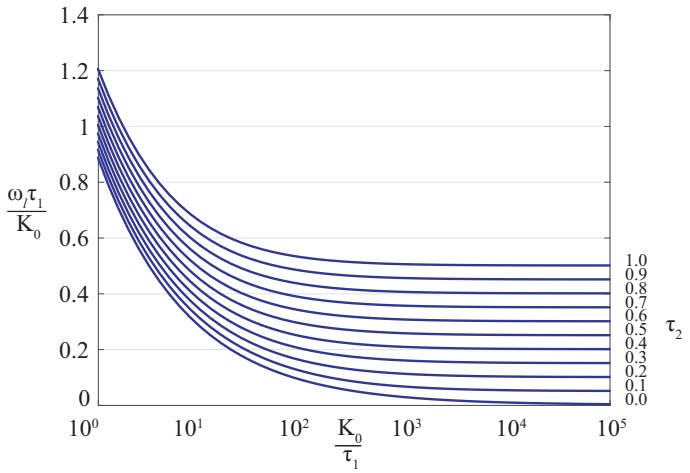

FIGURE 11 Diagrams for the lock-in frequency ω_l calculation in the case of triangular PD characteristic.

For this case, the exact formulae of the lock-in range are derived in (PII) (re-definitions $a = \frac{\tau_2}{\tau_1}$, $b = \frac{1}{\tau_1}$ are used to reduce the analytical formulae):

A. $(aK_0)^2 - 2bK_0\pi > 0$:

$$\omega_l = \frac{1}{\pi} c_1 \sqrt{(aK_0)^2 - 2bK_0\pi}\, \left(-\frac{c_2}{c_1}\right)^{\left(\frac{1}{2} - \frac{aK_0}{2\sqrt{(aK_0)^2 - 2bK_0\pi}}\right)}, \tag{19}$$

$$\text{where } c_1 = \frac{\pi}{4}\left(\frac{\sqrt{(aK_0)^2 + 2bK_0\pi}}{\sqrt{(aK_0)^2 - 2bK_0\pi}} + 1\right), c_2 = \frac{\pi}{4}\left(1 - \frac{\sqrt{(aK_0)^2 + 2bK_0\pi}}{\sqrt{(aK_0)^2 - 2bK_0\pi}}\right);$$

B. $(aK_0)^2 - 2bK_0\pi = 0$:

$$\omega_l = \frac{1}{2}c_2\, e^{\left(\frac{aK_0}{2c_2}\right)}, \text{where } c_2 = \frac{\sqrt{(aK_0)^2 + 2bK_0\pi}}{2}; \tag{20}$$

C. $(aK_0)^2 - 2bK_0\pi < 0$:

$$\omega_l = -\frac{aK_0\, e^{t_0 \operatorname{Re}\lambda_1^s}}{2\pi}\left(c_1 \cos\left(t_0 \operatorname{Im}\lambda_1^s\right) + c_2 \sin\left(t_0 \operatorname{Im}\lambda_1^s\right)\right) +$$
$$+ \frac{e^{t_0 \operatorname{Re}\lambda_1^s}\sqrt{2bK_0\pi - (aK_0)^2}}{2\pi}\left(c_2 \cos\left(t_0 \operatorname{Im}\lambda_1^s\right) - c_1 \sin\left(t_0 \operatorname{Im}\lambda_1^s\right)\right), \tag{21}$$
$$\text{where } t_0 = \frac{\operatorname{arctg}\left(-\frac{c_1}{c_2}\right)}{\operatorname{Im}\lambda_1^s}, c_1 = \frac{\pi}{2},\ c_2 = \frac{\pi\sqrt{(aK_0)^2 + 4bK_0(\pi - \frac{1}{k})}}{2\sqrt{2bK_0\pi - (aK_0)^2}},$$
$$\lambda_1^s = \frac{-aK_0 + i\sqrt{2bK_0\pi - (aK_0)^2}}{\pi}.$$

The formulae (19), (20), and (21) confirm the adequacy of the numerical diagrams in Figure 11.

3 CONCLUSIONS

In the present work, the lock-in range of PLL with active PI filter is studied. The nonlinear model of PLL in the signal's phase space is considered as well. The lock-in range is studied according to a rigorous mathematical definition from (Kuznetsov et al., 2015; Leonov et al., 2015b).

The phase plane analysis is applied to obtain the relation for the lock-in range computation. For the case of sinusoidal characteristics of phase detector the analytical estimates of the lock-in range, which improve the estimates in (Gardner, 2005; Huque, 2011; Huque and Stensby, 2013), are obtained. For the case of triangular characteristics of phase detector, the exact formulae of the lock-in range are derived, and the problem of the lock-in range computation is completely solved. Numerical methods are used to obtain diagrams for the lock-in range computation. The constructed diagrams confirm the adequacy of analytical results.

The study of the lock-in range for PLLs with other first-order filters (e.g., lead-lag filter) and PD characteristics (e.g., piecewise continuous sawtooth PD characteristic) by methods of phase plane analysis may form the next step of this research. Further work includes the study of the lock-in range of PLLs with higher-order filters, which is a challenging task since the methods of phase plane analysis can not be applied for the study of multidimensional phase space. Further research steps may include generalization of the existing analytical methods, development of new methods for analytical estimation of the lock-in range, and development of new methods for numerical computation of the lock-in range.

YHTEENVETO (FINNISH SUMMARY)

Aktiivisuodatettujen vaihelukittujen piirien lukkiutumisalueista

Tässä työssä tutkitaan vaihelukittuja silmukoita (phase-locked loops (PLL)) suljetuissa etäisyyksissä (lock-in range). PLL-variaatioita sovelletaan radiojärjestelmissä (esimerkiksi AM/FM-radio), telekommunikaatiojärjestelmissä (esimerkiksi GSM ja CDMA), GPS-paikannuksissa ja tietokonearkkitehtuureissa. Viime aikoina PLL on muodostunut aktiiviseksi tutkimusaiheeksi sen lukuisten potentiaalisten sovelluksien takia, esimerkkinä näistä optinen PLL.

Perusperiaatteena PLL:ssä on oikaista paikallisen (muokattavan) oskillaattorin vaihetta annettuun viiteoskillattoriin. F.M. Gardner esitteli suljetun etäisyyden konseptin, joka kuvailee oskillaattorien nopeaa synkronointia ilman epätoivottuja vaihe-eroja. F.M. Gardner tosin huomautti v. 1979 kirjassaan “Phaselock Techniques”, että suljetun etäisyyden määritelmä ei ole yleisissä tapauksissa tarpeeksi tiukka. Tästä huolimatta, suljetun etäisyyden määritelmä on hyödyllinen konsepti ja sitä hyödynnetään monissa PLL-sovelluksissa.

Tässä työssä tutkitaan epälineaarisen PLL-mallin suljettuja etäisyyksiä uuden matemaattisen määritelmän mukaan. Kyseistä PLL-mallia tutkitaan sen signaalin vaiheavaruudessa käyttämällä aktiivista suhteellis-sopeutettua (active proportionally-integrating (PI)) suodatinta. Työssä johdetaan analyyttisiä arvioita vaihdeilmaisimen suljettuun etäisyyteen, jolla on sinimuotoisia ominaisuuksia. Johdetut arviot ovat tiukempia arvioita tunnettuihin PLL:n suljettuihin etäisyyksiin joilla on PI-suodattimia. Lisäksi työssä johdetaan tiukempia arvioita vaihdeilmaisimiin joilla on kolmionmuotoisia ominaisuuksia. Mallien arviot validoitiin käyttämällä numeerisia simulaatioita.

REFERENCES

Aaltonen, L., Saukoski, M. & Halonen, K. 2005. Design of clock generating fully integrated PLL using low frequency reference signal. In Proceedings of the 2005 European Conference on Circuit Theory and Design, Vol. 1, I/161-I/164. doi: 10.1109/ECCTD.2005.1522935.

Abramovich, S. & Leonov, G. 1978. On approximation of capture bands in phase locked loop (in Russian). Radiotekhnika i Elektronika 23 (10), 2177-2183.

Abramovitch, D. 2002. Phase-locked loops: A control centric tutorial. In American Control Conf. Proc., Vol. 1. IEEE, 1-15.

Ahissar, E. 2003. Neuronal phase-locked loops. (US Patent 6,581,046).

Ahola, R. & Halonen, K. 2003. A 1.76-GHz 22.6-mW $\Delta\Sigma$ fractional-n frequency synthesizer. IEEE Journal of Solid-State Circuits 38 (1), 138–140. doi:10.1109/JSSC.2002.806261.

Ahola, R., Vikla, J., Lindfors, S., Routama, J. & Halonen, K. 1999. A 2 GHz phase-locked loop frequency synthesizer with on-chip VCO. Analog Integrated Circuits and Signal Processing 18 (1), 43–54.

Alexander, S. 1997. Optical communication receiver design. SPIE Optical engineering press Bellingham, Washington, USA.

Andronov, A. A., Vitt, E. A. & Khaikin, S. E. 1937. Theory of Oscillators (in Russian). ONTI NKTP SSSR. (English transl. 1966, Pergamon Press).

Armstrong, E. H. 1921. A new system of short wave amplification. Proceedings of the Institute of Radio Engineers 9 (1), 3–11.

Ascheid, G. & Meyr, H. 1982. Cycle slips in phase-locked loops: A tutorial survey. IEEE Transactions on Communications 30 (10), 2228-2241.

Bakaev, Y. N. & Guzh, A. A. 1965. Optimal reception of frequency modulated signals under doppler effect conditions (in Russian). Radiotekhnika i Elektronika 10 (1), 171–175.

Bakaev, Y. N. 1963. Stability and dynamical properties of astatic frequency synchronization system (in Russian). Radiotekhnika i Elektronika 8 (3), 513–516.

Baker, R. 2011. CMOS: Circuit Design, Layout, and Simulation. Wiley-IEEE Press. IEEE Press Series on Microelectronic Systems.

Banerjee, D. 2006. PLL performance, simulation and design. Dog Ear Publishing.

Bellescize, H. 1932. La réception synchrone. L'onde Électrique 11, 230-340.

Bellescize, H. d. 1935. Synchronizing system. (US Patent 1,990,428).

Best, R., Kuznetsov, N., Kuznetsova, O., Leonov, G., Yuldashev, M. & Yuldashev, R. 2015. A short survey on nonlinear models of the classic Costas loop: rigorous derivation and limitations of the classic analysis. In Proceedings of the American Control Conference. IEEE, 1296–1302. doi:10.1109/ACC.2015.7170912.

Best, R. 2007. Phase-Lock Loops: Design, Simulation and Application (6th edition). McGraw-Hill.

Bianchi, G., Kuznetsov, N., Leonov, G., Yuldashev, M. & Yuldashev, R. 2015. Limitations of PLL simulation: hidden oscillations in MATLAB and SPICE. In 2015 7th International Congress on Ultra Modern Telecommunications and Control Systems and Workshops (ICUMT), 79–84.

Blanchard, A. 1976. Phase-Locked Loops. Wiley.

Chan, V. W. 2000. Optical space communications. IEEE Journal of Selected Topics in Quantum Electronics 6 (6), 959–975.

Costas, J. 1956. Synchoronous communications. In Proc. IRE, Vol. 44, 1713–1718.

Costas, J. P. 1962. Receiver for communication system. (US Patent 3,047,659).

Crawford, J. A. 1994. Frequency synthesizer design handbook. Artech House Publishers.

DeLange, O. E. 1968. Optical heterodyne detection. IEEE Spectrum 5 (10), 77–85.

Dudkowski, D., Jafari, S., Kapitaniak, T., Kuznetsov, N. V., Leonov, G. A. & Prasad, A. 2016. Hidden attractors in dynamical systems. Physics Reports. doi:10.1016/j.physrep.2016.05.002.

Egan, W. F. 2000. Frequency synthesis by phase lock. Wiley New York.

Ershova, O. B. & Leonov, G. A. 1983. Frequency estimates of the number of cycle slidings in phase control systems. Automation and Remove Control 44 (5), 600-607.

Gantmacher, F. R. & Brenner, J. L. 2005. Applications of the Theory of Matrices. Courier Corporation.

Gardner, F. 1966. Phase-lock techniques. New York: John Wiley & Sons.

Gardner, F. 1979. Phase-lock techniques (2nd edition). New York: John Wiley & Sons.

Gardner, F. 2005. Phaselock Techniques (3rd edition). Wiley.

Gelig, A., Leonov, G. & Yakubovich, V. 1978. Stability of Nonlinear Systems with Nonunique Equilibrium (in Russian). Nauka. (English transl: Stability of Stationary Sets in Control Systems with Discontinuous Nonlinearities, 2004, World Scientific).

George, T. S. 1951. Analysis of synchronizing systems for dot-interlaced color television. Proceedings of the IRE 39 (2), 124–131.

Goldman, S. 2007. Phase-Locked Loops Engineering Handbook for Integrated Circuits. Artech House.

Gopal, M. 2002. Control systems: principles and design. Tata McGraw-Hill Education.

Grebene, A. & Camenzind, H. 1969. Phase locking as a new approach for tuned integrated circuits. In Solid-State Circuits Conference. Digest of Technical Papers. 1969 IEEE International, Vol. 12. IEEE, 100–101.

Gruen, W. 1953. Theory of afc synchronization. Proceedings of the IRE 8 (41), 1043–1048.

Gubar', N. A. 1961. Investigation of a piecewise linear dynamical system with three parameters. Journal of Applied Mathematics and Mechanics 25 (6), 1519–1535.

Hershey, J. E., Grabb, M. L. & Kenneth Brakeley Welles, I. 2002. Use of wideband DTV overlay signals for brevity signaling and public safety. (US Patent 6,498,627).

Hoppensteadt, F. C. & Izhikevich, E. M. 2000. Pattern recognition via synchronization in phase-locked loop neural networks. IEEE Transactions on Neural Networks 11 (3), 734–738.

Huque, A. S. & Stensby, J. 2013. An analytical approximation for the pull-out frequency of a PLL employing a sinusoidal phase detector. ETRI Journal 35 (2), 218–225.

Huque, A. S. 2011. A new derivation of the pull-out frequency for second-order phase lock loops employing triangular and sinusoidal phase detectors. The Univerrsity of Alabama in Huntsville. (Ph. D. thesis).

Huygens, C. 1966. Horologium oscillatorium: 1673. Dawson.

Janc, R. & Jasper, S. 1988. Digital global positioning system receiver. (US Patent 4,785,463).

Johnson, C., Ward, P., Lindley, J., Maher, R., Holmes, J. & Fuchser, T. 1984. Global position system (GPS) multiplexed receiver. (US Patent 4,468,793).

Jorgensen, K. 1999. Frequency modulation using a phase-locked loop. (US Patent 5,920,556).

Kaplan, E. & Hegarty, C. 2005. Understanding GPS: principles and applications. Artech house.

Kauraniemi, J. & Vuori, J. 1997. Narrowband digital phase-locked loop using delta operator filters. In 1997 IEEE 47th Vehicular Technology Conference, Vol. 3, 1734–1737.

Kazovsky, L. G. 1985. Optical heterodyning versus optical homodyning: A comparison. Journal of optical communications 6 (1), 18–24.

Keliu, S. & Sánchez-Sinencio, E. 2006. CMOS PLL synthesizers: analysis and design, Vol. 783. Springer Science & Business Media.

Kihara, M., Ono, S. & Eskelinen, P. 2002. Digital Clocks for Synchronization and Communications. Artech House.

Kim, J., Horowitz, M. A. & Wei, G. Y. 2003. Design of CMOS adaptive-bandwidth pll/dlls: a general approach. Circuits and Systems II: Analog and Digital Signal Processing, IEEE Transactions on 50 (11), 860–869.

Kroupa, V. 2003. Phase Lock Loops and Frequency Synthesis. John Wiley & Sons.

Kudrewicz, J. & Wasowicz, S. 2007. Equations of phase-locked loop. Dynamics on circle, torus and cylinder. World Scientific.

Kudryashova, E., Kuznetsova, O., Kuznetsov, N., Leonov, G., Seledzhi, S., Yuldashev, M. & Yuldashev, R. 2014. Nonlinear models of BPSK Costas loop. ICINCO 2014 - Proceedings of the 11th International Conference on Informatics in Control, Automation and Robotics 1, 704-710. doi:10.5220/0005050707040710.

Kung, S. 1988. VLSI array processors. Prentice Hall.

Kuznetsov, N., Kuznetsova, O., Leonov, G., Neittaanmaki, P., Yuldashev, M. & Yuldashev, R. 2015. Limitations of the classical phase-locked loop analysis. Proceedings - IEEE International Symposium on Circuits and Systems 2015-July, 533-536. doi:10.1109/ISCAS.2015.7168688.

Kuznetsov, N., Leonov, G., Neittaanmäki, P., Seledzhi, S., Yuldashev, M. & Yuldashev, R. 2012a. Nonlinear mathematical models of Costas loop for general waveform of input signal. In IEEE 4th International Conference on Nonlinear Science and Complexity, NSC 2012 - Proceedings, 109-112. doi:10.1109/NSC.2012.6304729.

Kuznetsov, N., Leonov, G., Neittaanmäki, P., Seledzhi, S., Yuldashev, M. & Yuldashev, R. 2012b. Simulation of phase-locked loops in phase-frequency domain. In International Congress on Ultra Modern Telecommunications and Control Systems and Workshops. IEEE, 351-356 (art. no. 6459692). doi:10.1109/ICUMT.2012.6459692.

Kuznetsov, N., Leonov, G., Neittaanmäki, P., Seledzhi, S., Yuldashev, M. & Yuldashev, R. 2013. Phase-frequency domain model of Costas loop with mixer discriminator. In Proceedings of the 10th International Conference on Informatics in Control, Automation and Robotics, 427-433. doi:10.5220/0004479104270433.

Kuznetsov, N., Leonov, G., Seledzgi, S., Yuldashev, M. & Yuldashev, R. 2015. Elegant analytic computation of phase detector characteristic for non-sinusoidal signals. IFAC-PapersOnLine 48 (11), 960-963. doi:10.1016/j.ifacol.2015.09.316.

Kuznetsov, N., Leonov, G. & Seledzhi, S. 2009. Nonlinear analysis of the Costas loop and phase-locked loop with squarer. In Proceedings of the IASTED International Conference on Signal and Image Processing, SIP 2009, 1-7.

Kuznetsov, N., Leonov, G., Yuldashev, M. & Yuldashev, R. 2011. Analytical methods for computation of phase-detector characteristics and PLL design. In ISSCS 2011 - International Symposium on Signals, Circuits and Systems, Proceedings, 7-10. doi:10.1109/ISSCS.2011.5978639.

Kuznetsov, N., Leonov, G., Yuldashev, M. & Yuldashev, R. 2014. Nonlinear analysis of classical phase-locked loops in signal's phase space. IFAC Proceedings Volumes (IFAC-PapersOnline) 19, 8253-8258. doi:10.3182/20140824-6-ZA-1003.02772.

Kuznetsov, N., Leonov, G., Yuldashev, M. & Yuldashev, R. 2015. Rigorous mathematical definitions of the hold-in and pull-in ranges for phase-locked loops. IFAC-PapersOnLine 48 (11), 710-713. doi:10.1016/j.ifacol.2015.09.272.

Kuznetsov, N. 2008. Stability and Oscillations of Dynamical Systems: Theory and Applications. Jyvaskyla University Printing House.

Kuznetsov, N., Kuznetsova, O., Leonov, G. & Vagaitsev, V. 2013. Analytical-numerical localization of hidden attractor in electrical Chua's circuit. Informatics in Control, Automation and Robotics, Lecture Notes in Electrical Engineering, Volume 174, Part 4 174 (4), 149-158. doi:10.1007/978-3-642-31353-0_11.

Kuznetsov, N. V. 2016. Analytical-numerical methods for the study of hidden oscillations (in Russian). (Habilitation Thesis).

Leonov, G., Kuznetsov, N. & Mokaev, T. 2015. Homoclinic orbits, and self-excited and hidden attractors in a Lorenz-like system describing convective fluid motion. Eur. Phys. J. Special Topics 224 (8), 1421-1458. doi:10.1140/epjst/e2015-02470-3.

Leonov, G., Kuznetsov, N. & Vagaitsev, V. 2011. Localization of hidden Chua's attractors. Physics Letters A 375 (23), 2230-2233. doi:10.1016/j.physleta.2011.04.037.

Leonov, G., Kuznetsov, N. & Vagaitsev, V. 2012. Hidden attractor in smooth Chua systems. Physica D: Nonlinear Phenomena 241 (18), 1482-1486. doi:10.1016/j.physd.2012.05.016.

Leonov, G., Kuznetsov, N., Yuldahsev, M. & Yuldashev, R. 2011. Computation of phase detector characteristics in synchronization systems. Doklady Mathematics 84 (1), 586-590. doi:10.1134/S1064562411040223.

Leonov, G., Kuznetsov, N., Yuldahsev, M. & Yuldashev, R. 2012. Analytical method for computation of phase-detector characteristic. IEEE Transactions on Circuits and Systems - II: Express Briefs 59 (10), 633-647. doi:10.1109/TCSII.2012.2213362.

Leonov, G., Kuznetsov, N., Yuldashev, M. & Yuldashev, R. 2015a. Computation of the phase detector characteristic of classical PLL. Doklady Mathematics 91 (2), 246-249.

Leonov, G., Kuznetsov, N., Yuldashev, M. & Yuldashev, R. 2015b. Hold-in, pull-in, and lock-in ranges of PLL circuits: rigorous mathematical definitions and limitations of classical theory. IEEE Transactions on Circuits and Systems–I: Regular Papers 62 (10), 2454–2464. doi:10.1109/TCSI.2015.2476295.

Leonov, G., Kuznetsov, N., Yuldashev, M. & Yuldashev, R. 2015c. Mathematical models of the Costas loop. Doklady Mathematics 92 (2), 594–598. doi:10.1134/S1064562415050270.

Leonov, G., Kuznetsov, N., Yuldashev, M. & Yuldashev, R. 2015d. Nonlinear dynamical model of Costas loop and an approach to the analysis of its stability in the large. Signal processing 108, 124-135. doi:10.1016/j.sigpro.2014.08.033.

Leonov, G. & Kuznetsov, N. 2013. Hidden attractors in dynamical systems. From hidden oscillations in Hilbert-Kolmogorov, Aizerman, and Kalman problems to hidden chaotic attractors in Chua circuits. International Journal of Bifurcation and Chaos 23 (1). doi:10.1142/S0218127413300024. (art. no. 1330002).

Leonov, G. & Kuznetsov, N. 2014. Nonlinear Mathematical Models of Phase-Locked Loops. Stability and Oscillations. Cambridge Scientific Publisher.

Leonov, G. A., Kuznetsov, N. V., M.V., Y. & R.V., Y. 2015. Hold-in, pull-in, and lock-in ranges of PLL circuits: Rigorous mathematical definitions and limitations of classical theory. IEEE Transactions on Circuits and Systems – I: Regular Papers 62 (10), 2454–2464.

Lerber, T., Honkanen, S., Tervonen, A., Ludvigsen, H. & Kuppers, F. 2009. Optical clock recovery method: review. Elsevier Opt. Fiber Technol 15, 363–372.

Lindgren, N. 1970. Optical communications—a decade of preparations. Proceedings of the IEEE 58 (10), 1410–1418.

Lindsey, W. & Tausworthe, R. 1973. A Bibliography of the Theory and Application of the Phase-lock Principle. Jet Propulsion Laboratory, California Institute of Technology. JPL technical report.

Lyapunov, A. M. 1892. The General Problem of the Stability of Motion (in Russian). Kharkov: . (English transl. Academic Press, NY, 1966).

Meyr, H. & Ascheid, G. 1990. Synchronization in digital communications: Phase-, frequency-locked loops and Amplitude Control, Vol. 9. Wiley-Interscience.

Meyr, H. 1975. Nonlinear analysis of correlative tracking systems using renewal process theory. IEEE Transactions on Communications 23 (2), 192–203.

Mitola, J. 1995. The software radio architecture. IEEE Communications Magazine 33 (5), 26–38.

Mitropolsky, Y. & Bogolubov, N. 1961. Asymptotic Methods in the Theory of Non-Linear Oscillations. New York: Gordon and Breach.

Moon, S. T., Valero-López, A. Y. & Sánchez-Sinencio, E. 2005. Fully integrated frequency synthesizers: A tutorial. International journal of high speed electronics and systems 15 (02), 353–375.

Proakis, J. & Salehi, M. 2008. Digital Communications. McGraw-Hill Higher Education.

Rapeli, J. 1992. Interpolating phase-locked loop frequency synthesizer. (US Patent 5,079,520).

Rapinoja, T., Stadius, K. & Halonen, K. 2006. Behavioral model based simulation methods for charge-pump PLL's. In 2006 International Baltic Electronics Conference, 1-4. doi:10.1109/BEC.2006.311073.

Razavi, B. 1996. Monolithic phase-locked loops and clock recovery circuits: theory and design. John Wiley & Sons.

Richman, D. 1953. Theory of synchronization, applied to NTSC color television. In Proceedings of the IRE, Vol. 41, 403–403.

Richman, D. 1954. Color-carrier reference phase synchronization accuracy in NTSC color television. Proceedings of the IRE 42 (1), 106–133.

Rosenkranz, W. 1985. Design and optimization of a digital fm receiver using dpll techniques. In IEEE International Conference on Acoustics, Speech, and Signal Processing (ICASSP'85), Vol. 10. IEEE, 592–595.

Samoilenko, A. & Petryshyn, R. 2004. Multifrequency Oscillations of Nonlinear Systems. Springer. Mathematics and Its Applications.

Saukoski, M., Aaltonen, L., Salo, T. & Halonen, K. A. 2008. Interface and control electronics for a bulk micromachined capacitive gyroscope. Sensors and Actuators A: Physical 147 (1), 183 – 193.

Shakhgildyan, V. & Lyakhovkin, A. 1966. Fazovaya avtopodstroika chastoty (in Russian). Moscow: Svyaz'.

Shakhtarin, B. 2012. The dynamic characteristics of phase locking in the presence of a harmonic noise. Journal of Communications Technology and Electronics 57 (6), 588–594.

Shalfeev, V. D. & Matrosov, V. V. 2013. Nonlinear dynamics of phase synchronization systems (in Russian).

Speeti, T., Aaltonen, L. & Halonen, K. 2009. Integrated charge-pump phase-locked loop with sc-loop filter for capacitive microsensor readout. In IEEE International Symposium on Circuits and Systems (ISCAS 2009), 1373-1376. doi:10.1109/ISCAS.2009.5118020.

Tokunaga, M. & Mori, S. 1990. Digital neuron model with dpll for associative memory. In IEEE International Symposium on Circuits and Systems (ISCAS 1990). IEEE, 1069–1072.

Tretter, S. A. 2008. Communication System Design Using DSP Algorithms with Laboratory Experiments for the $TMS320C6713^{TM}$ DSK. Springer.

Tricomi, F. 1933. Integrazione di unequazione differenziale presentatasi in elettrotechnica. Annali della R. Shcuola Normale Superiore di Pisa 2 (2), 1-20.

Tucker, D. G. 1954. The history of the homodyne and synchrodyne. Journal of the British Institution of Radio Engineers 14 (4), 143–154.

Vankka, J. 1997. Digital frequency synthesizer/modulator for continuous-phase modulations with slow frequency hopping. IEEE Transactions on Vehicular Technology 46 (4), 933-940. doi:10.1109/25.653067.

Viterbi, A. 1959. Acquisition range and tracking behavior of phase-locked loops. JPL, California Institute of Technology, Pasadena, External Publ 673.

Viterbi, A. 1966. Principles of coherent communications. New York: McGraw-Hill.

Wei-Ping, L. & Chin-Kan, C. 1998. Phase-locked loop with neurocontroller. In Proceedings of the 37th SICE Annual Conference, International Session Papers, 1133–1138.

Wendt, K. & Fredentall, G. 1943. Automatic frequency and phase control of synchronization in TV receivers. Proceedings of the IRE 31 (1), 1-15.

APPENDIX 1 NUMERICAL COMPUTATION OF THE LOCK-IN RANGE

The implementation of the PLL model (6) with sinusoidal PD characteristic is given in Listing 1.1.

```
function dz = PLLSysSin(t, z)
% Function for defining differential equations, which ODE solver will
    integrate
% Sinusoidal PD characteristic
global omega_e tau_1 tau_2 L;
dz = zeros(2,1);
dz(1) = sin(z(2));
dz(2) = omega_e - L*(z(1) + tau_2*sin(z(2)))/tau_1;
end
```

LISTING 1.1 Equations for the PLL model with active PI filter and sinusoidal PD characteristic in the signal's phase space.

The implementation of the PLL model (6) with triangular PD characteristic is given in Listing 1.2.

```
function dz = PLLSysTriangle(t,z)
% Function for defining differential equations, which ODE solver will
    integrate
% Triangular PD characteristic
global omega_e tau_1 tau_2 L;
dz = zeros(2,1);
dz(1) = sawtooth(z(2)+pi/2, 0.5);
dz(2) = omega_e - L*(z(1) + tau_2*sawtooth(z(2)+pi/2, 0.5))/tau_1;
end
```

LISTING 1.2 Equations for the PLL model with active PI filter and triangular PD characteristic in the signal's phase space.

The event for stopping the numerical integration of phase trajectory reaching $\theta_\Delta = \text{initial\_value} \pm \text{halt\_value}$ is given in Listing 1.3.

```
function [value,isterminal,direction] = Event(t, y, initial_value,
    halt_value)
% Event function for ODE solver to stop when halt_value is reached

value = (y(2) - initial_value)^2 - halt_value^2;
isterminal=1;
direction=0;
end
```

LISTING 1.3 Event MATLAB function.

The MATLAB script for constructing the lock-in range diagrams from Section 2.3 is given in Listing 1.4.

```
clear all;
global omega_e tau_1 tau_2 L;
%Setting figure options
figure;
hold on;
```

```
grid on;
text(-0.05, 0.5, '\tau_2', 'Units', 'normalized');
xlabel('K_0 / \tau_1');
ylabel('\omega_l*\tau_1/K_0');
ax = gca;
ax.YAxisLocation = 'right';
set(ax,'XScale','log');
set(ax,'fontsize',20);
%Setting PLL parameters
omega_e = 0;
tau_1 = 0.5;
initial_value = pi; %theta_delta coordinate of saddle equilibrium
halt_value = pi; %theta_delta maximum deviation from initial_value
%Setting ODE solver options, system, and event
xoverFcn = @(t, y) Event(t, y, initial_value, halt_value); %event for
    stopping integration
options = odeset('RelTol', 1.e-10, 'AbsTol', 1.e-10, 'events', xoverFcn
    );
len = 1.e4; % time of integration

%the case of sinusoidal/triangular PD characteristic;
%one of two possible should be chosen
sys = @PLLSysSin;
% sys = @PLLSysTriangle;

tau2_values = 0:0.5:1; %vector of tau_2 values
%The outer cycle for plotting curves for each value stored in
    tau2_values
for i=1:size(tau2_values,2)
    tau_2 = tau2_values(i);
    plotNum = zeros (0,2);
    % The inner cycle for computing the values of omega_l for fixed
        tau_2
    for j=0:1:5
        L_tau1 = 10^j;
        L = L_tau1*tau_1;
        % Numerical integration of trajectory close to separatrix Q
        [T,Y,Te,Ye,De] = ode15s(sys, -[0 len], [omega_e/L*tau_1
            initial_value+1.e-4], options);
        plotNum = [plotNum; [L_tau1 Y(end, 1)/2]];
        clear T Y Te Ye De;
    end;
    % Plot the computed array of omega_l
    semilogx(plotNum(:, 1), plotNum(:, 2), 'blue', 'LineWidth', 3);
    text(plotNum(1, 1), plotNum(1, 2), sprintf(' %.2f', tau_2), '
        HorizontalAlignment', 'right');
end;
```

LISTING 1.4 MATLAB script for constructing the diagram from Figure 9a and Figure 11.

ORIGINAL PAPERS

PI

THE LOCK-IN RANGE OF PLL-BASED CIRCUITS WITH PROPORTIONALLY-INTEGRATING FILTER AND SINUSOIDAL PHASE DETECTOR CHARACTERISTIC

by

K. D. Aleksandrov, N. V. Kuznetsov, G. A. Leonov, M. V. Yuldashev,
R. V. Yuldashev 2016

arXiv:1603.08401

Lock-in range of PLL-based circuits with proportionally-integrating filter and sinusoidal phase detector characteristic

K. D. Aleksandrov, N.V. Kuznetsov, G. A. Leonov, M. V. Yuldashev, R. V. Yuldashev

Faculty of Mathematics and Mechanics, Saint-Petersburg State University, Russia

Dept. of Mathematical Information Technology, University of Jyväskylä, Finland

Institute of Problems of Mechanical Engineering RAS, Russia

Abstract

In the present work PLL-based circuits with sinusoidal phase detector characteristic and active proportionally-integrating (PI) filter are considered. The notion of lock-in range – an important characteristic of PLL-based circuits, which corresponds to the synchronization without cycle slipping, is studied. For the lock-in range a rigorous mathematical definition is discussed. Numerical and analytical estimates for the lock-in range are obtained.

Keywords: phase-locked loop, nonlinear analysis, PLL, two-phase PLL, lock-in range, Gardner's problem on unique lock-in frequency, pull-out frequency

1. Model of PLL-based circuits in the signal's phase space

For the description of PLL-based circuits a physical model in the signals space and a mathematical model in the signal's phase space are used (Gardner, 1966; Shakhgil'dyan and Lyakhovkin, 1966; Viterbi, 1966).

The equations describing the model of PLL-based circuits in the signals space are difficult for the study, since that equations are nonautonomous (see, e.g., (Kudrewicz and Wasowicz, 2007)). By contrast, the equations of model in the signal's phase space are autonomous (Gardner, 1966; Shakhgil'dyan and Lyakhovkin, 1966; Viterbi, 1966), what simplifies the study of PLL-based circuits. The application of averaging methods (Mitropolsky and Bogolubov, 1961; Samoilenko and Petryshyn, 2004) allows one to reduce the model of PLL-based circuits in the signals space to the model in the signal's phase space (see, e.g., (Leonov et al., 2012; Leonov and Kuznetsov, 2014; Leonov et al., 2015a; Kuznetsov et al., 2015b,a; Best et al., 2015).

Consider a model of PLL-based circuits in the signal's phase space (see Fig. 1). A reference oscillator (Input) and a voltage-controlled oscillator (VCO) generate phases $\theta_1(t)$ and $\theta_2(t)$, respectively. The frequency of reference signal usually assumed to be constant:

$$\dot{\theta}_1(t) = \omega_1. \tag{1}$$

The phases $\theta_1(t)$ and $\theta_2(t)$ enter the inputs of the phase detector (PD). The output of the phase detector in the signal's phase space is called a phase detector characteristic and

Email address: nkuznetsov239@gmail.com (N.V. Kuznetsov)

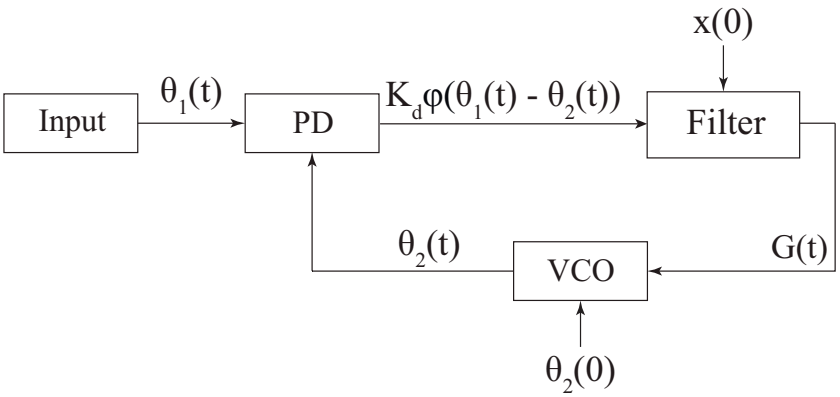

Figure 1: Model of PLL-based circuit in the signal's phase space.

has the form

$$K_d\varphi(\theta_1(t)-\theta_2(t)).$$

The maximum absolute value of PD output $K_d > 0$ is called a phase detector gain (see, e.g., (Best, 2007; Goldman, 2007)). The periodic function $\varphi(\theta_\Delta(t))$ depends on difference $\theta_1(t)-\theta_2(t)$ (which is called a phase error and denoted by $\theta_\Delta(t)$). The PD characteristic depends on the design of PLL-based circuit and the signal waveforms $f_1(\theta_1)$ of Input and $f_2(\theta_2)$ of VCO. In the present work a sinusoidal PD characteristic with

$$\varphi(\theta_\Delta(t)) = \sin(\theta_\Delta(t))$$

is considered (which corresponds, e.g., to the classical PLL with $f_1(\theta_1(t)) = \sin(\theta_1(t))$ and $f_2(\theta_2(t)) = \cos(\theta_2(t))$).

The output of phase detector is processed by Filter. Further we consider the active PI filter (see, e.g., (Baker, 2011)) with transfer function $W(s) = \frac{1+\tau_2 s}{\tau_1 s}$, $\tau_1 > 0$, $\tau_2 > 0$. The considered filter can be described as

$$\begin{cases} \dot{x}(t) = K_d \sin(\theta_\Delta(t)), \\ G(t) = \frac{1}{\tau_1} x(t) + \frac{\tau_2}{\tau_1} K_d \sin(\theta_\Delta(t)), \end{cases} \tag{2}$$

where $x(t)$ is the filter state. The output of Filter $G(t)$ is used as a control signal for VCO:

$$\dot{\theta}_2(t) = \omega_2^{\text{free}} + K_v G(t), \tag{3}$$

where ω_2^{free} is the VCO free-running frequency and $K_v > 0$ is the VCO gain coefficient.

Relations (1), (2), and (3) result in autonomous system of differential equations

$$\begin{cases} \dot{x} = K_d \sin(\theta_\Delta), \\ \dot{\theta}_\Delta = \omega_1 - \omega_2^{\text{free}} - \frac{K_v}{\tau_1}\left(x + \tau_2 K_d \sin(\theta_\Delta)\right). \end{cases} \tag{4}$$

Denote the difference of the reference frequency and the VCO free-running frequency $\omega_1 - \omega_2^{\text{free}}$ by $\omega_\Delta^{\text{free}}$. By the linear transformation $x \to K_d x$ we have

$$\begin{cases} \dot{x} = \sin(\theta_\Delta), \\ \dot{\theta}_\Delta = \omega_\Delta^{\text{free}} - \frac{K_0}{\tau_1}\left(x + \tau_2 \sin(\theta_\Delta)\right), \end{cases} \tag{5}$$

where $K_0 = K_v K_d$ is the loop gain. For signal waveforms listed in Table 1, relations (5) describe the models of the classical PLL and two-phase PLL in the signal's phase space. The models of classical Costas loop and two-phase Costas loop in the signal's phase space can be described by relations similar to (5) (PD characteristic of the circuits usually is a π-periodic function, and the approaches presented in this paper can be applied to these circuits as well) (see, e.g., (Best et al., 2014; Leonov et al., 2015a; Best et al., 2015)).

Signal waveforms	PD characteristic
Classical PLL	
$f_1(\theta_1) = \sin(\theta_1)$ $f_2(\theta_2) = \cos(\theta_2)$	$\frac{1}{2}\sin(\theta_\Delta)$
$f_1(\theta_1) = \sin(\theta_1)$ $f_2(\theta_2) = \operatorname{sign}(\cos(\theta_2))$	$\frac{2}{\pi}\sin(\theta_\Delta)$
$f_1(\theta_1) = \begin{cases} \frac{2}{\pi}\theta_1 + 1, \theta_1 \in [0;\pi], \\ 1 - \frac{2}{\pi}\theta_1, \theta_1 \in [\pi;2\pi] \end{cases}$ $f_2(\theta_2) = \sin(\theta_2)$	$\frac{4}{\pi^2}\sin(\theta_\Delta)$
Two-phase PLL	
$f_1(\theta_1) = \cos(\theta_1)$ $f_2(\theta_2) = \cos(\theta_2)$	$\sin(\theta_\Delta)$

Table 1: The dependency PD characteristics of PLL-based circuits on signal waveforms.

By the transformation

$$\left(\omega_\Delta^{\text{free}}, x, \theta_\Delta\right) \to \left(-\omega_\Delta^{\text{free}}, -x, -\theta_\Delta\right),$$

(5) is not changed. This property allows one to use the concept of frequency deviation

$$\left|\omega_\Delta^{\text{free}}\right| = \left|\omega_1 - \omega_2^{\text{free}}\right|$$

and consider (5) with $\omega_\Delta^{\text{free}} > 0$ only.

The state of PLL-based circuits for which the VCO frequency is adjusted to the reference frequency of Input is called a locked state. The locked states correspond to the locally asymptotically stable equilibria of (5), which can be found from the relations

$$\begin{cases} \sin(\theta_{eq}) = 0, \\ \omega_\Delta^{\text{free}} - \frac{K_0}{\tau_1} x_{eq} = 0. \end{cases}$$

Here x_{eq} depends on $\omega_\Delta^{\text{free}}$ and further is denoted by $x_{eq}(\omega_\Delta^{\text{free}})$.

Since (5) is 2π-periodic in θ_Δ, we can consider (5) in a 2π-interval of θ_Δ, $\theta_\Delta \in (-\pi, \pi]$. In interval $\theta_\Delta \in (-\pi, \pi]$ there exist two equilibria: $\left(0, \frac{\omega_\Delta^{\text{free}} \tau_1}{K_0}\right)$ and $\left(\pi, \frac{\omega_\Delta^{\text{free}} \tau_1}{K_0}\right)$. To define

type of the equilibria let us write out corresponding characteristic polynomials and find the eigenvalues:

$$\text{equilibrium } (0, \tfrac{\omega_\Delta^{\text{free}}\tau_1}{K_0}): \qquad \lambda^2 + \tfrac{K_0\tau_2}{\tau_1}\lambda + \tfrac{K_0}{\tau_1} = 0;$$

$$\begin{aligned}
&\lambda_{1,2} = \tfrac{-K_0\tau_2 \pm \sqrt{(K_0\tau_2)^2 - 4K_0\tau_1}}{2\tau_1}, && (K_0\tau_2)^2 - 4K_0\tau_1 > 0;\\
&\lambda_1 = \lambda_2 = \tfrac{-K_0\tau_2}{2\tau_1}, && (K_0\tau_2)^2 - 4K_0\tau_1 = 0;\\
&\lambda_{1,2} = \tfrac{-K_0\tau_2 \pm i\sqrt{4K_0\tau_1 - (K_0\tau_2)^2}}{2\tau_1}, && (K_0\tau_2)^2 - 4K_0\tau_1 < 0;
\end{aligned}$$

$$\text{equilibrium } (\pi, \tfrac{\omega_\Delta^{\text{free}}\tau_1}{K_0}): \qquad \lambda^2 - \tfrac{K_0\tau_2}{\tau_1}\lambda - \tfrac{K_0}{\tau_1} = 0;$$

$$\lambda_{1,2} = \tfrac{K_0\tau_2 \pm \sqrt{(K_0\tau_2)^2 + 4K_0\tau_1}}{2\tau_1}.$$

Denote the stable equilibrium as

$$\left(\theta_{eq}^s, x_{eq}(\omega_\Delta^{\text{free}})\right) = \left(0, \frac{\omega_\Delta^{\text{free}}\tau_1}{K_0}\right)$$

and the unstable equilibrium as

$$\left(\theta_{eq}^u, x_{eq}(\omega_\Delta^{\text{free}})\right) = \left(\pi, \frac{\omega_\Delta^{\text{free}}\tau_1}{K_0}\right).$$

Thus, for any arbitrary $\omega_\Delta^{\text{free}}$ the equilibria

$$\left(\theta_{eq}^s + 2\pi k, x_{eq}(\omega_\Delta^{\text{free}})\right) = \left(2\pi k, \frac{\omega_\Delta^{\text{free}}\tau_1}{K_0}\right)$$

are locally asymptotically stable. Hence, the locked states of (5) are given by equilibria $\left(\theta_{eq}^s + 2\pi k, x_{eq}(\omega_\Delta^{\text{free}})\right)$. The remaining equilibria

$$\left(\theta_{eq}^u + 2\pi k, x_{eq}(\omega_\Delta^{\text{free}})\right) = \left(\pi + 2\pi k, \frac{\omega_\Delta^{\text{free}}\tau_1}{K_0}\right)$$

are unstable saddle equilibria.

2. The global stability of PLL-based circuit model

In order to consider the lock-in range of PLL-based circuits let us discuss the global asymptotic stability. *If for a certain $\omega_\Delta^{\text{free}}$ any solution of (5) tends to an equilibrium, then the system with such $\omega_\Delta^{\text{free}}$ is called globally asymptotically stable* (see, e.g., (Leonov et al., 2015b)). To prove the global asymptotic stability of (5) two approaches can be applied: the phase plane analysis (Tricomi, 1933; Andronov et al., 1937) and construction of the Lyapunov functions (Lyapunov, 1892).

By methods of the phase plane analysis, in (Viterbi, 1966) the global asymptotic stability of (5) for any $\omega_\Delta^{\text{free}}$ is stated. However, to complete rigorously the proof given in (Viterbi, 1966), the additional explanations are required (i.e., the absence of heteroclinic

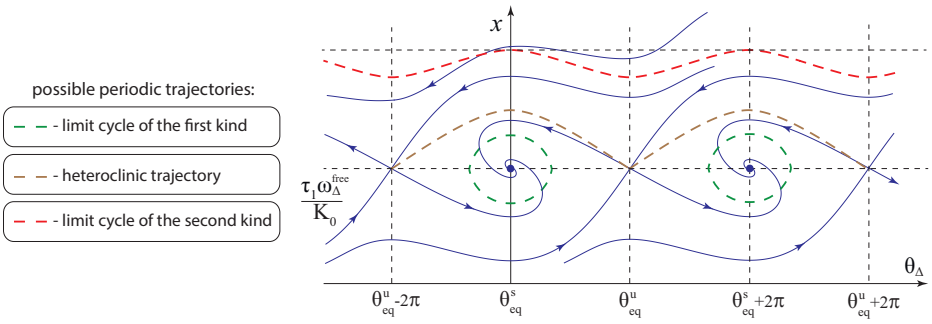

Figure 2: Phase portrait and possible periodic trajectories of (5).

trajectory and limit cycles of the first kind (see Fig. 2) is needed to be explained; e.g., for the case of lead-lag filter a number of works (Kapranov, 1956; Gubar', 1961; Shakhtarin, 1969; Belyustina et al., 1970) is devoted to the study of these periodic trajectories).

To overcome these difficulties, the methods of the Lyapunov functions construction can be applied. The modifications of the classical global stability criteria for cylindrical phase space are developed in (Gelig et al., 1978; Leonov and Kuznetsov, 2014; Leonov et al., 2015b). The global asymptotic stability of (5) for any $\omega_\Delta^{\text{free}}$ can be using the Lyapunov function

$$V(x,\theta_\Delta) = \frac{1}{2}\left(x - \frac{\tau_1\omega_\Delta^{\text{free}}}{K_0}\right)^2 + \frac{2\tau_1}{K_0}\sin^2\left(\frac{\theta_\Delta}{2}\right) \geq 0;$$
$$\dot{V}(x,\theta_\Delta) = -\tau_2\sin^2(\theta_\Delta) < 0, \quad \forall\theta_\Delta \neq \{\theta^s_{eq} + 2\pi k, \theta^u_{eq} + 2\pi k\}.$$

3. The lock-in range definition and analysis

Since the considered model of PLL-based circuits in the signal's phase space is globally asymptotically stable, it achieves locked state for any initial VCO phase $\theta_2(0)$ and filter state $x(0)$. However, the phase error θ_Δ may substantially increase during the acquisition process. In order to consider the property of the model to synchronize without undesired growth of the phase error θ_Δ, a lock-in range concept was introduced in (Gardner, 1966): "*If, for some reason, the frequency difference between input and VCO is less than the loop bandwidth, the loop will lock up almost instantaneously without slipping cycles. The maximum frequency difference for which this fast acquisition is possible is called the lock-in frequency*". The lock-in range concept is widely used in engineering literature on the PLL-based circuits study (see, e.g., (Stensby, 1997; Kihara et al., 2002; Kroupa, 2003; Gardner, 2005; Best, 2007)). Remark, that it is said that cycle slipping occurs if (see, e.g., (Ascheid and Meyr, 1982; Ershova and Leonov, 1983; Smirnova et al., 2014))

$$\limsup_{t\to+\infty} |\theta_\Delta(0) - \theta_\Delta(t)| \geq 2\pi.$$

For (5) with fixed $\omega_\Delta^{\text{free}}$ a domain of loop states for which the synchronization without cycle slipping occurs is called the lock-in domain $D_{\text{lock-in}}(\omega_\Delta^{\text{free}})$ (see Fig. 3). However, in general, even for zero frequency deviation ($\omega_\Delta^{\text{free}} = 0$) and a sufficiently large initial state of filter ($x(0)$), cycle slipping may take place, thus in 1979 Gardner wrote: *"There is no natural way to define exactly any unique lock-in frequency"* and *"despite its vague reality,*

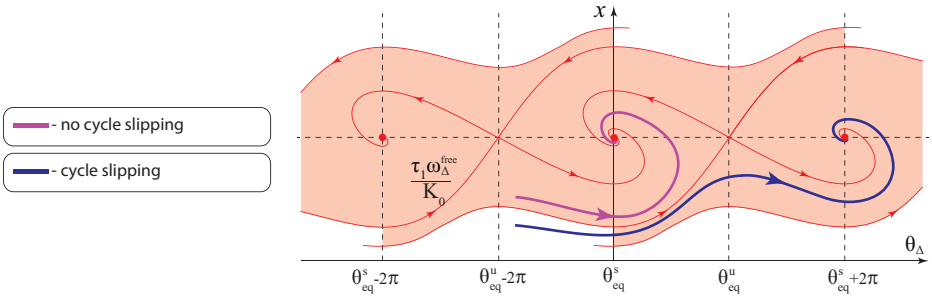

Figure 3: The lock-in domain $D_{\text{lock}-\text{in}}(\omega_\Delta^{\text{free}})$ of (5).

lock-in range is a useful concept" (Gardner, 1979). To overcome the stated problem, in (Kuznetsov et al., 2015c; Leonov et al., 2015b) the rigorous mathematical definition of a lock-in range is suggested:

Definition 1. *(Kuznetsov et al., 2015c; Leonov et al., 2015b) The lock-in range of model (5) is a range $[0,\omega_l)$ such that for each frequency deviation $\left|\omega_\Delta^{\text{free}}\right| \in [0,\omega_l)$ the model (5) is globally asymptotically stable and the following domain*

$$D_{\text{lock}-\text{in}}((-\omega_l,\omega_l)) = \bigcap_{\left|\omega_\Delta^{\text{free}}\right|<\omega_l} D_{\text{lock}-\text{in}}(\omega_\Delta^{\text{free}})$$

contains all corresponding equilibria $\left(\theta^s_{eq}, x_{eq}(\omega_\Delta^{\text{free}})\right)$.

For model (5) each lock-in domain from intersection $\bigcap_{\left|\omega_\Delta^{\text{free}}\right|<\omega_l} D_{\text{lock}-\text{in}}(\omega_\Delta^{\text{free}})$ is bounded by the separatrices of saddle equilibria $\left(\theta^u_{eq}, x_{eq}(\omega_\Delta^{\text{free}})\right)$ and vertical lines $\theta_\Delta = \theta^s_{eq} \pm 2\pi$. Thus, the behavior of separatrices on the phase plane is the key to the lock-in range study (see Fig. 4).

4. Phase plane analysis for the lock-in range estimation

Consider an approach to the lock-in range computation of (5), based on the phase plane analysis. To compute the lock-in range of (5) we need to consider the behavior of the lower separatrix $Q(\theta_\Delta,\omega_\Delta^{\text{free}})$, which tends to the saddle point $\left(\theta^u_{eq}, x_{eq}(\omega_\Delta^{\text{free}})\right) = \left(\pi, \frac{\omega_\Delta^{\text{free}}\tau_1}{K_0}\right)$ as $t \to +\infty$ (by the symmetry of the lower and the upper half-planes, the consideration of the upper separatrix is also possible).

The parameter $\omega_\Delta^{\text{free}}$ shifts the phase plane vertically. To check this, we use a linear transformation $x \to x + \frac{\omega_\Delta^{\text{free}}\tau_1}{K_0}$. Thus, to compute the lock-in range of (5), we need to find $\omega_\Delta^{\text{free}} = \omega_l$ (where ω_l is called a lock-in frequency) such that (see Fig. 4)

$$x_{eq}(-\omega_l) = Q(\theta^s_{eq},\omega_l). \tag{6}$$

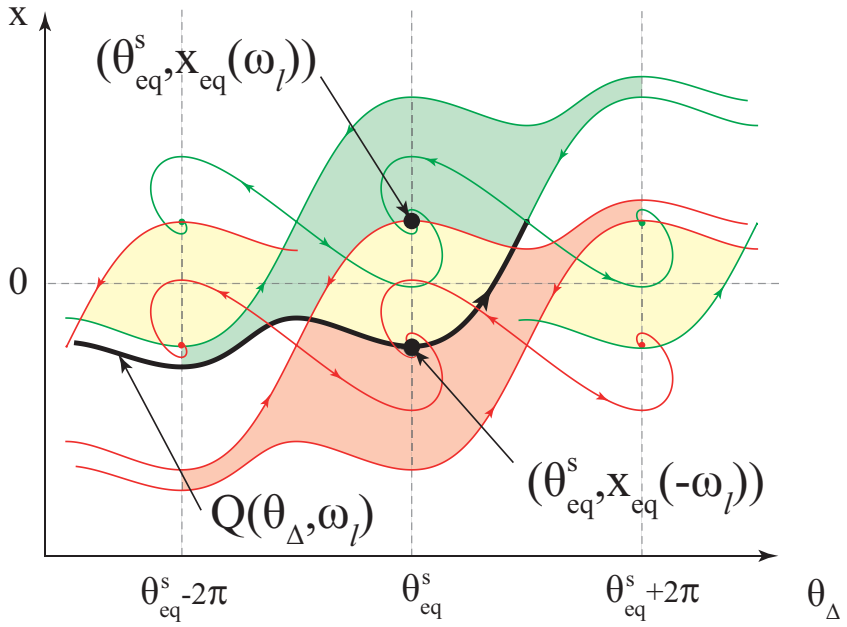

Figure 4: The domain $D_{\text{lock-in}}((-\omega_l,\omega_l))$ of (5).

By (6), we obtain an exact formula for the lock-in frequency ω_l:

$$-\frac{\omega_l}{K_0/\tau_1} = \frac{\omega_l}{K_0/\tau_1} + Q(\theta^s_{eq}, 0).$$
$$\omega_l = -\frac{K_0 Q(\theta^s_{eq}, 0)}{2\tau_1}, \tag{7}$$

Numerical simulations are used to compute the lock-in range of (5) applying (7). The separatrix $Q(\theta_\Delta,0)$ is numerically integrated and the corresponding ω_l is approximated. The obtained numerical results can be illustrated by a diagram (see Fig. 5)[1].

Note that (5) depends on the value of two coefficients $\frac{K_0}{\tau_1}$ and τ_2. In Fig. 5, choosing X-axis as $\frac{K_0}{\tau_1}$, we can plot a single curve for every fixed value of τ_2. The results of numerical simulations show that for sufficiently large $\frac{K_0}{\tau_1}$, the value of ω_l grows almost proportionally to $\frac{K_0}{\tau_1}$. Hence, $\frac{\omega_l \tau_1}{K_0}$ is almost constant for sufficiently large $\frac{K_0}{\tau_1}$ and in Fig. 5 the Y-axis can be chosen as $\frac{\omega_\Delta^{\text{free}} \tau_1}{K_0}$.

To obtain the lock-in frequency ω_l for fixed τ_1, τ_2, and K_0 using Fig. 5, we consider the curve corresponding to the chosen τ_2. Next, for X-value equal $\frac{K_0}{\tau_1}$ we get the Y-value of the curve. Finally, we multiply the Y-value by $\frac{K_0}{\tau_1}$ (see Fig. 6).

Consider an analytical approach to the lock-in range estimation. Main stages of the approach are presented in Subsection 4.1.

[1]These results submitted to IFAC PSYCO 2016

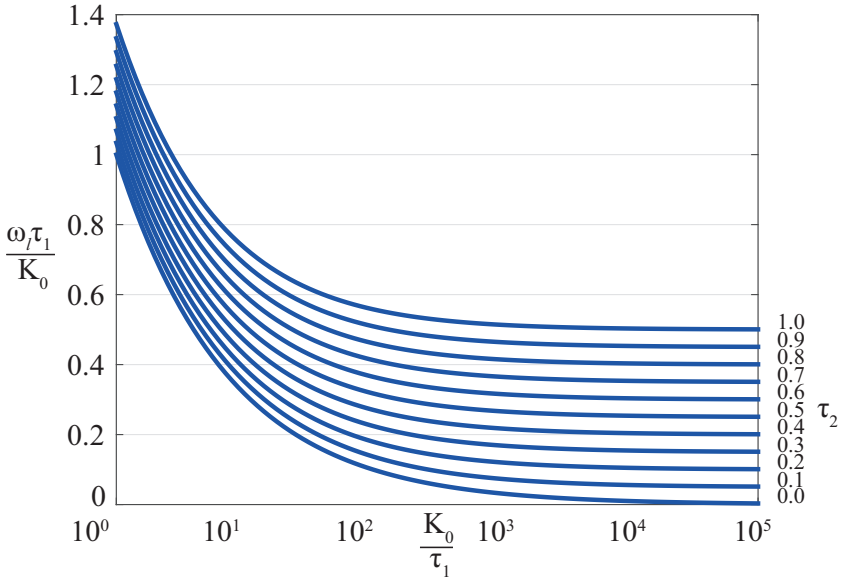

Figure 5: Values of $\frac{\omega_l}{K_0/\tau_1}$ for various K_0, τ_1, τ_2.

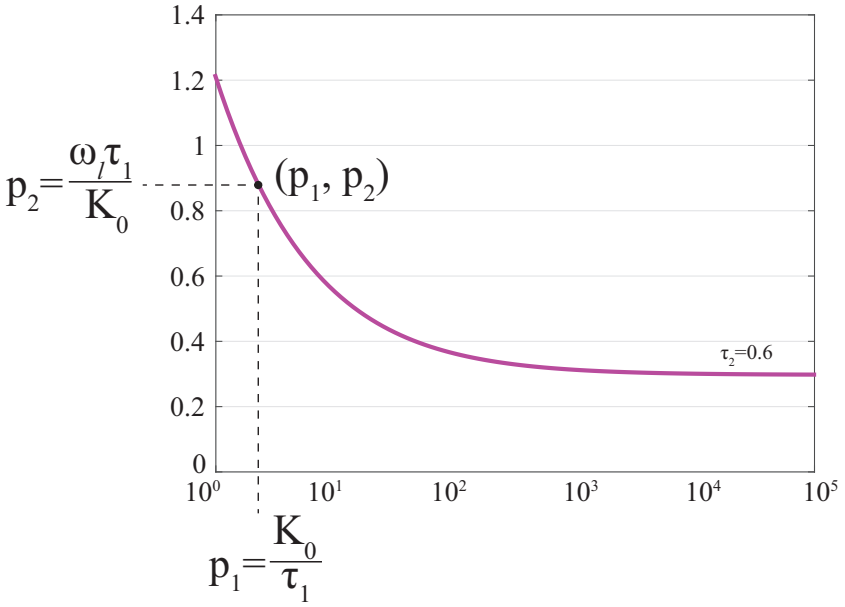

Figure 6: The lock-in frequency calculation: $\omega_l = p_1 p_2$.

4.1. Analytical approach to the lock-in range estimation

Consider an active PI filter with small parameter $0 < \frac{\tau_2}{\tau_1} \ll 1$ (see, e.g., (Alexandrov et al., 2014)). The consideration of (5) with such active PI filter allows us to estimate the lower separatrix $Q(\theta_\Delta, 0)$ and the lock-in range. For this purpose the approximations of separatrix $Q(\theta_\Delta, 0)$ in interval $0 \le \theta_\Delta < \pi$ are used.

The separatrix $Q(\theta_\Delta, 0)$, which is a solution of (5), can be expanded in a Taylor series in variable τ_2/τ_1 (since the parameter τ_2/τ_1 is considered as a variable, the separatrix $Q(\theta_\Delta, 0) = Q(\theta_\Delta, 0, \tau_2/\tau_1)$ depends on it). The first-order approximation of the lower separatrix $Q(\theta_\Delta, 0, \tau_2/\tau_1)$ has the form

$$\hat{Q}_1(\theta_\Delta, 0, \tau_2/\tau_1) = -2\sqrt{K_0/\tau_1}\cos\frac{\theta_\Delta}{2} - \\ - \frac{\tau_2}{\tau_1}\frac{K_0\left(\frac{2}{3} - \sin\frac{\theta_\Delta}{2} - \frac{1}{3}\sin\frac{3\theta_\Delta}{2}\right)}{\cos\frac{\theta_\Delta}{2}}. \tag{8}$$

The second-order approximation of $Q(\theta_\Delta, 0, \tau_2/\tau_1)$ has the form

$$\hat{Q}_2(\theta_\Delta, 0, \tau_2/\tau_1) = -2\sqrt{K_0/\tau_1}\cos\frac{\theta_\Delta}{2} - \frac{\tau_2}{\tau_1}\frac{K_0\left(\frac{2}{3} - \sin\frac{\theta_\Delta}{2} - \frac{1}{3}\sin\frac{3\theta_\Delta}{2}\right)}{\cos\frac{\theta_\Delta}{2}} - \\ - \left(\frac{\tau_2}{\tau_1}\right)^2 \frac{K_0^2(6\frac{1}{2} - 4\ln 2)}{6\sqrt{K_0/\tau_1}\cos\frac{\theta_\Delta}{2}} + \frac{K_0^2\left(\frac{2}{3} - \sin\frac{\theta_\Delta}{2} - \frac{1}{3}\sin\frac{3\theta_\Delta}{2}\right)^2}{4\sqrt{K_0/\tau_1}\cos^3\frac{\theta_\Delta}{2}} + \\ + \left(\frac{\tau_2}{\tau_1}\right)^2 \frac{K_0^2\left(8\sin(\frac{\theta_\Delta}{2}) - 4\ln\left|\sin\frac{\theta_\Delta}{2} + 1\right|\right)}{6\sqrt{K_0/\tau_1}\cos\frac{\theta_\Delta}{2}} + \left(\frac{\tau_2}{\tau_1}\right)^2 \frac{K_0^2\left(\frac{1}{2}\cos 2\theta_\Delta + 2\cos\theta_\Delta\right)}{6\sqrt{K_0/\tau_1}\cos\frac{\theta_\Delta}{2}}. \tag{9}$$

For approximations (8), (9) of separatrix $Q(\theta_\Delta, 0, \tau_2/\tau_1)$ the following relations are valid:

$$Q(\theta_\Delta, 0, \tau_2/\tau_1) = \hat{Q}_1(\theta_\Delta, 0, \tau_2/\tau_1) + O\left((\tau_2/\tau_1)^2\right),$$
$$Q(\theta_\Delta, 0, \tau_2/\tau_1) = \hat{Q}_2(\theta_\Delta, 0, \tau_2/\tau_1) + O\left((\tau_2/\tau_1)^3\right).$$

For $\theta_\Delta = \theta^s_{eq}$ the relations (8), (9) take the following values:

$$\hat{Q}_1(\theta^s_{eq}, 0, \tau_2/\tau_1) = -2\sqrt{K_0/\tau_1} - \frac{2K_0\tau_2}{3\tau_1},$$
$$\hat{Q}_2(\theta^s_{eq}, 0, \tau_2/\tau_1) = -2\sqrt{K_0/\tau_1} - \frac{2K_0\tau_2}{3\tau_1} - \\ - \frac{K_0\tau_2^2(5 - 6\ln 2)}{9\tau_1}\sqrt{K_0/\tau_1}.$$

Using relation (7) the lock-in frequency ω_l is approximated as follows:

$$\omega_l = \frac{K_0\sqrt{K_0/\tau_1}}{\tau_1} + \frac{K_0^2\tau_2}{3\tau_1^2} + O\left((\tau_2/\tau_1)^2\right), \tag{10}$$

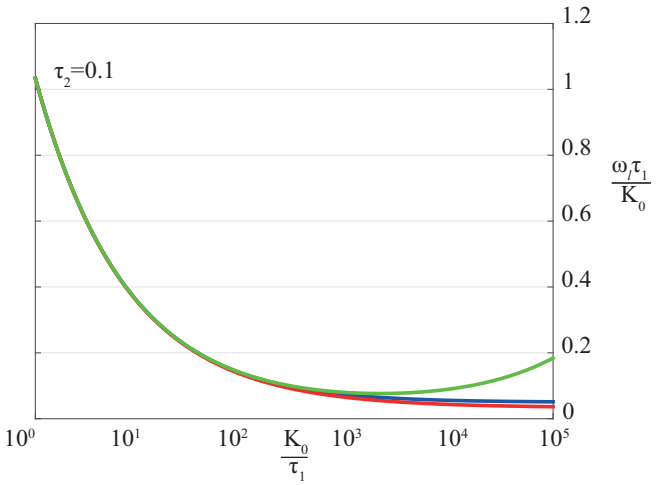

Figure 7: Estimates on $\frac{\omega_l}{K_0/\tau_1}$ for various K_0, τ_1.

$$\omega_l = \frac{K_0\sqrt{K_0/\tau_1}}{\tau_1} + \frac{K_0^2\tau_2}{3\tau_1^2} + \\ + \frac{K_0^2\tau_2^2(5-6\ln 2)}{18\tau_1^2}\sqrt{K_0/\tau_1} + O\left((\tau_2/\tau_1)^3\right). \tag{11}$$

For fixed $\tau_2 = 0.1$ the three curves are shown in Fig. 7. The values of ω_l (the blue curve, which is obtained numerically using relation (7)) are estimated from below by (10) and from above by (11) (the red and green curves correspondingly). Since the lock-in frequency ω_l is approximated under the condition of small parameter τ_2/τ_1, the estimates (10) and (11) give less precise result in the case of large K_0/τ_1.

4.2. The pull-out frequency and lock-in range

An another characteristic related to the cycle slipping effect is the pull-out frequency ω_{po} (see, e.g., (Gardner, 1979; Stensby, 1997; Kroupa, 2003). In (Gardner, 2005) the pull-out frequency is defined as a frequency-step limit, *"below which the loop does not skip cycles but remains in lock"*. However, in general case of Filter (see, e.g., (Pinheiro and Piqueira, 2014; Banerjee and Sarkar, 2008)) the pull-out frequency may depend on the value of $\omega_\Delta^{\text{free}}$.

However, in the case of active PI filter, the pull-out frequency can be defined and approximated (see, e.g., (Gardner, 1979; Huque and Stensby, 2013)), since the parameter $\omega_\Delta^{\text{free}}$ only shifts the phase plane vertically. The pull-out frequency can be found as follows (see Fig. 8):

$$x_{eq}(\omega_\Delta^{\text{free}}) = Q(\theta_{eq}^s, \omega_\Delta^{\text{free}} + \omega_{po}), \\ \frac{\omega_\Delta^{\text{free}}}{K_0/\tau_1} = \frac{\omega_\Delta^{\text{free}} + \omega_{po}}{K_0/\tau_1} + Q(\theta_{eq}^s, 0). \\ \omega_{po} = -\frac{K_0 Q(\theta_{eq}^s, 0)}{\tau_1} = 2\omega_l. \tag{12}$$

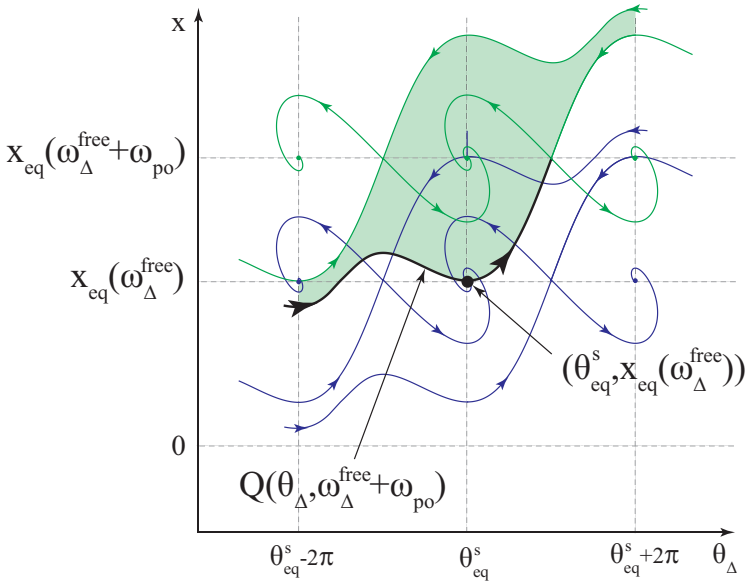

Figure 8: The frequency step of (5) equals to pull-out frequency ω_{po}.

In Fig. 9 the estimates from (Gardner, 1979; Huque and Stensby, 2013) are compared with estimates based on (10) and (11). The pull-out frequency estimate, which is obtained according to Fig. 5 and (12), is drawn in blue color. Analytical estimates based on (10), (11), and (12) are drawn in red and green colors correspondingly. The black curve is the estimate of the pull-out frequency from (Huque and Stensby, 2013). The dashed curve corresponds to the empirical estimate

$$\omega_{po} \approx 1.85 \left(\frac{1}{2} + \frac{\tau_1}{K_0 \tau_2^2} \right), \tag{13}$$

presented in (Gardner, 1979).

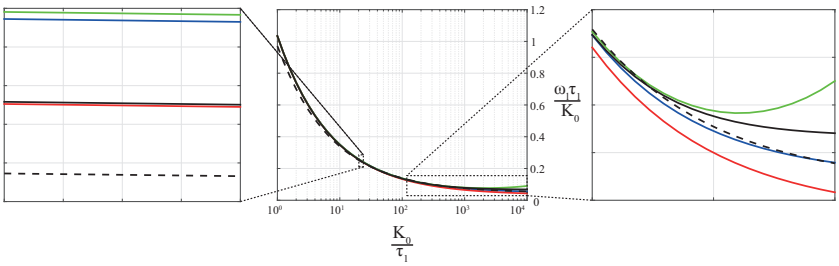

Figure 9: Comparison of the pull-out frequency estimates.

For K_0/τ_1 not very large the relation (11) is the most precise estimate compared to the presented ones.

5. Conclusion

In the present work models of the PLL-based circuits in the signal's phase space are described. The lock-in range of PLL-based circuits with sinusoidal PD characteristic and active PI filter is considered. The rigorous definition of the lock-in range is discussed, and relation (7) for the lock-in range computation is derived. For the lock-in range estimation two approaches – numerical and analytical – are presented. The methods are based on the integration of phase trajectories. In Subsection 4.1 the numerical estimates are verified by analytical estimates, which are obtained under the condition of small parameter.

Appendix A. The lock-in range estimation for small parameter of the loop filter.

Let us write out (5) in a different form with $a = \frac{\tau_2}{\tau_1}$ and $b = \frac{1}{\tau_1}$:

$$\begin{cases} \dot{x} = \sin(\theta_\Delta), \\ \dot{\theta}_\Delta = \omega_\Delta^{\text{free}} - bK_0 x - aK_0 \sin(\theta_\Delta). \end{cases} \tag{A.1}$$

Consider the following system, which is equivalent to (A.1):

$$\begin{cases} \dot{\theta}_\Delta = y, \\ \dot{y} = -aK_0 \cos(\theta_\Delta) y - bK_0 \sin(\theta_\Delta), \end{cases} \tag{A.2}$$

where $y = \omega_\Delta^{\text{free}} - bK_0 x - aK_0 \sin(\theta_\Delta)$.

In virtue of 2π-periodicity of (A.2) in variable θ_Δ, phase trajectories of (A.2) coincides for each interval $\theta_\Delta \in (-\pi + 2\pi k, \pi + 2\pi k]$, $k \in \mathbb{Z}$. Thus, one can study (A.2) in interval $\theta_\Delta \in (-\pi, \pi]$ only.

Let us find equilibria of (A.2) from the following system of equations:

$$\begin{cases} \sin(\theta_{eq}) = 0, \\ aK_0 \cos(\theta_{eq}) y_{eq} = 0. \end{cases}$$

In interval $\theta_\Delta \in (-\pi, \pi]$ there exist two equilibria $\left(\theta_{eq}^s, y_{eq}\right) = (0;0)$ and $\left(\theta_{eq}^u, y_{eq}\right) = (\pi;0)$. To define type of the equilibria points let us write out corresponding characteristic polynomials and find the eigenvalues:

$$\text{equilibrium } (0;0): \qquad \lambda^2 + aK_0\lambda + bK_0 = 0;$$

$$\begin{aligned} &\lambda_{1,2} = \tfrac{-aK_0 \pm \sqrt{(aK_0)^2 - 4bK_0}}{2}, && (aK_0)^2 - 4bK_0 > 0; \\ &\lambda_1 = \lambda_2 = \tfrac{-aK_0}{2}, && (aK_0)^2 - 4bK_0 = 0; \\ &\lambda_{1,2} = \tfrac{-aK_0 \pm i\sqrt{4bK_0 - (aK_0)^2}}{2}, && (aK_0)^2 - 4bK_0 < 0; \end{aligned}$$

$$\text{equilibrium } (\pi;0): \qquad \lambda^2 - aK_0\lambda - bK_0 = 0;$$

$$\lambda_{1,2} = \tfrac{aK_0 \pm \sqrt{(aK_0)^2 + 4bK_0}}{2}.$$

Thus, equilibrium $\left(\theta_{eq}^s, y_{eq}\right)$ is a stable node, a stable degenerated node, or a stable focus (that depends on the sign of $(aK_0)^2 - 4bK_0$). Equilibrium $\left(\theta_{eq}^u, y_{eq}\right)$ is a saddle point for

all $a>0$, $b>0$, $K_0>0$. Moreover, in virtue of periodicity each equilibrium $\left(\theta^u_{eq}+2\pi k, y_{eq}\right)$ is a saddle point, and each equilibrium $\left(\theta^s_{eq}+2\pi k, y_{eq}\right)$ is a stable equilibrium of the same type as $\left(\theta^s_{eq}, y_{eq}\right)$. Note also that equilibria (θ_{eq}, y_{eq}) of (A.2) and corresponding equilibria (θ_{eq}, x_{eq}) of (A.1) are of the same type, and related as follows:

$$(\theta_{eq}, y_{eq}) = \left(\theta_{eq}, \omega_\Delta^{\text{free}} - bK_0 x_{eq}\right).$$

Let us consider the following differential equation:

$$y'(\theta_\Delta) = -\frac{aK_0\cos(\theta_\Delta)y(\theta_\Delta) + bK_0\sin(\theta_\Delta)}{y(\theta_\Delta)}. \tag{A.3}$$

The right side of equation (A.3) is discontinuous in each point of line $y=0$. This line is an isocline line of vertical angular inclination of (A.3) (Barbashin and Tabueva, 1969). Equation (A.3) is equivalent to (A.2) in the upper and the lower open half planes of the phase plane.

Let the solutions $y(\theta_\Delta, a)$ of equation (A.3) be considered as functions of two variables θ_Δ, a. Consider the solution of differential equation (A.3), which range of values lies in the upper open half plane of its phase plane. Right side of equation (A.3) in the upper open half plane is function of class C^m for m arbitrary large. Solutions of the Cauchy problem with initial conditions $x=x_0$, $y=y_0$ (which solutions are on the upper half plane) are also of class C^m on their domain of existence for m arbitrary large (Hartman, 1964).

Let us study the separatrix $S(\theta_\Delta, a)$ in interval $[0,\pi)$, which tends to saddle point $(\theta^u_{eq}; x_{eq}) = (\pi; 0)$ and is situated in its second quadrant. Separatrix $S(\theta_\Delta, a)$ is the solution of the corresponding Cauchy problem for equation (A.3). The separatrix $S(\theta_\Delta, a)$ is of class C^m on its domain of existence for m arbitrary large.

Consider separatrix $S(\theta_\Delta, a)$ as a Taylor series in variable a in the neighborhood of $a_0 = 0$:

$$S(\theta_\Delta, a) = S(\theta_\Delta, 0) + a\frac{\partial S(\theta_\Delta, a)}{\partial a}\Big|_{a=0} + \cdots + \frac{a^n}{n!}\frac{\partial^n S(\theta_\Delta, a)}{\partial a^n}\Big|_{a=0} + \ldots. \tag{A.4}$$

Let us denote

$$\begin{aligned} &S_0(\theta_\Delta) = S(\theta_\Delta, 0), \\ &S_i(\theta_\Delta) = \frac{1}{i!}\frac{\partial^i S(\theta_\Delta, a)}{\partial a^i}\Big|_{a=0}, \quad i \geq 1. \end{aligned}$$

$\hat{S}_n(\theta_\Delta, a)$ as the n-th approximation of $S(\theta_\Delta, a)$ in variable a:

$$\hat{S}_n(\theta_\Delta, a) = S(\theta_\Delta, 0) + \sum_{i=1}^{n} a^i S_i(\theta_\Delta).$$

The Taylor remainder is denoted as follows:

$$\tilde{S}_n(\theta_\Delta, a) = \sum_{i=n+1}^{+\infty} a^i S_i(\theta_\Delta). \tag{A.5}$$

For the convergent Taylor series its remainder $\tilde{S}_n(\theta_\Delta, a) = O(a^{n+1})$ for each point x_0 of interval $[0,\pi)$.

Separatrix $S(\theta_\Delta, a)$ satisfies the following relation, which follows from (A.3):

$$S(\theta_\Delta,a)S'(\theta_\Delta,a) = -aK_0\cos(\theta_\Delta)S(\theta_\Delta,a) - bK_0\sin(\theta_\Delta).$$

$$\int_{\theta_\Delta}^{\pi} S(s,a)dS(s,a) = -aK_0\int_{\theta_\Delta}^{\pi}\cos(s)S(s,a)ds - bK_0\int_{\theta_\Delta}^{\pi}\sin(s)ds.$$

$$\frac{1}{2}\lim_{s\to\pi-0}S^2(s,a) - \frac{1}{2}S^2(\theta_\Delta,a) = -aK_0\int_{\theta_\Delta}^{\pi}\cos(s)S(s,a)ds - bK_0\int_{\theta_\Delta}^{\pi}\sin(s)ds. \tag{A.6}$$

Let us represent $S(\theta_\Delta, a)$ as Taylor series (A.4) in relation (A.6).

$$-\frac{1}{2}\left(S_0(\theta_\Delta) + aS_1(\theta_\Delta) + a^2S_2(\theta_\Delta) + \tilde{S}_2(\theta_\Delta,a)\right)^2 = -bK_0\int_{\theta_\Delta}^{\pi}\sin(s)ds -$$

$$-aK_0\int_{\theta_\Delta}^{\pi}\cos(s)\left(S_0(s) + S_1(s) + S_2(s) + \tilde{S}_2(s,a)\right)ds.$$

$$-\frac{1}{2}S_0^2(\theta_\Delta) - aS_0(\theta_\Delta)S_1(\theta_\Delta) - \frac{1}{2}a^2S_1^2(\theta_\Delta) - a^2S_0(\theta_\Delta)S_2(\theta_\Delta) + O(a^3) =$$

$$-bK_0\int_{\theta_\Delta}^{\pi}\sin(s)ds - aK_0\int_{\theta_\Delta}^{\pi}\cos(s)S_0(s) - a^2K_0\int_{\theta_\Delta}^{\pi}\cos(s)S_1(s)ds - O(a^3).$$

$$-\frac{1}{2}S_0^2(\theta_\Delta) - aS_0(\theta_\Delta)S_1(\theta_\Delta) - a^2\left(\frac{1}{2}S_1^2(\theta_\Delta) + S_0(\theta_\Delta)S_2(\theta_\Delta)\right) + O(a^3) =$$

$$-bK_0\int_{\theta_\Delta}^{\pi}\sin(s)ds - aK_0\int_{\theta_\Delta}^{\pi}\cos(s)S_0(s) - a^2K_0\int_{\theta_\Delta}^{\pi}\cos(s)S_1(s)ds + O(a^3). \tag{A.7}$$

Let us write out the corresponding members of (A.7) for each a^n, $n = 0, 1, 2$.
For a^0:

$$\frac{1}{2}S_0^2(\theta_\Delta) = bK_0\int_{\theta_\Delta}^{\pi}\sin(s)ds. \tag{A.8}$$

For a^1:

$$S_0(\theta_\Delta)S_1(\theta_\Delta) = K_0\int_{\theta_\Delta}^{\pi}\cos(s)S_0(s)ds. \tag{A.9}$$

For a^2:

$$S_0(\theta_\Delta)S_2(\theta_\Delta) + \frac{1}{2}S_1^2(\theta_\Delta) = K_0\int_{\theta_\Delta}^{\pi}\cos(s)S_1(s)ds. \tag{A.10}$$

Let us consequently find $S_0(\theta_\Delta)$, $S_1(\theta_\Delta)$, $S_2(\theta_\Delta)$ using relations (A.8), (A.9) and (A.10). Begin with evaluation of $S_0(\theta_\Delta)$:

$$\frac{1}{2}S_0^2(\theta_\Delta) = bK_0\int_{\theta_\Delta}^{\pi}\sin(s)ds = -bK_0\cos(s)\Big|_x^{\pi}ds =$$

$$= bK_0(1+\cos(\theta_\Delta)).$$

$$S_0(\theta_\Delta) = \sqrt{2bK_0(1+\cos(\theta_\Delta))}. \tag{A.11}$$

According to (A.11)

$$S_0(0) = 2\sqrt{bK_0}. \tag{A.12}$$

Using equation (A.9) and relations (A.11) evaluate $S_1(\theta_\Delta)$:

$$S_1(\theta_\Delta) = \frac{K_0 \int\limits_{\theta_\Delta}^{\pi} \cos(s) S_0(s) ds}{S_0(\theta_\Delta)}.$$

$$S_1(\theta_\Delta) = \frac{K_0\sqrt{2bK_0} \int\limits_{\theta_\Delta}^{\pi} \cos(s)\sqrt{(1+\cos(s))} ds}{\sqrt{2bK_0(1+\cos(\theta_\Delta))}}.$$

Let us evaluate the integral

$$\int\limits_{\theta_\Delta}^{\pi} \cos(s)\sqrt{(1+\cos(s))} ds$$

in the interval $\theta_\Delta \in [0;\pi)$ using the following substitutions:

$$u = 1+\cos(s), du = -\sin(s)ds$$
$$v = \sqrt{2-u}, dv = -\frac{du}{2\sqrt{2-u}}.$$

$$\int\limits_{\theta_\Delta}^{\pi} \cos(s)\sqrt{(1+\cos(s))} ds = \int\limits_{\theta_\Delta}^{\pi} \frac{\cos(s)\sin(s)}{\sqrt{(1-\cos(s))}} ds =$$
$$= -\int\limits_{1+\cos(\theta_\Delta)}^{0} \frac{u-1}{\sqrt{2-u}} du = 2\int\limits_{\sqrt{1-\cos(\theta_\Delta)}}^{\sqrt{2}} (1-v^2) dv =$$
$$= 2\left(\sqrt{2} - \sqrt{1-\cos(\theta_\Delta)}\right) - \frac{2}{3}\left(2\sqrt{2} - \sqrt{1-\cos(\theta_\Delta)}^{3}\right) =$$
$$= -\frac{2}{3}(2+\cos(\theta_\Delta))\sqrt{1-\cos(\theta_\Delta)} + \frac{2\sqrt{2}}{3}.$$

Hence, an expression for $S_1(\theta_\Delta)$ in interval $\theta_\Delta \in [0;\pi)$ is obtained:

$$S_1(\theta_\Delta) = \frac{K_0\sqrt{2bK_0}\left(\frac{2\sqrt{2}}{3} - \frac{2}{3}(2+\cos(\theta_\Delta))\sqrt{1-\cos(\theta_\Delta)}\right)}{\sqrt{2bK_0(1+\cos(\theta_\Delta))}}. \tag{A.13}$$

Moreover,

$$S_1(0) = \frac{2K_0}{3}. \tag{A.14}$$

To shorten the further evaluation of $S_2(\theta_\Delta)$, write out $S_1(\theta_\Delta)$ in equivalent form (in interval $\theta_\Delta \in [0;\pi)$).

$$S_1(\theta_\Delta) = \frac{K_0\sqrt{2bK_0}\left(\frac{2\sqrt{2}}{3} - \frac{2}{3}(2+\cos(\theta_\Delta))\sqrt{1-\cos(\theta_\Delta)}\right)}{\sqrt{2bK_0(1+\cos(\theta_\Delta))}} =$$

$$= \frac{K_0\sqrt{2bK_0}\left(\frac{2\sqrt{2}}{3} - \frac{2}{3}(2+\cos\theta_\Delta)\sqrt{2}\sin\frac{\theta_\Delta}{2}\right)}{\sqrt{2bK_0}\sqrt{2}\cos\frac{\theta_\Delta}{2}} = \frac{K_0\left(\frac{2}{3} - \frac{2}{3}(2+\cos\theta_\Delta)\sin\frac{\theta_\Delta}{2}\right)}{\cos\frac{\theta_\Delta}{2}} =$$

$$= \frac{K_0\left(\frac{2}{3} - \frac{2}{3}(3-2\sin^2\frac{\theta_\Delta}{2})\sin\frac{\theta_\Delta}{2}\right)}{\cos\frac{\theta_\Delta}{2}} = \frac{K_0\left(\frac{2}{3} - 2\sin\frac{\theta_\Delta}{2} - \frac{4}{3}\sin^3\frac{\theta_\Delta}{2}\right)}{\cos\frac{\theta_\Delta}{2}} =$$

$$= \frac{K_0\left(\frac{2}{3} - \sin\frac{\theta_\Delta}{2} - \frac{1}{3}\sin\frac{3\theta_\Delta}{2}\right)}{\cos\frac{\theta_\Delta}{2}}.$$

Let us evaluate $S_2(\theta_\Delta)$ using (A.10), (A.11) and (A.13).

$$S_2(\theta_\Delta) = \frac{K_0\int\limits_{\theta_\Delta}^{\pi}\cos(s)S_1(s)ds - \frac{1}{2}S_1^2(\theta_\Delta)}{S_0(\theta_\Delta)} =$$
$$= \frac{K_0^2\int\limits_{\theta_\Delta}^{\pi}\frac{\cos(s)\left(\frac{2}{3}-\sin\frac{s}{2}-\frac{1}{3}\sin\frac{3s}{2}\right)}{\cos\frac{s}{2}}ds}{2\sqrt{bK_0}\cos\frac{\theta_\Delta}{2}} - \frac{K_0^2\left(\frac{2}{3} - \sin\frac{\theta_\Delta}{2} - \frac{1}{3}\sin\frac{3\theta_\Delta}{2}\right)^2}{4\sqrt{bK_0}\cos^3\frac{\theta_\Delta}{2}}.$$

Evaluate the integral $\int\limits_{\theta_\Delta}^{\pi}\frac{\cos(s)\left(\frac{2}{3} - \sin\frac{s}{2} - \frac{1}{3}\sin\frac{3s}{2}\right)}{\cos\frac{s}{2}}ds$:

I

$$\int\limits_{\theta_\Delta}^{\pi}\frac{2}{3}\frac{\cos(s)}{\cos\frac{s}{2}}ds = \frac{2}{3}\int\limits_{\theta_\Delta}^{\pi}\frac{2\cos^2(\frac{s}{2})-1}{\cos\frac{s}{2}}ds = \frac{2}{3}\int\limits_{\theta_\Delta}^{\pi}\left(2\cos\frac{s}{2} - \frac{1}{\cos\frac{s}{2}}\right)ds =$$
$$= \frac{8}{3}\left(\sin(\frac{s}{2})\right)\Big|_x^\pi - \frac{2}{3}\int\limits_{\theta_\Delta}^{\pi}\frac{1}{\cos\frac{s}{2}}ds =$$

$$u = \frac{s}{2}; \quad du = \frac{1}{2}ds$$

$$= \frac{8}{3}\left(\sin(\frac{s}{2})\right)\Big|_x^\pi - \frac{4}{3}\int\limits_{\frac{\theta_\Delta}{2}}^{\frac{\pi}{2}}\frac{1}{\cos u}du = \left(\frac{8}{3}\sin(\frac{s}{2}) - \frac{4}{3}\ln\left|\operatorname{tg}\frac{s}{2} + \frac{1}{\cos\frac{s}{2}}\right|\right)\Big|_x^\pi.$$

II

$$-\int\limits_{\theta_\Delta}^{\pi}\frac{\cos(s)\left(\sin\frac{s}{2} + \frac{1}{3}\sin\frac{3s}{2}\right)}{\cos\frac{s}{2}}ds = -\int\limits_{\theta_\Delta}^{\pi}\frac{\cos(s)\left(\sin\frac{s}{2} + \frac{1}{3}\left(3\sin\frac{s}{2} - 4\sin^3\frac{s}{2}\right)\right)}{\cos\frac{s}{2}}ds =$$
$$-\int\limits_{\theta_\Delta}^{\pi}\frac{\cos(s)\left(2\sin\frac{s}{2} - \frac{4}{3}\sin^3\frac{s}{2}\right)}{\cos\frac{s}{2}}ds = -2\int\limits_{\theta_\Delta}^{\pi}\frac{\cos(s)\sin\frac{s}{2}\cos\frac{s}{2}\left(1 - \frac{2}{3}\sin^2\frac{s}{2}\right)}{\cos^2\frac{s}{2}}ds =$$
$$-2\int\limits_{\theta_\Delta}^{\pi}\frac{\cos(s)\sin s\left(1 - \frac{2}{3}\sin^2\frac{s}{2}\right)}{\cos s + 1}ds = -\frac{2}{3}\int\limits_{\theta_\Delta}^{\pi}\frac{\cos(s)\sin s\,(2+\cos s)}{\cos s + 1}ds =$$

$$u=\cos s;\quad du=-\sin(s)ds$$

$$
\begin{aligned}
&=\frac{2}{3}\int\limits_{\cos(\theta_\Delta)}^{-1}\frac{u(2+u)}{u+1}du=\frac{2}{3}\int\limits_{\cos(\theta_\Delta)}^{\cos\pi}\left(u+1-\frac{1}{u+1}\right)du=\\
&=\frac{2}{3}\left(\frac{1}{2}\cos^2 s+\cos s-\ln\left|\cos s+1\right|\right)\Big|_x^\pi=\\
&=\frac{2}{3}\left(\frac{1}{2}\cos^2 s+\cos s-2\ln\left|\sqrt{2}\cos\frac{s}{2}\right|\right)\Big|_x^\pi=\\
&=\frac{2}{3}\left(\frac{1}{2}\cos^2 s+\cos s-2\ln\left|\cos\frac{s}{2}\right|\right)\Big|_x^\pi.
\end{aligned}
$$

I+II

$$
\begin{aligned}
&\left(\frac{8}{3}\sin(\frac{s}{2})-\frac{4}{3}\ln\left|\operatorname{tg}\frac{s}{2}+\frac{1}{\cos\frac{s}{2}}\right|\right)\Big|_x^\pi+\frac{2}{3}\left(\frac{1}{2}\cos^2 s+\cos s-2\ln\left|\cos\frac{s}{2}\right|\right)\Big|_x^\pi=\\
&\frac{1}{3}\left(8\sin(\frac{s}{2})-4\ln\left|\frac{\sin\frac{s}{2}+1}{\cos\frac{s}{2}}\right|+\cos^2 s+2\cos s-4\ln\left|\cos\frac{s}{2}\right|\right)\Big|_x^\pi=\\
&\frac{1}{3}\left(8\sin(\frac{s}{2})-4\ln\left|\sin\frac{s}{2}+1\right|+\frac{1}{2}\cos 2s+\frac{1}{2}+2\cos s\right)\Big|_x^\pi=\\
&=\frac{6\frac{1}{2}-4\ln 2}{3}-\frac{1}{3}\left(8\sin(\frac{\theta_\Delta}{2})-4\ln\left|\sin\frac{\theta_\Delta}{2}+1\right|+\frac{1}{2}\cos 2\theta_\Delta+2\cos\theta_\Delta\right).
\end{aligned}
$$

Hence,

$$
S_2(\theta_\Delta)=\frac{K_0^2(6\frac{1}{2}-4\ln 2)-K_0^2\left(8\sin(\frac{\theta_\Delta}{2})-4\ln\left|\sin\frac{\theta_\Delta}{2}+1\right|+\frac{1}{2}\cos 2\theta_\Delta+2\cos\theta_\Delta\right)}{6\sqrt{bK_0}\cos\frac{\theta_\Delta}{2}}- \tag{A.15}
$$

$$
-\frac{K_0^2\left(\frac{2}{3}-\sin\frac{\theta_\Delta}{2}-\frac{1}{3}\sin\frac{3\theta_\Delta}{2}\right)^2}{4\sqrt{bK_0}\cos^3\frac{\theta_\Delta}{2}}.
$$

In $\theta_\Delta=0$

$$
S_2(0)=\frac{2K_0^2(1-\ln 2)}{3\sqrt{bK_0}}-\frac{1K_0^2}{9\sqrt{bK_0}}=\frac{K_0^2(5-6\ln 2)}{9\sqrt{bK_0}}. \tag{A.16}
$$

Hence, $S_0(\theta_\Delta)$, $S_1(\theta_\Delta)$, $S_2(\theta_\Delta)$ are evaluated (equations (A.11), (A.13) and (A.15), correspondingly). I. e. the first and the second approximations $\hat{S}_1(\theta_\Delta,a)$, $\hat{S}_2(\theta_\Delta,a)$ of separatrix $S(\theta_\Delta,a)$ are found. Furthermore, using (A.12), (A.14) and (A.16) the following relations are valid:

$$
\begin{aligned}
&\hat{S}_1(0,a)=2\sqrt{bK_0}+a\frac{2K_0}{3},\\
&\hat{S}_2(0,a)=\hat{S}_2(0)=2\sqrt{bK_0}+a\frac{2K_0}{3}+a^2\frac{K_0(5-6\ln 2)}{9b}\sqrt{K_0 b}.
\end{aligned}
$$

ACKNOWLEDGEMENTS

This work was supported by the Russian Scientific Foundation and Saint-Petersburg State University. The authors would like to thank Roland E. Best, the founder of the Best Engineering Company, Oberwil, Switzerland and the author of the bestseller on PLL-based circuits Best (2007) for valuable discussion.

References

K.D. Alexandrov, N.V. Kuznetsov, G.A. Leonov, and S.M. Seledzhi. Best's conjecture on pull-in range of two-phase Costas loop. In *2014 6th International Congress on Ultra Modern Telecommunications and Control Systems and Workshops (ICUMT)*, volume 2015-January, pages 78–82. IEEE, 2014. doi: 10.1109/ICUMT.2014.7002082.

A. A. Andronov, E. A. Vitt, and S. E. Khaikin. *Theory of Oscillators (in Russian)*. ONTI NKTP SSSR, 1937. [English transl. 1966, Pergamon Press].

G. Ascheid and H. Meyr. Cycle slips in phase-locked loops: A tutorial survey. *Communications, IEEE Transactions on*, 30(10):2228–2241, 1982.

R.J. Baker. *CMOS: Circuit Design, Layout, and Simulation*. IEEE Press Series on Microelectronic Systems. Wiley-IEEE Press, 2011.

T. Banerjee and B.C. Sarkar. Chaos and bifurcation in a third-order digital phase-locked loop. *International Journal of Electronics and Communications*, (62):86–91, 2008.

E. A. Barbashin and V. A. Tabueva. *Dynamical systems with cylindrical phase space (in Russian)*. Nauka, Moscow, 1969.

L.N. Belyustina, V.V. Bykov, K.G. Kiveleva, and V.D. Shalfeev. On the size of pull-in range of pll with proportional-integrating filter. *Izv. vuzov. Radiofizika (in Russian)*, 13(4), 1970.

R.E. Best. *Phase-Lock Loops: Design, Simulation and Application*. McGraw-Hill, 6th edition, 2007.

R.E. Best, N.V. Kuznetsov, G.A. Leonov, M.V. Yuldashev, and R.V. Yuldashev. Simulation of analog Costas loop circuits. *International Journal of Automation and Computing*, 11(6):571–579, 2014. 10.1007/s11633-014-0846-x.

R.E. Best, N.V. Kuznetsov, O.A. Kuznetsova, G.A. Leonov, M.V. Yuldashev, and R.V. Yuldashev. A short survey on nonlinear models of the classic Costas loop: rigorous derivation and limitations of the classic analysis. In *Proceedings of the American Control Conference*, pages 1296–1302. IEEE, 2015. doi: 10.1109/ACC.2015.7170912. art. num. 7170912, http://arxiv.org/pdf/1505.04288v1.pdf.

O. B. Ershova and G. A. Leonov. Frequency estimates of the number of cycle slidings in phase control systems. *Avtomat. Remove Control*, 44(5):600–607, 1983.

F.M. Gardner. *Phase-lock techniques*. John Wiley & Sons, New York, 1966.

F.M. Gardner. *Phase-lock techniques*. John Wiley & Sons, New York, 2nd edition, 1979.

F.M. Gardner. *Phaselock Techniques*. Wiley, 3rd edition, 2005.

A.Kh. Gelig, G.A. Leonov, and V.A. Yakubovich. *Stability of Nonlinear Systems with Nonunique Equilibrium (in Russian)*. Nauka, 1978. (English transl: Stability of Stationary Sets in Control Systems with Discontinuous Nonlinearities, 2004, World Scientific).

S.J. Goldman. *Phase-Locked Loops Engineering Handbook for Integrated Circuits*. Artech House, 2007.

N. A. Gubar'. Investigation of a piecewise linear dynamical system with three parameters. *J. Appl. Math. Mech.*, 25(6):1011–1023, 1961.

P. Hartman. *Ordinary differential equations*. John Willey & Sons, New-York, 1964.

A. S. Huque and J. Stensby. An analytical approximation for the pull-out frequency of a pll employing a sinusoidal phase detector. *ETRI Journal*, 35(2):218–225, 2013.

M.V. Kapranov. Locking band for phase-locked loop. *Radiofizika (in Russian)*, 2(12): 37–52, 1956.

M. Kihara, S. Ono, and P. Eskelinen. *Digital Clocks for Synchronization and Communications*. Artech House, 2002.

V.F. Kroupa. *Phase Lock Loops and Frequency Synthesis*. John Wiley & Sons, 2003.

J. Kudrewicz and S. Wasowicz. *Equations of phase-locked loop. Dynamics on circle, torus and cylinder*. World Scientific, 2007.

N.V. Kuznetsov, O.A. Kuznetsova, G.A. Leonov, P. Neittaanmaki, M.V. Yuldashev, and R.V. Yuldashev. Limitations of the classical phase-locked loop analysis. *Proceedings - IEEE International Symposium on Circuits and Systems*, 2015-July:533–536, 2015a. doi: http://dx.doi.org/10.1109/ISCAS.2015.7168688.

N.V. Kuznetsov, G.A. Leonov, S.M. Seledzgi, M.V. Yuldashev, and R.V. Yuldashev. Elegant analytic computation of phase detector characteristic for non-sinusoidal signals. *IFAC-PapersOnLine*, 48(11):960–963, 2015b. doi: http://dx.doi.org/10.1016/j.ifacol.2015.09.316.

N.V. Kuznetsov, G.A. Leonov, M.V. Yuldashev, and R.V. Yuldashev. Rigorous mathematical definitions of the hold-in and pull-in ranges for phase-locked loops. *IFAC-PapersOnLine*, 48(11):710–713, 2015c. doi: http://dx.doi.org/10.1016/j.ifacol.2015.09.272.

G.A. Leonov and N.V. Kuznetsov. *Nonlinear Mathematical Models of Phase-Locked Loops. Stability and Oscillations*. Cambridge Scientific Publisher, 2014.

G.A. Leonov, N.V. Kuznetsov, M.V. Yuldahsev, and R.V. Yuldashev. Analytical method for computation of phase-detector characteristic. *IEEE Transactions on Circuits and Systems - II: Express Briefs*, 59(10):633–647, 2012. doi: 10.1109/TCSII.2012.2213362.

G.A. Leonov, N.V. Kuznetsov, M.V. Yuldashev, and R.V. Yuldashev. Nonlinear dynamical model of Costas loop and an approach to the analysis of its stability in the large. *Signal processing*, 108:124–135, 2015a. doi: 10.1016/j.sigpro.2014.08.033.

G.A. Leonov, N.V. Kuznetsov, M.V. Yuldashev, and R.V. Yuldashev. Hold-in, pull-in, and lock-in ranges of PLL circuits: rigorous mathematical definitions and limitations of classical theory. *IEEE Transactions on Circuits and Systems–I: Regular Papers*, 62 (10):2454–2464, 2015b. doi: http://dx.doi.org/10.1109/TCSI.2015.2476295.

A. M. Lyapunov. *The General Problem of the Stability of Motion (in Russian)*. Kharkov, 1892. [English transl. Academic Press, NY, 1966].

Y.A. Mitropolsky and N.N. Bogolubov. *Asymptotic Methods in the Theory of Non-Linear Oscillations*. Gordon and Breach, New York, 1961.

R.B. Pinheiro and J.R.C. Piqueira. Designing all-pole filters for high-frequency phase-locked loops. *Mathematical Problems in Engineering*, 2014, 2014. art. num. 682318.

A.M. Samoilenko and R. Petryshyn. *Multifrequency Oscillations of Nonlinear Systems*. Mathematics and Its Applications. Springer, 2004.

V.V. Shakhgil'dyan and A.A. Lyakhovkin. *Fazovaya avtopodstroika chastoty (in Russian)*. Svyaz', Moscow, 1966.

B.I. Shakhtarin. Study of a piecewise-linear system of phase-locked frequency control. *Radiotechnica and electronika (in Russian)*, (8):1415–1424, 1969.

V. Smirnova, A. Proskurnikov, and N. Utina. Problem of cycle-slipping for infinite dimensional systems with mimo nonlinearities. In *Ultra Modern Telecommunications and Control Systems and Workshops (ICUMT), 2014 6th International Congress on*, pages 590–595. IEEE, 2014.

J.L. Stensby. *Phase-Locked Loops: Theory and Applications*. Phase-locked Loops: Theory and Applications. Taylor & Francis, 1997.

F. Tricomi. Integrazione di unequazione differenziale presentatasi in elettrotechnica. *Annali della R. Shcuola Normale Superiore di Pisa*, 2(2):1–20, 1933.

A. Viterbi. *Principles of coherent communications*. McGraw-Hill, New York, 1966.

PII

THE LOCK-IN RANGE OF CLASSICAL PLL WITH IMPULSE SIGNALS AND PROPORTIONALLY-INTEGRATING FILTER

by

K. D. Aleksandrov, N. V. Kuznetsov, G. A. Leonov, M. V. Yuldashev,
R. V. Yuldashev 2016

arXiv:1603.09363

Lock-in range of classical PLL with impulse signals and proportionally-integrating filter

K. D. Aleksandrov, N.V. Kuznetsov, G. A. Leonov, M. V. Yuldashev, R. V. Yuldashev

Faculty of Mathematics and Mechanics, Saint-Petersburg State University, Russia

Dept. of Mathematical Information Technology, University of Jyväskylä, Finland

Institute of Problems of Mechanical Engineering RAS, Russia

Abstract

In the present work the model of PLL with impulse signals and active PI filter in the signal's phase space is described. For the considered PLL the lock-in range is computed analytically and obtained result are compared with numerical simulations.

Keywords: phase-locked loop, nonlinear analysis, PLL, two-phase PLL, lock-in range, Gardner's problem on unique lock-in frequency, pull-out frequency

1. Models of classical PLL with impulse signals

Consider a physical model of classical PLL in the signals space (see Fig. 1).

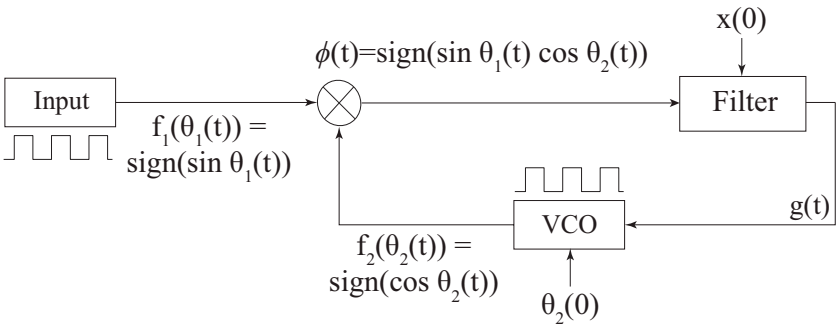

Figure 1: Model of PLL with impulse signals in the signals space.

This model contains the following blocks: a reference oscillator (Input), a voltage-controlled oscillator (VCO), a filter (Filter), and an analog multiplier as a phase detector (PD). The signals $\operatorname{sign}(\sin\theta_1(t))$ and $\operatorname{sign}(\cos\theta_2(t))$ of the Input and the VCO (here $\theta_2(0)$ is the initial phase of VCO) enter the multiplier block. The resulting impulse signal $\phi(t) = \operatorname{sign}(\sin\theta_1(t)\cos\theta_2(t))$ is filtered by low-pass filter Filter (here $x(0)$ is an initial state of Filter). The filtered signal $g(t)$ is used as a control signal for VCO.

The equations describing the model of PLL-based circuits in the signals space are difficult for the study, since that equations are nonautonomous (see, e.g., (Kudrewicz

Email address: nkuznetsov239@gmail.com (N.V. Kuznetsov)

and Wasowicz, 2007)). By contrast, the equations of model in the signal's phase space are autonomous (Gardner, 1966; Shakhgil'dyan and Lyakhovkin, 1966; Viterbi, 1966), what simplifies the study of PLL-based circuits. The application of averaging methods (Mitropolsky and Bogolubov, 1961; Samoilenko and Petryshyn, 2004) allows one to reduce the model of PLL-based circuits in the signals space to the model in the signal's phase space (see, e.g., (Leonov et al., 2012; Leonov and Kuznetsov, 2014; Leonov et al., 2015a; Kuznetsov et al., 2015b,a; Best et al., 2015).

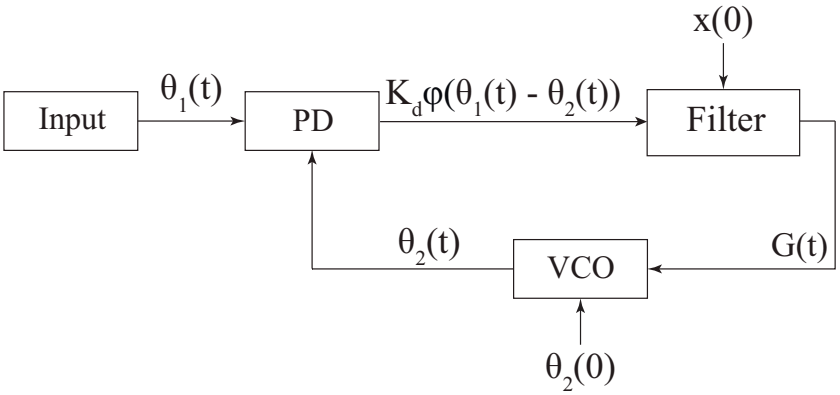

Figure 2: Model of the classical PLL in the signal's phase space.

The main difference between the physical model (Fig. 1) and the simplified mathematical model in the signal's phase space (Fig. 2) is the absence of high-frequency component of the phase detector output. The output of the phase detector in the signal's phase space is called a phase detector characteristic and has the form

$$K_d\varphi(\theta_1(t)-\theta_2(t)).$$

The maximum absolute value of PD output $K_d > 0$ is called a phase detector gain (see, e.g., (Best, 2007; Goldman, 2007)). The periodic function $\varphi(\theta_\Delta(t))$ depends on difference $\theta_1(t)-\theta_2(t)$ (which is called a phase error and denoted by $\theta_\Delta(t)$). The PD characteristic depends on the design of PLL-based circuit and the signal waveforms $f_1(\theta_1)$ of Input and $f_2(\theta_2)$ of VCO. For PLL with impulse signals the PD characteristic is as follows (see, e.g., (Viterbi, 1966; Gardner, 1966; Leonov et al., 2012)):

$$\begin{aligned} &K_d = 1; \\ &\varphi(\theta_\Delta(t)) = \begin{cases} \frac{2}{\pi}\theta_\Delta(t), & \text{if } -\frac{\pi}{2} \le \theta_\Delta(t) \le \frac{\pi}{2}, \\ -\frac{2}{\pi}\theta_\Delta(t)+2, & \text{if } \frac{\pi}{2} \le \theta_\Delta(t) \le \frac{3\pi}{2}. \end{cases} \end{aligned} \tag{1}$$

Let us describe a model of classical PLL with impulse signals in the signal's phase space (see Fig. 2). A reference oscillator and a voltage-controlled oscillator generate the phases $\theta_1(t)$ and $\theta_2(t)$, respectively. The frequency of reference signal usually assumed to be constant:

$$\dot{\theta}_1(t) = \omega_1. \tag{2}$$

The phases $\theta_1(t)$ and $\theta_2(t)$ enter the inputs of the phase detector. The output of phase detector is processed by Filter. Further we consider the active PI filter (see, e.g., (Baker,

2011)) with transfer function $W(s) = \frac{1+\tau_2 s}{\tau_1 s}$, $\tau_1 > 0$, $\tau_2 > 0$. The considered filter can be described as

$$\begin{cases} \dot{x}(t) = K_d \varphi(\theta_\Delta(t)), \\ G(t) = \frac{1}{\tau_1} x(t) + \frac{\tau_2}{\tau_1} K_d \varphi(\theta_\Delta(t)), \end{cases} \tag{3}$$

where $x(t)$ is the filter state.

The output of Filter $G(t)$ is used as a control signal for VCO:

$$\dot{\theta}_2(t) = \omega_2^{\text{free}} + K_v G(t), \tag{4}$$

where ω_2^{free} is the VCO free-running frequency and $K_v > 0$ is the VCO gain.

Relations (2), (3), and (4) result in autonomous system of differential equations

$$\begin{cases} \dot{x} = K_d \varphi(\theta_\Delta), \\ \dot{\theta}_\Delta = \omega_1 - \omega_2^{\text{free}} - \frac{K_v}{\tau_1} \left(x + \tau_2 K_d \varphi(\theta_\Delta) \right). \end{cases} \tag{5}$$

Denote the difference of the reference frequency and the VCO free-running frequency $\omega_1 - \omega_2^{\text{free}}$ by $\omega_\Delta^{\text{free}}$. By the linear transformation $x \to K_d x$ we have

$$\begin{cases} \dot{x} = \varphi(\theta_\Delta), \\ \dot{\theta}_\Delta = \omega_\Delta^{\text{free}} - \frac{K_0}{\tau_1} \left(x + \tau_2 \varphi(\theta_\Delta) \right), \end{cases} \tag{6}$$

where $K_0 = K_v K_d$ is the loop gain. Here (6) describes the model of PLL with the impulse signals and active PI filter in the signal's phase space.

By the transformation

$$\left(\omega_\Delta^{\text{free}}, x, \theta_\Delta \right) \to \left(-\omega_\Delta^{\text{free}}, -x, -\theta_\Delta \right),$$

(6) with odd PD characteristic (1) is not changed. This property allows one to use the concept of frequency deviation

$$\left| \omega_\Delta^{\text{free}} \right| = \left| \omega_1 - \omega_2^{\text{free}} \right|$$

and consider (6) with $\omega_\Delta^{\text{free}} > 0$ only.

The PLL state for which the VCO frequency is adjusted to the reference frequency of Input is called a locked state. The locked states of the PLL correspond to the locally asymptotically stable equilibria of (6), which can be found from the relations

$$\begin{cases} \varphi(\theta_{eq}) = 0, \\ \omega_\Delta^{\text{free}} - \frac{K_0}{\tau_1} x_{eq} = 0. \end{cases}$$

Since (6) is 2π-periodic in θ_Δ, we can consider (6) in a 2π-interval of θ_Δ, $\theta_\Delta \in (-\pi, \pi]$. In interval $\theta_\Delta \in (-\pi, \pi]$ there exist two equilibria:

$$\left(\theta_{eq}^s, x_{eq}(\omega_\Delta^{\text{free}}) \right) = (0, \frac{\omega_\Delta^{\text{free}} \tau_1}{K_0}) \text{ and } \left(\theta_{eq}^u, x_{eq}(\omega_\Delta^{\text{free}}) \right) = (\pi, \frac{\omega_\Delta^{\text{free}} \tau_1}{K_0}).$$

As is shown below (see Appendix A) the equilibria

$$\left(\theta_{eq}^s + 2\pi k, x_{eq}(\omega_\Delta^{\text{free}}) \right) = \left(2\pi k, \frac{\omega_\Delta^{\text{free}} \tau_1}{K_0} \right)$$

are locally asymptotically stable. Hence, the locked states of (6) are given by equilibria $\left(\theta^s_{eq}, x_{eq}(\omega^{\text{free}}_\Delta)\right)$. The remaining equilibria

$$\left(\theta^u_{eq} + 2\pi k, x_{eq}(\omega^{\text{free}}_\Delta)\right) = \left(\pi + 2\pi k, \frac{\omega^{\text{free}}_\Delta \tau_1}{K_0}\right)$$

are saddle equilibria (see Appendix A).

2. The lock-in range

The model of classical PLL with impulse signals and active PI filter in the signal's phase space is globally asymptotically stable (see, e.g., (Gubar', 1961; Leonov and Aleksandrov, 2015)). The PLL achieves locked state for any initial VCO phase $\theta_2(0)$ and filter state $x(0)$. So, there exist no limit cycles of the first kind, heteroclinic trajectories, and limit cycles of the second kind on the phase plane of (6) (see Fig. 3).

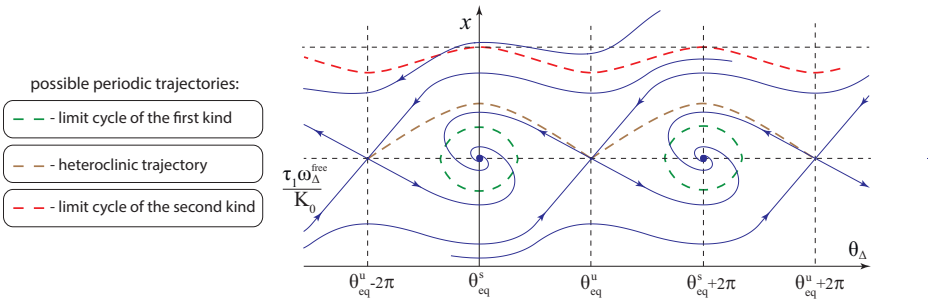

Figure 3: Possible periodic trajectories on the phase plane of (6).

However, the phase error θ_Δ may significantly increase during the acquisition process. In order to consider the property of the model to synchronize without undesired growth of the phase error θ_Δ, a lock-in range concept was introduced in (Gardner, 1966): "*If, for some reason, the frequency difference between input and VCO is less than the loop bandwidth, the loop will lock up almost instantaneously without slipping cycles. The maximum frequency difference for which this fast acquisition is possible is called the lock-in frequency*". The lock-in range concept is widely used in engineering literature on the PLL-based circuits study (see, e.g., (Stensby, 1997; Kihara et al., 2002; Kroupa, 2003; Gardner, 2005; Best, 2007)). It is said that a cycle slipping occurs if (see, e.g., (Ascheid and Meyr, 1982; Ershova and Leonov, 1983; Smirnova et al., 2014))

$$\limsup_{t\to+\infty} |\theta_\Delta(0) - \theta_\Delta(t)| \geq 2\pi.$$

However, in general, even for zero frequency deviation ($\omega^{\text{free}}_\Delta = 0$) and a sufficiently large initial state of filter ($x(0)$), cycle slipping may take place, thus in 1979 Gardner wrote: *"There is no natural way to define exactly any unique lock-in frequency"* and *"despite its vague reality, lock-in range is a useful concept"* (Gardner, 1979).

To overcome the stated problem, in (Kuznetsov et al., 2015c; Leonov et al., 2015b) the rigorous mathematical definition of a lock-in range is suggested:

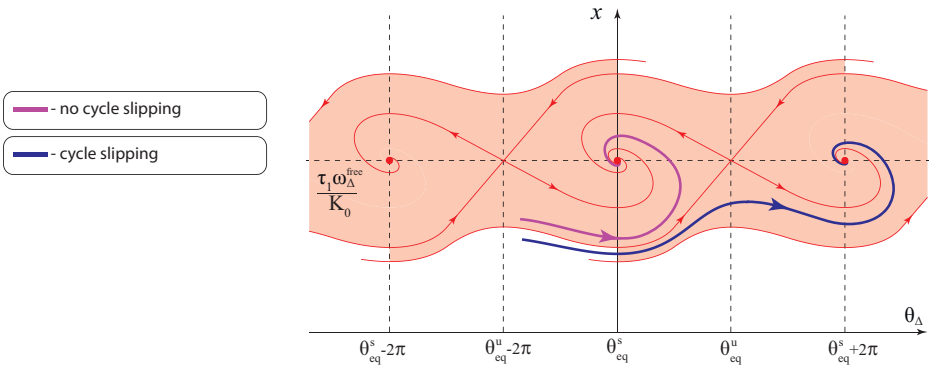

Figure 4: The lock-in domain and cycle slipping.

Definition 1. *(Kuznetsov et al., 2015c; Leonov et al., 2015b) The lock-in range of model (6) is a range $[0,\omega_l)$ such that for each frequency deviation $\left|\omega_\Delta^{\text{free}}\right| \in [0,\omega_l)$ the model (6) is globally asymptotically stable and the following domain*

$$D_{\text{lock}-\text{in}}((-\omega_l,\omega_l)) = \bigcap_{|\omega_\Delta^{\text{free}}|<\omega_l} D_{\text{lock}-\text{in}}(\omega_\Delta^{\text{free}})$$

contains all corresponding equilibria $\left(\theta^s_{eq}, x_{eq}(\omega_\Delta^{\text{free}})\right)$.

For model (6) each lock-in domain from intersection $\bigcap_{|\omega_\Delta^{\text{free}}|<\omega_l} D_{\text{lock}-\text{in}}(\omega_\Delta^{\text{free}})$ is bounded by the separatrices of saddle equilibria $\left(\theta^u_{eq}, x_{eq}(\omega_\Delta^{\text{free}})\right)$ and vertical lines $\theta_\Delta = \theta^s_{eq} \pm 2\pi$. Thus, the behavior of separatrices on the phase plane is the key to the lock-in range study (see Fig. 5).

3. Phase plane analysis for the lock-in range estimation

Consider an approach to the lock-in range computation of (6), based on the phase plane analysis. To compute the lock-in range of (6) we need to consider the behavior of the lower separatrix $Q(\theta_\Delta,\omega_\Delta^{\text{free}})$, which tends to the saddle point $\left(\theta^u_{eq}, x_{eq}(\omega_\Delta^{\text{free}})\right) = \left(\pi, \frac{\omega_\Delta^{\text{free}}\tau_1}{K_0}\right)$ as $t \to +\infty$ (by the symmetry of the lower and the upper half-planes, the consideration of the upper separatrix is also possible). The parameter $\omega_\Delta^{\text{free}}$ shifts the phase plane vertically. To check this, we use a linear transformation $x \to x + \frac{\omega_\Delta^{\text{free}}\tau_1}{K_0}$. Thus, to compute the lock-in range of (6), we need to find $\omega_\Delta^{\text{free}} = \omega_l$ (where ω_l is called a lock-in frequency) such that (see Fig. 5)

$$x_{eq}(-\omega_l) = Q(\theta^s_{eq},\omega_l). \tag{7}$$

By (7), we obtain an exact formula for the lock-in frequency ω_l:

$$-\frac{\omega_l}{K_0/\tau_1} = \frac{\omega_l}{K_0/\tau_1} + Q(\theta^s_{eq},0).$$
$$\omega_l = -\frac{K_0 Q(\theta^s_{eq},0)}{2\tau_1}, \tag{8}$$

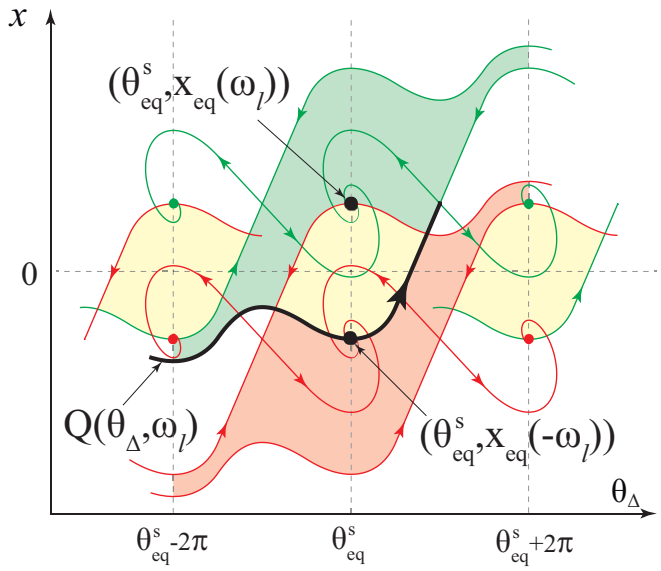

Figure 5: The lock-in domain of (6) for $|\omega_\Delta^{\text{free}}| = \omega_l$.

Numerical simulations are used to compute the lock-in range of (6) applying (8). The separatrix $Q(\theta_\Delta, 0)$ is numerically integrated and the corresponding ω_l is approximated. The obtained numerical results can be illustrated by special diagram (see Fig. 6). Note that (6) depends on the value of two coefficients $\frac{K_0}{\tau_1}$ and τ_2. In Fig. 6, choosing X-axis as $\frac{K_0}{\tau_1}$, we can plot a single curve for every fixed value of τ_2. The results of numerical simulations show that for sufficiently large $\frac{K_0}{\tau_1}$, the value of ω_l grows almost proportionally to $\frac{K_0}{\tau_1}$. Hence, $\frac{\omega_l \tau_1}{K_0}$ is almost constant for sufficiently large $\frac{K_0}{\tau_1}$ and in Fig. 6 the Y-axis can be chosen as $\frac{\omega_\Delta^{\text{free}} \tau_1}{K_0}$.

To obtain the lock-in frequency ω_l for fixed τ_1, τ_2, and K_0 using Fig. 6, we consider the curve corresponding to the chosen τ_2. Next, for X-value equal $\frac{K_0}{\tau_1}$ we get the Y-value of the curve. Finally, we multiply the Y-value by $\frac{K_0}{\tau_1}$.

Consider an analytical approach to the exact lock-in range computation. Main stages of computation are presented in Subsection 3.1.

3.1. Analytical approach to the lock-in range computation

Consider a system

$$\begin{cases} \dot\theta_\Delta(t) = y(t), \\ \dot y(t) = -\frac{K_0\tau_2}{\tau_1}\dot\varphi(\theta_\Delta(t))y(t) - \frac{K_0}{\tau_1}\varphi(\theta_\Delta(t)), \end{cases} \tag{9}$$

where $y(t) = \omega_\Delta^{\text{free}} - \frac{K_0}{\tau_1}(x(t) + \tau_2\varphi(\theta_\Delta(t)))$. Relations (9) are equivalent to (6) and allow one to exclude $\omega_\Delta^{\text{free}}$ from the computation. Note that equilibria (θ_{eq}, y_{eq}) of (9) and the corresponding equilibria (θ_{eq}, x_{eq}) of (6) are of the same type and related as

$$(\theta_{eq}, y_{eq}) = \left(\theta_{eq}, \omega_\Delta^{\text{free}} - K_0 b x_{eq}\right).$$

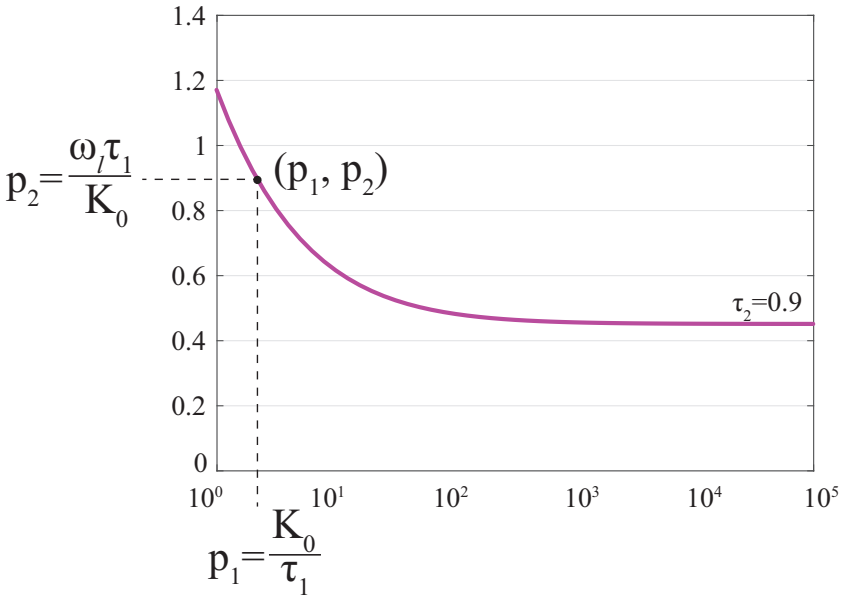

Figure 6: Diagram for the lock-in frequency ω_l calculation.

The separatrix $Q(\theta_\Delta, \omega_\Delta^{\text{free}})$ from (8) corresponds to the upper separatrix $S'(\theta_\Delta)$ of the phase plane of (9) (see Fig. 7) and the following relation

$$Q(\theta_{eq}^s, \omega_\Delta^{\text{free}}) = \frac{\tau_1}{K_0}\left(\omega_\Delta^{\text{free}} - S'(\theta_{eq}^s)\right)$$

is valid.

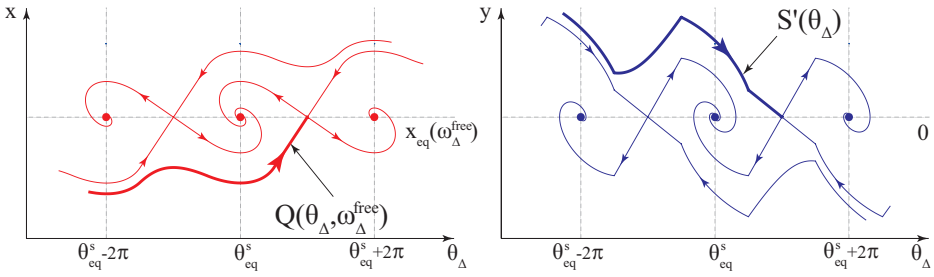

Figure 7: Phase plane portraits of (6) and (9).

Relation (8) takes the form

$$\omega_l = \frac{1}{2}S'(\theta_{eq}^s). \tag{10}$$

The computation of the separatrix $S'(\theta_\Delta)$ is in two steps. Step 1: we integrate the separatrix $S'(\theta_\Delta)$ in the interval $\left(\frac{\pi}{2}, \pi\right)$ (in which the function $\varphi(\theta_\Delta)$ is continuously differentiable) and compute $S'(\frac{\pi}{2})$. For this purpose, we need to find the eigenvector that

corresponds to separatrix $S'(\theta_\Delta)$ on the considered interval. Step 2: we find a general solution of (9) on the interval $\left(-\frac{\pi}{2},\frac{\pi}{2}\right)$. Here there exist three cases depending on the type stable equilibrium $\left(\theta^s_{eq},0\right)$: a stable focus, stable node, and stable degenerated node. For every case described above we perform separate computations. Using the computed $S'(\frac{\pi}{2})$ as the initial data of the Cauchy problem, it is possible to obtain an exact expression for $S'(\theta^s_{eq})$.

The obtained analytical results are illustrated in Fig. 8. The red line in Fig. 8 is used for the case of stable focus, and the green line for the case of stable node. The crosses are used for the case of stable degenerated node.

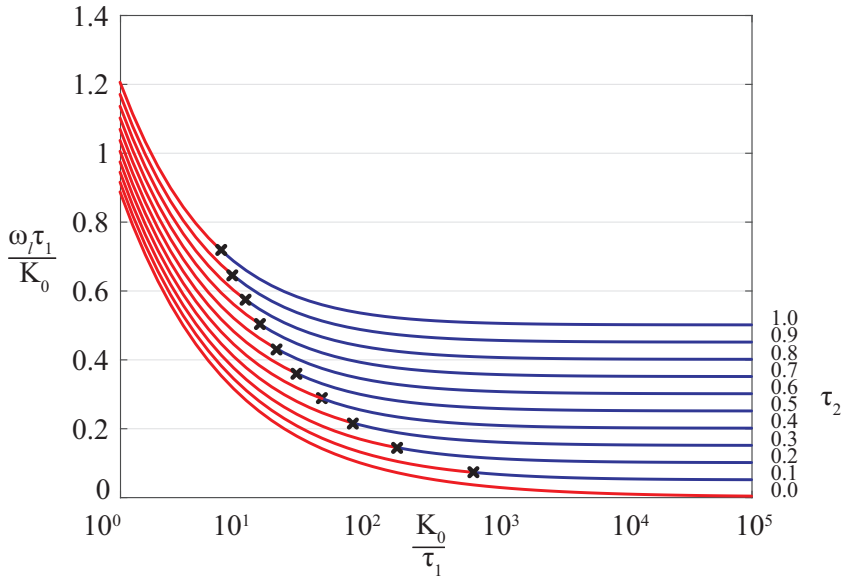

Figure 8: Diagram for the lock-in frequency ω_l calculation.

The formulae for three possible cases are given below (redefinitions $a=\frac{\tau_2}{\tau_1}$, $b=\frac{1}{\tau_1}$ are used to reduce the analytical formulae):

A. $(aK_0)^2-2bK_0\pi>0$ that corresponds to a stable node:

$$\omega_l=\frac{1}{\pi}c_1\sqrt{(aK_0)^2-2bK_0\pi}\,\left(-\frac{c_2}{c_1}\right)^{\left(\frac{1}{2}-\frac{aK_0}{2\sqrt{(aK_0)^2-2bK_0\pi}}\right)}, \tag{11}$$

$$\text{where } c_1=\frac{\pi}{4}\left(\frac{\sqrt{(aK_0)^2+2bK_0\pi}}{\sqrt{(aK_0)^2-2bK_0\pi}}+1\right), c_2=\frac{\pi}{4}\left(1-\frac{\sqrt{(aK_0)^2+2bK_0\pi}}{\sqrt{(aK_0)^2-2bK_0\pi}}\right).$$

B. $(aK_0)^2-2bK_0\pi=0$ that corresponds to a stable degenerated node:

$$\omega_l=\frac{1}{2}c_2\,e^{\left(\frac{aK_0}{2c_2}\right)}, \text{where } c_2=\frac{\sqrt{(aK_0)^2+2bK_0\pi}}{2}. \tag{12}$$

C. $(aK_0)^2 - 2bK_0\pi < 0$ that corresponds to a stable focus:

$$\omega_l = -\frac{aK_0\, e^{t_0 \operatorname{Re}\lambda_1^s}}{2\pi}\left(c_1 \cos\left(t_0 \operatorname{Im}\lambda_1^s\right) + c_2 \sin\left(t_0 \operatorname{Im}\lambda_1^s\right)\right) +$$
$$+ \frac{e^{t_0 \operatorname{Re}\lambda_1^s}\sqrt{2bK_0\pi - (aK_0)^2}}{2\pi}\left(c_2 \cos\left(t_0 \operatorname{Im}\lambda_1^s\right) - c_1 \sin\left(t_0 \operatorname{Im}\lambda_1^s\right)\right), \tag{13}$$
$$\text{where } t_0 = \frac{\operatorname{arctg}\left(-\dfrac{c_1}{c_2}\right)}{\operatorname{Im}\lambda_1^s}, c_1 = \frac{\pi}{2},\ c_2 = \frac{\pi\sqrt{(aK_0)^2 + 4bK_0(\pi - \frac{1}{k})}}{2\sqrt{2bK_0\pi - (aK_0)^2}},$$
$$\lambda_1^s = \frac{-aK_0 + i\sqrt{2bK_0\pi - (aK_0)^2}}{\pi}.$$

Rigorous derivation of (11), (12), and (13) is given in Appendix A. The analytical and numerical results are compared in Fig. 9.

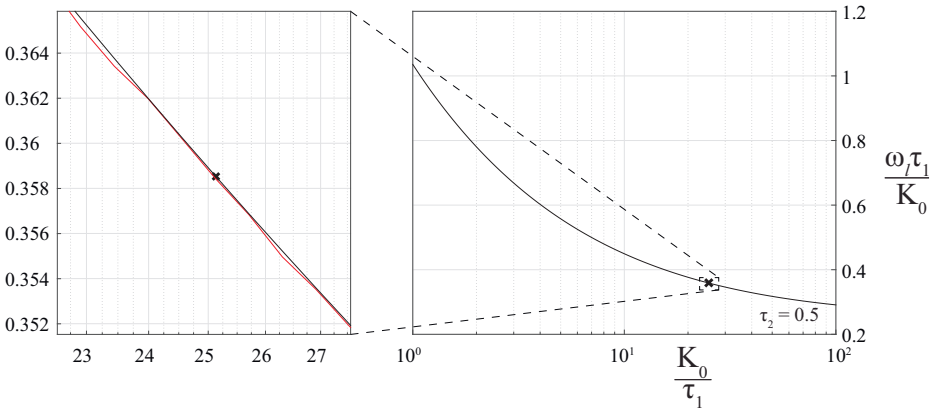

Figure 9: Comparison of analytical and numerical results on the lock-in computation.

4. Conclusion

In the present work the model of PLL with impulse signals and active PI filter in the signal's phase space is described. For the considered PLL the lock-in range is computed analytically and obtained result are compared with numerical simulations.

Appendix A. The lock-in computation

In this section equations (11), (12), and (13) are rigorously derived. Consider the following relations

$$\begin{cases} \dot\theta_\Delta = y, \\ \dot y = -aK_0\dot\varphi(\theta_\Delta)y - bK_0\varphi(\theta_\Delta). \end{cases} \tag{A.1}$$

Also we consider a normalized 2π-periodic zigzag function

$$\varphi(\theta_\Delta) = \begin{cases} k\theta_\Delta, & \text{if } -\frac{1}{k} \le \theta_\Delta \le \frac{1}{k}; \\ -\frac{k}{\pi k - 1}\theta_\Delta + \frac{\pi k}{\pi k - 1}, & \text{if } \frac{1}{k} \le \theta_\Delta \le 2\pi - \frac{1}{k} \end{cases} \tag{A.2}$$

for finite $k > \frac{1}{\pi}$ in the interval $\theta_\Delta \in \left[-\frac{1}{k}, 2\pi - \frac{1}{k}\right)$. For $k = \frac{2}{\pi}$ the function $\varphi(\theta_\Delta)$ is triangular and corresponds to (1).

From 2π-periodicity of (A.1) it follows that for each interval the behavior of phase trajectories on the system phase plane is the same

$$\theta_\Delta \in \left(-\frac{1}{k} + 2\pi j, -\frac{1}{k} + 2\pi(j+1)\right], \ j \in \mathbb{Z}.$$

Thus, we can consider a single interval $\left(-\frac{1}{k}, 2\pi - \frac{1}{k}\right]$ of the phase plane of (A.1).

In the intervals inside $\left(-\frac{1}{k}, 2\pi - \frac{1}{k}\right]$, (A.1) takes the form:

I. $-\frac{1}{k} < \theta_\Delta < \frac{1}{k}$

$$\begin{cases} \dot{\theta_\Delta} = y, \\ \dot{y} = -aK_0 k y - bK_0 k \theta_\Delta; \end{cases} \tag{A.3}$$

II. $\frac{1}{k} < \theta_\Delta < 2\pi - \frac{1}{k}$

$$\begin{cases} \dot{\theta_\Delta} = y, \\ \dot{y} = aK_0 \frac{k}{\pi k - 1} y + bK_0 \left(\frac{k}{\pi k - 1} \theta_\Delta - \frac{\pi k}{\pi k - 1}\right). \end{cases} \tag{A.4}$$

In each interval there exists only one equilibrium:

I. $-\frac{1}{k} < \theta_\Delta < \frac{1}{k}$

$$\begin{cases} y_{\text{eq}} = 0, \\ -aK_0 k y - bK_0 k \theta_{\text{eq}} = 0; \end{cases} \qquad \begin{cases} y_{\text{eq}} = 0, \\ \theta_{\text{eq}} = 0; \end{cases}$$

II. $\frac{1}{k} < \theta_\Delta < 2\pi - \frac{1}{k}$

$$\begin{cases} y_{\text{eq}} = 0, \\ \frac{aK_0 k}{\pi k - 1} y_{\text{eq}} + \frac{bK_0 k}{\pi k - 1} (\theta_{\text{eq}} - \pi) = 0. \end{cases} \qquad \begin{cases} y_{\text{eq}} = 0, \\ \theta_{\text{eq}} = \pi. \end{cases}$$

To define a type of the equilibria points, we compute the corresponding characteristic polynomial and eigenvalues. For the first equilibrium $(\theta_{\text{eq}}, y_{\text{eq}}) = (0,0)$ the characteristic polynomial is as follows

$$\chi(\lambda) = \begin{vmatrix} -\lambda & 1 \\ -bK_0 k & -aK_0 k - \lambda \end{vmatrix} = \lambda^2 + aK_0 k \lambda + bK_0 k.$$

The eigenvalues of the equilibrium $(\theta_{\text{eq}}, y_{\text{eq}}) = (0,0)$ depend on a sign of $(aK_0)^2 - \frac{4bK_0}{k}$. Here, there exist three cases:

A. $(aK_0)^2 - \frac{4bK_0}{k} > 0$:

$$\lambda^s_{1,2} = \frac{-aK_0 k \pm \sqrt{(aK_0 k)^2 - 4bK_0 k}}{2},$$

the equilibrium $(0,0)$ is a stable node.

B. $(aK_0)^2 - \frac{4bK_0}{k} = 0$:

$$\lambda^s_1 = \lambda^s_2 = \frac{-aK_0 k}{2},$$

the equilibrium $(0,0)$ is a stable degenerated node, or stable proper node.
C. $(aK_0)^2 - \frac{4bK_0}{k} < 0$:

$$\lambda^s_{1,2} = \frac{-aK_0k \pm i\sqrt{4bK_0k - (aK_0k)^2}}{2},$$

the equilibrium $(0,0)$ is a stable focus.
Denote $(\theta^s_{\text{eq}}, y_{\text{eq}}) = (0,0)$.

For the second equilibrium $(\theta_{\text{eq}}, y_{\text{eq}}) = (\pi, 0)$ we have

$$\chi(\lambda) = \begin{vmatrix} -\lambda & 1 \\ \frac{bK_0k}{\pi k-1} & \frac{aK_0k}{\pi k-1} - \lambda \end{vmatrix} = \lambda^2 - \frac{aK_0k}{\pi k-1}\lambda - \frac{bK_0k}{\pi k-1};$$

$$\lambda^u_{1,2} = \frac{\frac{aK_0k}{\pi k-1} \pm \sqrt{\left(\frac{aK_0k}{\pi k-1}\right)^2 + \frac{4bK_0k}{\pi k-1}}}{2},$$

which means that $(\pi, 0)$ is always an unstable saddle for the considered parameters of the PLL. Denote $(\theta^u_{\text{eq}}, y_{\text{eq}}) = (\pi, 0)$.

The calculation of $S'(\theta^s_{\text{eq}})$ from formula (10) for lock-in range is in some stages. First, find two-dimensional eigenvectors X^u_1, X^u_2 of saddle point $\left(\theta^u_{\text{eq}}, y_{\text{eq}}\right)$ from the interval $\theta_\Delta \in \left(\frac{1}{k}, 2\pi - \frac{1}{k}\right)$. Next, compute $S'(\frac{1}{k})$, which is possible due to the continuity of (A.1). Find two-dimensional eigenvectors X^s_1, X^s_2 of stable equilibrium $\left(\theta^s_{\text{eq}}, y_{\text{eq}}\right)$ in the interval $\theta_\Delta \in \left(-\frac{1}{k}, \frac{1}{k}\right)$. Find a general solution of (A.1) in the interval $\theta_\Delta \in \left(-\frac{1}{k}, \frac{1}{k}\right)$. Using the obtained $S'(\frac{1}{k})$ as the initial data of the Cauchy problem, we can compute $S'(\theta^s_{\text{eq}})$.

Let us find the eigenvectors X^u_1, X^u_2 of a saddle point $\left(\theta^u_{\text{eq}}, y_{\text{eq}}\right)$. First, find the eigenvector X^u_1:

$$\begin{pmatrix} -\lambda^u_1 & 1 \\ \frac{bK_0k}{\pi k-1} & \frac{aK_0k}{\pi k-1} - \lambda^u_1 \end{pmatrix} X^u_1 = \mathbb{O},$$

$$\begin{pmatrix} -\frac{\frac{aK_0k}{\pi k-1} + \sqrt{\left(\frac{aK_0k}{\pi k-1}\right)^2 + \frac{4bK_0k}{\pi k-1}}}{2} & 1 \\ \frac{bK_0k}{\pi k-1} & \frac{aK_0k}{\pi k-1} - \frac{\frac{aK_0k}{\pi k-1} + \sqrt{\left(\frac{aK_0k}{\pi k-1}\right)^2 + \frac{4bK_0k}{\pi k-1}}}{2} \end{pmatrix} X^u_1 = \mathbb{O},$$

$$\begin{pmatrix} -\frac{\frac{aK_0k}{\pi k-1} + \sqrt{\left(\frac{aK_0k}{\pi k-1}\right)^2 + \frac{4bK_0k}{\pi k-1}}}{2} & 1 \\ \frac{bK_0k}{\pi k-1} & -\frac{\frac{aK_0k}{\pi k-1} - \sqrt{\left(\frac{aK_0k}{\pi k-1}\right)^2 + \frac{4bK_0k}{\pi k-1}}}{2} \end{pmatrix} X^u_1 = \mathbb{O}. \qquad \text{(A.5)}$$

Multiply the second row of (A.5) by $\frac{\frac{aK_0k}{\pi k-1} + \sqrt{\left(\frac{aK_0k}{\pi k-1}\right)^2 + \frac{4bK_0k}{\pi k-1}}}{2}$ and divide it by $\frac{bK_0k}{\pi k-1}$.

Then we have

$$\begin{pmatrix} -\frac{\frac{aK_0k}{\pi k-1}+\sqrt{\left(\frac{aK_0k}{\pi k-1}\right)^2+\frac{4bK_0k}{\pi k-1}}}{2} & 1 \\ \frac{\frac{aK_0k}{\pi k-1}+\sqrt{\left(\frac{aK_0k}{\pi k-1}\right)^2+\frac{4bK_0k}{\pi k-1}}}{2} & -\frac{\left(\left(\frac{aK_0k}{\pi k-1}\right)^2-(\frac{aK_0k}{\pi k-1})^2+\frac{4bK_0k}{\pi k-1}\right)(\pi k-1)}{4bK_0k} \end{pmatrix} X_1^u = \mathbb{O},$$

$$\begin{pmatrix} -\frac{\frac{aK_0k}{\pi k-1}+\sqrt{\left(\frac{aK_0k}{\pi k-1}\right)^2+\frac{4bK_0k}{\pi k-1}}}{2} & 1 \\ \frac{\frac{aK_0k}{\pi k-1}+\sqrt{\left(\frac{aK_0k}{\pi k-1}\right)^2+\frac{4bK_0k}{\pi k-1}}}{2} & -1 \end{pmatrix} X_1^u = \mathbb{O}.$$

Hence,

$$X_1^u = \begin{pmatrix} c \\ c\frac{\sqrt{(aK_0k)^2+4bK_0k(\pi k-1)}+aK_0k}{2(\pi k-1)} \end{pmatrix}.$$

Let us choose $c = \frac{\sqrt{(aK_0k)^2+4bK_0k(\pi k-1)}-aK_0k}{2bK_0k}$. Then

$$X_1^u = \begin{pmatrix} \frac{\sqrt{(aK_0k)^2+4bK_0k(\pi k-1)}-aK_0k}{2bK_0k} \\ \frac{(aK_0k)^2+4bK_0k(\pi k-1)-(aK_0k)^2}{4bK_0k(\pi k-1)} \end{pmatrix},$$

$$X_1^u = \begin{pmatrix} \frac{\sqrt{(aK_0k)^2+4bK_0k(\pi k-1)}-aK_0k}{2bK_0k} \\ 1 \end{pmatrix}.$$

Next, find the second eigenvector X_2^u in the same way:

$$\begin{pmatrix} -\lambda_2^u & 1 \\ \frac{bK_0k}{\pi k-1} & \frac{aK_0k}{\pi k-1}-\lambda_2^u \end{pmatrix} X_2^u = \mathbb{O},$$

$$\begin{pmatrix} \frac{\sqrt{\left(\frac{aK_0k}{\pi k-1}\right)^2+\frac{4bK_0k}{\pi k-1}}-\frac{aK_0k}{\pi k-1}}{2} & 1 \\ \frac{bK_0k}{\pi k-1} & \frac{aK_0k}{\pi k-1}+\frac{\sqrt{\left(\frac{aK_0k}{\pi k-1}\right)^2+\frac{4bK_0k}{\pi k-1}}-\frac{aK_0k}{\pi k-1}}{2} \end{pmatrix} X_2^u = \mathbb{O},$$

$$\begin{pmatrix} \frac{\sqrt{\left(\frac{aK_0k}{\pi k-1}\right)^2+\frac{4bK_0k}{\pi k-1}}-\frac{aK_0k}{\pi k-1}}{2} & 1 \\ \frac{bK_0k}{\pi k-1} & \frac{\sqrt{\left(\frac{aK_0k}{\pi k-1}\right)^2+\frac{4bK_0k}{\pi k-1}}+\frac{aK_0k}{\pi k-1}}{2} \end{pmatrix} X_2^u = \mathbb{O}. \qquad \text{(A.6)}$$

Multiply the second row of (A.6) by $\dfrac{\sqrt{\left(\frac{aK_0k}{\pi k-1}\right)^2+\frac{4bK_0k}{\pi k-1}}-\frac{aK_0k}{\pi k-1}}{2}$, and divide it by $\dfrac{bK_0k}{\pi k-1}$. Then

$$\begin{pmatrix} \dfrac{\sqrt{\left(\frac{aK_0k}{\pi k-1}\right)^2+\frac{4bK_0k}{\pi k-1}}-\frac{aK_0k}{\pi k-1}}{2} & 1 \\ \dfrac{\sqrt{\left(\frac{aK_0k}{\pi k-1}\right)^2+\frac{4bK_0k}{\pi k-1}}-\frac{aK_0k}{\pi k-1}}{2} & \dfrac{\left(\left(\frac{aK_0k}{\pi k-1}\right)^2+\frac{4bK_0k}{\pi k-1}-\left(\frac{aK_0k}{\pi k-1}\right)^2\right)(\pi k-1)}{4bK_0k} \end{pmatrix} X_2^u=\mathbb{O},$$

$$\begin{pmatrix} \dfrac{\sqrt{\left(\frac{aK_0k}{\pi k-1}\right)^2+\frac{4bK_0k}{\pi k-1}}-\frac{aK_0k}{\pi k-1}}{2} & 1 \\ \dfrac{\sqrt{\left(\frac{aK_0k}{\pi k-1}\right)^2+\frac{4bK_0k}{\pi k-1}}-\frac{aK_0k}{\pi k-1}}{2} & 1 \end{pmatrix} X_2^u=\mathbb{O}.$$

Hence,

$$X_2^u=\begin{pmatrix} -c \\ c\dfrac{\sqrt{\left(\frac{aK_0k}{\pi k-1}\right)^2+\frac{4bK_0k}{\pi k-1}}-\frac{aK_0k}{\pi k-1}}{2} \end{pmatrix}.$$

Choose $c=\dfrac{\sqrt{(aK_0k)^2+4bK_0k(\pi k-1)}+aK_0k}{2bK_0k}$:

$$X_2^u=\begin{pmatrix} -\dfrac{\sqrt{(aK_0k)^2+4bK_0k(\pi k-1)}+aK_0k}{2bK_0k} \\ \dfrac{(aK_0k)^2+4bK_0k(\pi k-1)-(aK_0k)^2}{4bK_0k(\pi k-1)} \end{pmatrix},$$

$$X_2^u=\begin{pmatrix} -\dfrac{\sqrt{(aK_0k)^2+4bK_0k(\pi k-1)}+aK_0k}{2bK_0k} \\ 1 \end{pmatrix}.$$

We can show that the direction of separatrix $S'(\theta_\Delta)$ coincides with the direction of eigenvector X_2^u, which corresponds to eigenvalue λ_2^u. That allows us to find $S'(\frac{1}{k})$. For this purpose, we write an equation of straight line, which passes through two points

$$(x_1,y_1)=(\pi,0),$$
$$(x_2,y_2)=\left(\pi-\frac{\sqrt{(aK_0k)^2+4bK_0k(\pi k-1)}+aK_0k}{2bK_0k},1\right).$$

The equation takes the form

$$\frac{y-0}{1-0}=\frac{x-\pi}{\left(\pi-\dfrac{\sqrt{(aK_0k)^2+4bK_0k(\pi k-1)}+aK_0k}{2bK_0k}\right)-\pi},$$

$$y=\frac{2bK_0k}{\sqrt{(aK_0k)^2+4bK_0k(\pi k-1)}+aK_0k}\,(\pi-x)\,,$$

$$y=\frac{2bK_0k\left(\sqrt{(aK_0k)^2+4bK_0k(\pi k-1)}-aK_0k\right)}{(aK_0k)^2+4bK_0k(\pi k-1)-(aK_0k)^2}\,(\pi-x)\,,$$

$$y=\frac{\sqrt{(aK_0k)^2+4bK_0k(\pi k-1)}-aK_0k}{2(\pi k-1)}\,(\pi-x)\,.$$

Then

$$S'(\frac{1}{k})=\frac{\sqrt{(aK_0k)^2+4bK_0k(\pi k-1)}-aK_0k}{2(\pi k-1)}\left(\pi-\frac{1}{k}\right)=$$

$$=\frac{\sqrt{(aK_0)^2+4bK_0(\pi-\frac{1}{k})}-aK_0}{2}.$$

Next, we need to find the eigenvectors of equilibrium $(\theta^s_{\rm eq}, y_{\rm eq})$ and a general solution of (A.1) in the interval $\left(-\frac{1}{k},\frac{1}{k}\right)$. It was shown that for a stable equilibrium $(\theta^s_{\rm eq}, y_{\rm eq})$ in the interval $\left(-\frac{1}{k},\frac{1}{k}\right)$ there exist three different cases, which depend on a sign of $(aK_0)^2-\frac{4bK_0}{k}$. The eigenvectors X^s_1 and X^s_2 are computed in the case of stable focus only. For other cases the computation of X^s_1, X^s_2 is similar to that, considered in Appendix A.1.

Appendix A.1. Stable node

This case corresponds to $(aK_0)^2-\frac{4bK_0}{k}>0$. Let us find the eigenvectors X^s_1, X^s_2:

$$\begin{pmatrix} -\lambda^s_1 & 1 \\ -bK_0k & -aK_0k-\lambda^s_1 \end{pmatrix} X^s_1=\mathbb{O},$$

$$\begin{pmatrix} \dfrac{aK_0k-\sqrt{(aK_0k)^2-4bK_0k}}{2} & 1 \\ -bK_0k & -aK_0k+\dfrac{aK_0k-\sqrt{(aK_0k)^2-4bK_0k}}{2} \end{pmatrix} X^s_1=\mathbb{O},$$

$$\begin{pmatrix} \dfrac{aK_0k-\sqrt{(aK_0k)^2-4bK_0k}}{2} & 1 \\ -bK_0k & -\dfrac{aK_0k+\sqrt{(aK_0k)^2-4bK_0k}}{2} \end{pmatrix} X^s_1=\mathbb{O}. \qquad \text{(A.7)}$$

Multiply the second row of (A.7) by $\dfrac{aK_0k-\sqrt{(aK_0k)^2-4bK_0k}}{2}$, and divide it by bK_0k:

$$\begin{pmatrix} \dfrac{aK_0k-\sqrt{(aK_0k)^2-4bK_0k}}{2} & 1 \\ -\dfrac{aK_0k-\sqrt{(aK_0k)^2-4bK_0k}}{2} & -\dfrac{(aK_0k)^2-(aK_0k)^2+4bK_0k}{4bK_0k} \end{pmatrix} X^s_1=\mathbb{O},$$

$$\begin{pmatrix} \frac{aK_0k-\sqrt{(aK_0k)^2-4bK_0k}}{2} & 1 \\ -\frac{aK_0k-\sqrt{(aK_0k)^2-4bK_0k}}{2} & -1 \end{pmatrix} X_1^s = \mathbb{O},$$

$$X_1^s = \begin{pmatrix} -c \\ c\frac{aK_0k-\sqrt{(aK_0k)^2-4bK_0k}}{2} \end{pmatrix}.$$

Choose $c = -1$. Then

$$X_1^s = \begin{pmatrix} 1 \\ \frac{\sqrt{(aK_0k)^2-4bK_0k}-aK_0k}{2} \end{pmatrix}.$$

Next, find eigenvector X_2^s:

$$\begin{pmatrix} -\lambda_2^s & 1 \\ -bK_0k & -aK_0k-\lambda_2^s \end{pmatrix} X_2^s = \mathbb{O},$$

$$\begin{pmatrix} \frac{aK_0k+\sqrt{(aK_0k)^2-4bK_0k}}{2} & 1 \\ -bK_0k & -aK_0k+\frac{aK_0k+\sqrt{(aK_0k)^2-4bK_0k}}{2} \end{pmatrix} X_2^s = \mathbb{O},$$

$$\begin{pmatrix} \frac{aK_0k+\sqrt{(aK_0k)^2-4bK_0k}}{2} & 1 \\ -bK_0k & \frac{\sqrt{(aK_0k)^2-4bK_0k}-aK_0k}{2} \end{pmatrix} X_2^s = \mathbb{O}. \tag{A.8}$$

Multiply the second row of (A.8) by $\frac{aK_0k+\sqrt{(aK_0k)^2-4bK_0k}}{2}$, and divide it by bK_0k:

$$\begin{pmatrix} \frac{aK_0k+\sqrt{(aK_0k)^2-4bK_0k}}{2} & 1 \\ -\frac{aK_0k+\sqrt{(aK_0k)^2-4bK_0k}}{2} & \frac{(aK_0k)^2-4bK_0k-(aK_0k)^2}{4bK_0k} \end{pmatrix} X_2^s = \mathbb{O},$$

$$\begin{pmatrix} \frac{aK_0k+\sqrt{(aK_0k)^2-4bK_0k}}{2} & 1 \\ -\frac{aK_0k+\sqrt{(aK_0k)^2-4bK_0k}}{2} & -1 \end{pmatrix} X_2^s = \mathbb{O},$$

$$X_2^s = \begin{pmatrix} -c \\ c\frac{aK_0k+\sqrt{(aK_0k)^2-4bK_0k}}{2} \end{pmatrix}.$$

Choose $c=-1$. Then

$$X_2^s=\begin{pmatrix}1\\ -\dfrac{aK_0k+\sqrt{(aK_0k)^2-4bK_0k}}{2}\end{pmatrix}.$$

In the interval $\theta_\Delta\in\left(-\frac{1}{k},\frac{1}{k}\right)$ for $\left(\theta_{\rm eq}^s,y_{\rm eq}\right)=(0,0)$ being a node, a general solution of (A.1) has the form:

$$\begin{cases}\theta_\Delta(t)=c_1\,e^{\lambda_1^s t}+c_2\,e^{\lambda_2^s t},\\ \\ y(t)=-c_1\dfrac{aK_0k-\sqrt{(aK_0k)^2-4bK_0k}}{2}\,e^{\lambda_1^s t}-c_2\dfrac{aK_0k+\sqrt{(aK_0k)^2-4bK_0k}}{2}\,e^{\lambda_2^s t}.\end{cases}\tag{A.9}$$

Let us find coefficients c_1, c_2 of (A.9) for the solution of the Cauchy problem with initial conditions $\theta_\Delta(0)=\frac{1}{k}$, $y(0)=\frac{\sqrt{(aK_0)^2+4bK_0(\pi-\frac{1}{k})}-aK_0}{2}$, which coincide with $S'(\frac{1}{k})$.
At moment $t=0$ we have

$$\begin{cases}\dfrac{1}{k}=c_1+c_2,\\ \\ \dfrac{\sqrt{(aK_0)^2+4bK_0(\pi-\frac{1}{k})}-aK_0}{2}=\\ \\ \qquad=-c_1\dfrac{aK_0k-\sqrt{(aK_0k)^2-4bK_0k}}{2}-c_2\dfrac{aK_0k+\sqrt{(aK_0k)^2-4bK_0k}}{2},\end{cases}$$

$$\begin{cases}c_2=\dfrac{1}{k}-c_1,\\ \\ \dfrac{\sqrt{(aK_0)^2+4bK_0(\pi-\frac{1}{k})}-aK_0}{2}+\dfrac{aK_0k+\sqrt{(aK_0k)^2-4bK_0k}}{2k}=\\ =-c_1\dfrac{aK_0k-\sqrt{(aK_0k)^2-4bK_0k}}{2}+c_1\dfrac{aK_0k+\sqrt{(aK_0k)^2-4bK_0k}}{2},\end{cases}$$

$$\begin{cases}c_2=\dfrac{1}{k}-c_1,\\ \\ \dfrac{\sqrt{(aK_0)^2+4bK_0(\pi-\frac{1}{k})}}{2}+\dfrac{\sqrt{(aK_0)^2-\frac{4bK_0}{k}}}{2}=c_1k\sqrt{(aK_0)^2-\dfrac{4bK_0}{k}},\end{cases}$$

$$\begin{cases}c_2=\dfrac{1}{k}-c_1,\\ \\ c_1=\left(\dfrac{\sqrt{(aK_0)^2+4bK_0(\pi-\frac{1}{k})}}{\sqrt{(aK_0)^2-\frac{4bK_0}{k}}}+1\right):2k,\end{cases}$$

$$\begin{cases} c_1 = \left(\dfrac{\sqrt{(aK_0)^2 + 4bK_0(\pi - \frac{1}{k})}}{\sqrt{(aK_0)^2 - \frac{4bK_0}{k}}} + 1 \right) : 2k, \\ c_2 = \left(1 - \dfrac{\sqrt{(aK_0)^2 + 4bK_0(\pi - \frac{1}{k})}}{\sqrt{(aK_0)^2 - \frac{4bK_0}{k}}} \right) : 2k. \end{cases} \tag{A.10}$$

Finally, find $y(t_0)$ under the condition $\theta_\Delta(t_0) = 0$. The value of $y(t_0)$ corresponds to $S'(\theta^s_{\text{eq}})$. For this purpose, we express $y(t_0)$ in terms of c_1, c_2 from (A.10). Then

$$\begin{cases} 0 = c_1\, e^{\lambda_1^s t_0} + c_2\, e^{\lambda_2^s t_0}, \\ y(t_0) = -c_1 \dfrac{aK_0k - \sqrt{(aK_0k)^2 - 4bK_0k}}{2}\, e^{\lambda_1^s t_0} - c_2 \dfrac{aK_0k + \sqrt{(aK_0k)^2 - 4bK_0k}}{2}\, e^{\lambda_2^s t_0}, \end{cases}$$

$$\begin{cases} -\dfrac{c_1}{c_2} = e^{(\lambda_2^s - \lambda_1^s) t_0}, \\ y(t_0) = -c_1 \dfrac{aK_0k - \sqrt{(aK_0k)^2 - 4bK_0k}}{2}\, e^{\lambda_1^s t_0} - c_2 \dfrac{aK_0k + \sqrt{(aK_0k)^2 - 4bK_0k}}{2}\, e^{\lambda_2^s t_0}, \end{cases}$$

$$\begin{cases} -\dfrac{c_1}{c_2} = e^{\left(-\frac{\sqrt{(aK_0k)^2 - 4bK_0k} + aK_0k}{2} - \frac{\sqrt{(aK_0k)^2 - 4bK_0k} - aK_0k}{2} \right) t_0}, \\ y(t_0) = -c_1 \dfrac{aK_0k - \sqrt{(aK_0k)^2 - 4bK_0k}}{2}\, e^{\lambda_1^s t_0} - c_2 \dfrac{aK_0k + \sqrt{(aK_0k)^2 - 4bK_0k}}{2}\, e^{\lambda_2^s t_0}, \end{cases}$$

$$\begin{cases} -\dfrac{c_1}{c_2} = e^{\left(-\sqrt{(aK_0k)^2 - 4bK_0k} \right) t_0}, \\ y(t_0) = -c_1 \dfrac{aK_0k - \sqrt{(aK_0k)^2 - 4bK_0k}}{2}\, e^{\lambda_1^s t_0} - c_2 \dfrac{aK_0k + \sqrt{(aK_0k)^2 - 4bK_0k}}{2}\, e^{\lambda_2^s t_0}, \end{cases}$$

$$\begin{cases} \ln\left(-\dfrac{c_1}{c_2} \right) = -\left(\sqrt{(aK_0k)^2 - 4bK_0k} \right) t_0, \\ y(t_0) = -c_1 \dfrac{aK_0k - \sqrt{(aK_0k)^2 - 4bK_0k}}{2}\, e^{\lambda_1^s t_0} - c_2 \dfrac{aK_0k + \sqrt{(aK_0k)^2 - 4bK_0k}}{2}\, e^{\lambda_2^s t_0}, \end{cases}$$

$$\begin{cases} t_0 = \dfrac{\ln\left(-\dfrac{c_2}{c_1} \right)}{\sqrt{(aK_0k)^2 - 4bK_0k}}, \\ y(t_0) = -c_1 \dfrac{aK_0k - \sqrt{(aK_0k)^2 - 4bK_0k}}{2}\, e^{\lambda_1^s t_0} - c_2 \dfrac{aK_0k + \sqrt{(aK_0k)^2 - 4bK_0k}}{2}\, e^{\lambda_2^s t_0}, \end{cases}$$

Transform the following expression

$$e^{\lambda_1^s t_0} = e^{\left(\ln\left(-\frac{c_2}{c_1}\right)\frac{\lambda_1^s}{\sqrt{(aK_0k)^2-4bK_0k}}\right)} = e^{\left(\ln\left(-\frac{c_2}{c_1}\right)\frac{\sqrt{(aK_0k)^2-4bK_0k}-aK_0k}{2\sqrt{(aK_0k)^2-4bK_0k}}\right)} =$$

$$= \left(e^{\ln\left(-\frac{c_2}{c_1}\right)}\right)^{\left(\frac{1}{2}-\frac{aK_0k}{2\sqrt{(aK_0k)^2-4bK_0k}}\right)} = \left(-\frac{c_2}{c_1}\right)^{\left(\frac{1}{2}-\frac{aK_0k}{2\sqrt{(aK_0k)^2-4bK_0k}}\right)}.$$

Similarly,

$$e^{\lambda_2^s t_0} = e^{\left(\ln\left(-\frac{c_2}{c_1}\right)\frac{\lambda_2^s}{\sqrt{(aK_0k)^2-4bK_0k}}\right)} = e^{-\left(\ln\left(-\frac{c_2}{c_1}\right)\frac{\sqrt{(aK_0k)^2-4bK_0k}+aK_0k}{2\sqrt{(aK_0k)^2-4bK_0k}}\right)} =$$

$$= \left(e^{\ln\left(-\frac{c_2}{c_1}\right)}\right)^{-\left(\frac{1}{2}+\frac{aK_0}{2\sqrt{(aK_0)^2-\frac{4bK_0}{k}}}\right)} = \left(-\frac{c_2}{c_1}\right)^{\left(\frac{1}{2}-\frac{aK_0k}{2\sqrt{(aK_0k)^2-4bK_0k}}\right)-1}.$$

Then

$$y(t_0) = -c_1\frac{aK_0k-\sqrt{(aK_0k)^2-4bK_0k}}{2}\,e^{\lambda_1^s t_0} - c_2\frac{aK_0k+\sqrt{(aK_0k)^2-4bK_0k}}{2}\,e^{\lambda_2^s t_0},$$

$$y(t_0) = -c_1\frac{aK_0k-\sqrt{(aK_0k)^2-4bK_0k}}{2}\left(-\frac{c_2}{c_1}\right)^{\left(\frac{1}{2}-\frac{aK_0k}{2\sqrt{(aK_0k)^2-4bK_0k}}\right)} -$$

$$- c_2\frac{aK_0k+\sqrt{(aK_0k)^2-4bK_0k}}{2}\left(-\frac{c_2}{c_1}\right)^{\left(\frac{1}{2}-\frac{aK_0k}{2\sqrt{(aK_0k)^2-4bK_0k}}\right)-1},$$

$$y(t_0) = -c_1\frac{aK_0k-\sqrt{(aK_0k)^2-4bK_0k}}{2}\left(-\frac{c_2}{c_1}\right)^{\left(\frac{1}{2}-\frac{aK_0k}{2\sqrt{(aK_0k)^2-4bK_0k}}\right)} +$$

$$+ c_1\frac{aK_0k+\sqrt{(aK_0k)^2-4bK_0k}}{2}\left(-\frac{c_2}{c_1}\right)^{\left(\frac{1}{2}-\frac{aK_0k}{2\sqrt{(aK_0k)^2-4bK_0k}}\right)}.$$

As a result, for the case $(aK_0k)^2-4bK_0k>0$, when a stable equilibrium $\left(\theta_{\text{eq}}^s, y_{\text{eq}}\right)$ is a stable node, $S'(\theta_{\text{eq}}^s)$ can be found from the following formula

$$S'(\theta_{\text{eq}}^s) = c_1\sqrt{(aK_0k)^2-4bK_0k}\left(-\frac{c_2}{c_1}\right)^{\left(\frac{1}{2}-\frac{aK_0k}{2\sqrt{(aK_0k)^2-4bK_0k}}\right)}, \qquad \text{(A.11)}$$

where

$$c_1 = \left(\frac{\sqrt{(aK_0)^2 + 4bK_0(\pi - \frac{1}{k})}}{\sqrt{(aK_0)^2 - \frac{4bK_0}{k}}} + 1 \right) : 2k, \qquad c_2 = \left(1 - \frac{\sqrt{(aK_0)^2 + 4bK_0(\pi - \frac{1}{k})}}{\sqrt{(aK_0)^2 - \frac{4bK_0}{k}}} \right) : 2k.$$

Appendix A.2. Stable focus

This case corresponds to $(aK_0)^2 - \frac{4bK_0}{k} < 0$. The eigenvectors X_1^s, X_2^s are found in the same way as in Appendix A.1:

$$X_1^s = \begin{pmatrix} 1 \\ -\dfrac{aK_0k - i\sqrt{4bK_0k - (aK_0k)^2}}{2} \end{pmatrix}, \qquad X_2^s = \begin{pmatrix} 1 \\ -\dfrac{aK_0k + i\sqrt{4bK_0k - (aK_0k)^2}}{2} \end{pmatrix}.$$

The eigenvectors X_1^s, X_2^s can be represented as

$$X_{1,2}^s(t) = U_{1,2}^s + iV_{1,2}^s,$$

where $U_{1,2}^s$, $V_{1,2}^s$ are real two-dimensional vectors:

$$U_1^s = \begin{pmatrix} 1 \\ -\dfrac{aK_0k}{2} \end{pmatrix}, \qquad V_1^s = \begin{pmatrix} 0 \\ \dfrac{\sqrt{4bK_0k - (aK_0k)^2}}{2} \end{pmatrix},$$

$$U_2^s = \begin{pmatrix} 1 \\ -\dfrac{aK_0k}{2} \end{pmatrix}, \qquad V_2^s = \begin{pmatrix} 0 \\ -\dfrac{\sqrt{4bK_0k - (aK_0k)^2}}{2} \end{pmatrix}.$$

Consider a solution of (A.1), which corresponds to the eigenvalue λ_1^s:

$$\begin{aligned} &Y_1(t) = e^{\lambda_1^s t} X_1^s = e^{(\operatorname{Re}\lambda_1^s + i\operatorname{Im}\lambda_1^s)t}\ (U_1^s + iV_1^s) = \\ &= e^{t\operatorname{Re}\lambda_1^s} (\cos(t\operatorname{Im}\lambda_1^s) + i\sin(t\operatorname{Im}\lambda_1^s))\,(U_1^s + iV_1^s) = \\ &e^{t\operatorname{Re}\lambda_1^s} (U_1^s \cos(t\operatorname{Im}\lambda_1^s) - V_1^s \sin(t\operatorname{Im}\lambda_1^s)) + \\ &+ ie^{t\operatorname{Re}\lambda_1^s} (U_1^s \sin(t\operatorname{Im}\lambda_1^s) + V_1^s \cos(t\operatorname{Im}\lambda_1^s)). \end{aligned}$$

A general solution of (A.1) takes the form

$$\begin{aligned} &Y(t) = c_1 e^{t\operatorname{Re}\lambda_1^s} (U_1^s \cos(t\operatorname{Im}\lambda_1^s) - V_1^s \sin(t\operatorname{Im}\lambda_1^s)) + \\ &+ c_2 e^{t\operatorname{Re}\lambda_1^s} (U_1^s \sin(t\operatorname{Im}\lambda_1^s) + V_1^s \cos(t\operatorname{Im}\lambda_1^s)) = \\ &= e^{t\operatorname{Re}\lambda_1^s} U_1^s (c_1 \cos(t\operatorname{Im}\lambda_1^s) + c_2 \sin(t\operatorname{Im}\lambda_1^s)) + \\ &+ e^{t\operatorname{Re}\lambda_1^s} V_1^s (c_2 \cos(t\operatorname{Im}\lambda_1^s) - c_1 \sin(t\operatorname{Im}\lambda_1^s)). \end{aligned}$$

In other words,

$$\begin{cases} \theta_\Delta(t) = e^{t\operatorname{Re}\lambda_1^s} (c_1 \cos(t\operatorname{Im}\lambda_1^s) + c_2 \sin(t\operatorname{Im}\lambda_1^s)), \\ y(t) = -\dfrac{aK_0k\, e^{t\operatorname{Re}\lambda_1^s}}{2} (c_1 \cos(t\operatorname{Im}\lambda_1^s) + c_2 \sin(t\operatorname{Im}\lambda_1^s)) + \\ + \dfrac{e^{t\operatorname{Re}\lambda_1^s} \sqrt{4bK_0k - (aK_0k)^2}}{2} (c_2 \cos(t\operatorname{Im}\lambda_1^s) - c_1 \sin(t\operatorname{Im}\lambda_1^s)). \end{cases} \tag{A.12}$$

Let us find the coefficients c_1, c_2 for the solution of the Cauchy problem with the initial data $\theta_\Delta(0)=\frac{1}{k}$, $y(0)=\frac{\sqrt{(aK_0)^2+4bK_0(\pi-\frac{1}{k})}-aK_0}{2}$, similarly to Appendix A.1.

$$\begin{cases} \dfrac{1}{k}=e^{0\operatorname{Re}\lambda_1^s}\left(c_1\cos\left(0\operatorname{Im}\lambda_1^s\right)+c_2\sin\left(0\operatorname{Im}\lambda_1^s\right)\right), \\ \dfrac{\sqrt{(aK_0)^2+4bK_0(\pi-\frac{1}{k})}-aK_0}{2}= \\ =-\dfrac{aK_0k\,e^{0\operatorname{Re}\lambda_1^s}}{2}\left(c_1\cos\left(0\operatorname{Im}\lambda_1^s\right)+c_2\sin\left(0\operatorname{Im}\lambda_1^s\right)\right)+ \\ +\dfrac{e^{0\operatorname{Re}\lambda_1^s}\sqrt{4bK_0k-(aK_0k)^2}}{2}\left(c_2\cos\left(0\operatorname{Im}\lambda_1^s\right)-c_1\sin\left(0\operatorname{Im}\lambda_1^s\right)\right), \end{cases}$$

$$\begin{cases} \dfrac{1}{k}=c_1, \\ \dfrac{\sqrt{(aK_0)^2+4bK_0(\pi-\frac{1}{k})}-aK_0}{2}=-\dfrac{aK_0k}{2}c_1+\dfrac{\sqrt{4bK_0k-(aK_0k)^2}}{2}c_2, \end{cases}$$

$$\begin{cases} c_1=\dfrac{1}{k}, \\ c_2=\dfrac{\sqrt{(aK_0)^2+4bK_0(\pi-\frac{1}{k})}}{k\sqrt{\dfrac{4bK_0}{k}-(aK_0)^2}}. \end{cases}$$

Next, let us find t_0 such that $\theta_\Delta(t_0)=0$.

$$0=e^{t_0\operatorname{Re}\lambda_1^s}\left(c_1\cos\left(t_0\operatorname{Im}\lambda_1^s\right)+c_2\sin\left(t_0\operatorname{Im}\lambda_1^s\right)\right),$$

$$-\frac{c_1}{c_2}=\operatorname{tg}\left(t_0\operatorname{Im}\lambda_1^s\right),$$

$$t_0=\frac{\operatorname{arctg}\left(-\dfrac{c_1}{c_2}\right)}{\operatorname{Im}\lambda_1^s}.$$

Finally, all the unknowns for $y(t_0)$ from (A.12) are found and $S'(\theta_{\text{eq}}^s)$ is as follows

$$S'(\theta_{\text{eq}}^s)=y(t_0)=-\frac{aK_0k\,e^{t_0\operatorname{Re}\lambda_1^s}}{2}\left(c_1\cos\left(t_0\operatorname{Im}\lambda_1^s\right)+c_2\sin\left(t_0\operatorname{Im}\lambda_1^s\right)\right)+$$
$$+\frac{e^{t_0\operatorname{Re}\lambda_1^s}\sqrt{4bK_0k-(aK_0k)^2}}{2}\left(c_2\cos\left(t_0\operatorname{Im}\lambda_1^s\right)-c_1\sin\left(t_0\operatorname{Im}\lambda_1^s\right)\right), \qquad \text{(A.13)}$$

where

$$t_0=\frac{\operatorname{arctg}\left(-\dfrac{c_1}{c_2}\right)}{\operatorname{Im}\lambda_1^s}, \qquad \lambda_1^s=\frac{-aK_0k+i\sqrt{4bK_0k-(aK_0k)^2}}{2},$$
$$c_1=\frac{1}{k}, \qquad c_2=\frac{\sqrt{(aK_0)^2+4bK_0(\pi-\frac{1}{k})}}{k\sqrt{\dfrac{4bK_0}{k}-(aK_0)^2}}.$$

Appendix A.3. Stable degenerated node

This case corresponds to $(aK_0)^2 - \frac{4bK_0}{k} = 0$. In this case the eigenvalues λ_1^s and λ_1^s coincide:

$$\lambda^s := -\frac{aK_0k}{2} = \lambda_1^s = \lambda_2^s.$$

A stable equilibrium $\left(\theta_{\text{eq}}^s, y_{\text{eq}}\right)$ is a stable degenerated node, or a stable proper node.

For the characteristic matrix

$$\begin{pmatrix} -\lambda^s & 1 \\ -bK_0k & -aK_0k - \lambda^s \end{pmatrix}$$

of (A.1) it is shown that $\left(\theta_{\text{eq}}^s, y_{\text{eq}}\right)$ is a stable degenerated node. Find the eigenvector X^s corresponding to the eigenvalue λ^s of algebraic multiplicity two:

$$\begin{pmatrix} -\lambda^s & 1 \\ -bK_0k & -aK_0k - \lambda^s \end{pmatrix} X^s = \mathbb{O},$$

$$\begin{pmatrix} \frac{aK_0k}{2} & 1 \\ -bK_0k & -\frac{aK_0k}{2} \end{pmatrix} X^s = \mathbb{O}.$$

Adding the first row, multiplied by $\frac{aK_0k}{2}$, to the second row, we have:

$$\begin{pmatrix} \frac{aK_0k}{2} & 1 \\ \frac{(aK_0k)^2}{4} - bK_0k & 0 \end{pmatrix} X^s = \mathbb{O}.$$

The eigenvector X^s can be written as

$$X^s = \begin{pmatrix} c \\ -c\frac{aK_0k}{2} \end{pmatrix}.$$

Choose $c = 1$. To find a general solution of (A.1), we need to additionally find the first associated vector X_1^s:

$$\begin{pmatrix} \frac{aK_0k}{2} & 1 \\ -bK_0k & -\frac{aK_0k}{2} \end{pmatrix} X_1^s = \begin{pmatrix} 1 \\ -\frac{aK_0k}{2} \end{pmatrix},$$

$$\begin{pmatrix} \frac{aK_0k}{2} & 1 \\ \frac{(aK_0k)^2}{4} - bK_0k & 0 \end{pmatrix} X_1^s = \begin{pmatrix} 1 \\ 0 \end{pmatrix},$$

$$X_1^s = \begin{pmatrix} c \\ c - c\frac{aK_0k}{2} \end{pmatrix}.$$

Choose $c = 1$.

A general solution of (A.1) has the form

$$\begin{cases} \theta_\Delta(t) = e^{\left(-\dfrac{aK_0k}{2}t\right)}\,(c_1 + c_2\,(t+1))\,, \\ y(t) = e^{\left(-\dfrac{aK_0k}{2}t\right)}\,\left(-\dfrac{aK_0k}{2}c_1 + c_2\left(-\dfrac{aK_0k}{2}t + 1 - \dfrac{aK_0k}{2}\right)\right). \end{cases} \tag{A.14}$$

Similarly to Appendix A.1 and Appendix A.2, let us find the coefficients c_1 and c_2 for the solution of the Cauchy problem with the initial data $\theta_\Delta(0) = \frac{1}{k}$ and $y(0) = \frac{\sqrt{(aK_0)^2 + 4bK_0(\pi - \frac{1}{k})} - aK_0}{2}$. In this case we have:

$$\begin{cases} \dfrac{1}{k} = c_1 + c_2, \\ \dfrac{\sqrt{(aK_0)^2 + 4bK_0(\pi - \frac{1}{k})} - aK_0}{2} = -\dfrac{aK_0k}{2}c_1 + c_2\left(1 - \dfrac{aK_0k}{2}\right), \end{cases}$$

$$\begin{cases} c_1 = \dfrac{1}{k} - c_2, \\ \dfrac{\sqrt{(aK_0)^2 + 4bK_0(\pi - \frac{1}{k})} - aK_0}{2} = -\dfrac{aK_0k}{2}\left(\dfrac{1}{k} - c_2\right) + c_2 - c_2\dfrac{aK_0k}{2}, \end{cases}$$

$$\begin{cases} c_1 = \dfrac{1}{k} - c_2, \\ \dfrac{\sqrt{(aK_0)^2 + 4bK_0(\pi - \frac{1}{k})}}{2} = c_2, \end{cases}$$

$$\begin{cases} c_1 = \dfrac{1}{k} - \dfrac{\sqrt{(aK_0)^2 + 4bK_0(\pi - \frac{1}{k})}}{2}, \\ c_2 = \dfrac{\sqrt{(aK_0)^2 + 4bK_0(\pi - \frac{1}{k})}}{2}. \end{cases}$$

Find t_0 such that $\theta_\Delta(t_0) = 0$:

$$\begin{cases} 0 = e^{\left(-\dfrac{aK_0k}{2}t_0\right)}\,(c_1 + c_2\,(t_0+1))\,, \\ y(t_0) = e^{\left(-\dfrac{aK_0k}{2}t_0\right)}\,\left(-\dfrac{aK_0k}{2}c_1 + c_2\left(-\dfrac{aK_0k}{2}t_0 + 1 - \dfrac{aK_0k}{2}\right)\right), \end{cases}$$

$$\begin{cases} 0 = e^{\left(-\dfrac{aK_0k}{2}t_0\right)}\,((c_1 + c_2) + c_2t_0)\,, \\ y(t_0) = e^{\left(-\dfrac{aK_0k}{2}t_0\right)}\,\left(-\dfrac{aK_0k}{2}(c_1 + c_2) + c_2\left(-\dfrac{aK_0k}{2}t_0 + 1\right)\right), \end{cases}$$

$$\begin{cases} 0 = \dfrac{1}{k} + c_2 t_0, \\ y(t_0) = e^{\left(-\dfrac{aK_0 k}{2} t_0\right)} \left(-\dfrac{aK_0}{2} + c_2 \left(-\dfrac{aK_0 k}{2} t_0 + 1\right)\right), \end{cases}$$

$$\begin{cases} t_0 = -\dfrac{1}{c_2 k}, \\ y(t_0) = e^{\left(-\dfrac{aK_0 k}{2} t_0\right)} \left(-\dfrac{aK_0}{2} - \dfrac{aK_0 k c_2}{2} t_0 + c_2\right). \end{cases}$$

Finally, the expression for $S'(\theta^s_{\text{eq}})$ is as follows

$$S'(\theta^s_{\text{eq}}) = y(t_0) = c_2 \, e^{\left(\dfrac{aK_0}{2c_2}\right)}, \tag{A.15}$$

where

$$c_2 = \frac{\sqrt{(aK_0)^2 + 4bK_0(\pi - \frac{1}{k})}}{2}.$$

ACKNOWLEDGMENTS

This work was supported by the Russian Scientific Foundation and Saint-Petersburg State University. The authors would like to thank Roland E. Best, the founder of the Best Engineering Company, Oberwil, Switzerland and the author of the bestseller on PLL-based circuits Best (2007) for valuable discussion.

References

G. Ascheid and H. Meyr. Cycle slips in phase-locked loops: A tutorial survey. *Communications, IEEE Transactions on*, 30(10):2228–2241, 1982.

R Jacob Baker. *CMOS: Circuit Design, Layout, and Simulation*, volume 18. John Wiley & Sons, 2011.

R.E. Best. *Phase-Lock Loops: Design, Simulation and Application*. McGraw-Hill, 6th edition, 2007.

R.E. Best, N.V. Kuznetsov, O.A. Kuznetsova, G.A. Leonov, M.V. Yuldashev, and R.V. Yuldashev. A short survey on nonlinear models of the classic Costas loop: rigorous derivation and limitations of the classic analysis. In *Proceedings of the American Control Conference*, pages 1296–1302. IEEE, 2015. doi: 10.1109/ACC.2015.7170912. art. num. 7170912, http://arxiv.org/pdf/1505.04288v1.pdf.

O. B. Ershova and G. A. Leonov. Frequency estimates of the number of cycle slidings in phase control systems. *Avtomat. Remove Control*, 44(5):600–607, 1983.

F.M. Gardner. *Phase-lock techniques*. John Wiley & Sons, New York, 1966.

F.M. Gardner. *Phase-lock techniques*. John Wiley & Sons, New York, 2nd edition, 1979.

F.M. Gardner. *Phaselock Techniques*. Wiley, 3rd edition, 2005.

S.J. Goldman. *Phase-Locked Loops Engineering Handbook for Integrated Circuits*. Artech House, 2007.

N. A. Gubar'. Investigation of a piecewise linear dynamical system with three parameters. *J. Appl. Math. Mech.*, 25(6):1011–1023, 1961.

M. Kihara, S. Ono, and P. Eskelinen. *Digital Clocks for Synchronization and Communications*. Artech House, 2002.

V.F. Kroupa. *Phase Lock Loops and Frequency Synthesis*. John Wiley & Sons, 2003.

J. Kudrewicz and S. Wasowicz. *Equations of phase-locked loop. Dynamics on circle, torus and cylinder*. World Scientific, 2007.

N.V. Kuznetsov, O.A. Kuznetsova, G.A. Leonov, P. Neittaanmaki, M.V. Yuldashev, and R.V. Yuldashev. Limitations of the classical phase-locked loop analysis. *Proceedings - IEEE International Symposium on Circuits and Systems*, 2015-July:533–536, 2015a. doi: http://dx.doi.org/10.1109/ISCAS.2015.7168688.

N.V. Kuznetsov, G.A. Leonov, S.M. Seledzgi, M.V. Yuldashev, and R.V. Yuldashev. Elegant analytic computation of phase detector characteristic for non-sinusoidal signals. *IFAC-PapersOnLine*, 48(11):960–963, 2015b. doi: http://dx.doi.org/10.1016/j.ifacol.2015.09.316.

N.V. Kuznetsov, G.A. Leonov, M.V. Yuldashev, and R.V. Yuldashev. Rigorous mathematical definitions of the hold-in and pull-in ranges for phase-locked loops. *IFAC-PapersOnLine*, 48(11):710–713, 2015c. doi: http://dx.doi.org/10.1016/j.ifacol.2015.09.272.

G. A. Leonov and K. D. Aleksandrov. Frequency-Domain Criteria for the Global Stability of Phase Synchronization Systems. *Doklady Mathematics*, 92(3):764–768, 2015.

G.A. Leonov and N.V. Kuznetsov. *Nonlinear Mathematical Models of Phase-Locked Loops. Stability and Oscillations*. Cambridge Scientific Publisher, 2014.

G.A. Leonov, N.V. Kuznetsov, M.V. Yuldahsev, and R.V. Yuldashev. Analytical method for computation of phase-detector characteristic. *IEEE Transactions on Circuits and Systems - II: Express Briefs*, 59(10):633–647, 2012. doi: 10.1109/TCSII.2012.2213362.

G.A. Leonov, N.V. Kuznetsov, M.V. Yuldashev, and R.V. Yuldashev. Nonlinear dynamical model of Costas loop and an approach to the analysis of its stability in the large. *Signal processing*, 108:124–135, 2015a. doi: 10.1016/j.sigpro.2014.08.033.

G.A. Leonov, N.V. Kuznetsov, M.V. Yuldashev, and R.V. Yuldashev. Hold-in, pull-in, and lock-in ranges of PLL circuits: rigorous mathematical definitions and limitations of classical theory. *IEEE Transactions on Circuits and Systems–I: Regular Papers*, 62 (10):2454–2464, 2015b. doi: http://dx.doi.org/10.1109/TCSI.2015.2476295.

Y.A. Mitropolsky and N.N. Bogolubov. *Asymptotic Methods in the Theory of Non-Linear Oscillations*. Gordon and Breach, New York, 1961.

A.M. Samoilenko and R. Petryshyn. *Multifrequency Oscillations of Nonlinear Systems*. Mathematics and Its Applications. Springer, 2004.

V.V. Shakhgil'dyan and A.A. Lyakhovkin. *Fazovaya avtopodstroika chastoty (in Russian)*. Svyaz', Moscow, 1966.

V. Smirnova, A. Proskurnikov, and N. Utina. Problem of cycle-slipping for infinite dimensional systems with MIMO nonlinearities. In *Ultra Modern Telecommunications and Control Systems and Workshops (ICUMT), 2014 6th International Congress on*, pages 590–595. IEEE, 2014.

J.L. Stensby. *Phase-Locked Loops: Theory and Applications*. Phase-locked Loops: Theory and Applications. Taylor & Francis, 1997.

A. Viterbi. *Principles of coherent communications*. McGraw-Hill, New York, 1966.

PIII

FREQUENCY-DOMAIN CRITERIA FOR THE GLOBAL STABILITY OF PHASE SYNCHRONIZATION SYSTEMS

by

G. A. Leonov, K. D. Aleksandrov 2015

Doklady Mathematics, Vol. 92, No. 3, pp. 769 – 772

PIV

PULL-IN RANGE OF THE PLL-BASED CIRCUITS WITH PROPORTIONALLY-INTEGRATING FILTER

by

K. D. Aleksandrov, N. V. Kuznetsov, G. A. Leonov, P. Neittaanmäki, S. M. Seledzhi 2015

IFAC-PapersOnLine, Vol. 48, No. 11, pp. 720 – 724

Available online at www.sciencedirect.com

ScienceDirect

IFAC-PapersOnLine 48-11 (2015) 720–724

IFAC Papers Online
CONFERENCE PAPER ARCHIVE

Pull-in range of the PLL-based circuits with proportionally-integrating filter

Konstantin D. Alexandrov, **Nikolay V. Kuznetsov**, **Gennady A. Leonov**, **Pekka Neittaanmäki** **Svetlana M. Seledzhi**

Saint-Petersburg State University, Universitetsky pr. 28, Saint-Petersburg, 198504, Russia
Dept. of Mathematical Information Technology, University of Jyväskylä, P.O. Box 35 (Agora), FIN-40014, Finland
e-mail: nkuznetsov239@gmail.com

AbstractIn the present work the pull-in range of PLL-based circuits with proportionally-integrating filter is studied. Two approaches based on the methods of phase plane analysis and Lyapunov functions are discussed.

Keywords: phase-locked loop, nonlinear analysis, PLL, Costas loop, pull-in range, hidden oscillations

1. INTRODUCTION

The PLL circuit has been invented by French engineer Henri de Bellescize in 1932 (Bellescize, 1932) for the use in synchrodyne radio receivers – as alternative to a popular, at the time, superheterodyne. Since then, various modifications of PLL circuits (digital PLL, all-digital PLL, software PLL, neuronal PLL and so on) have been developed. Moreover, new circuits, based on PLL operation principles, were invented. One of such circuits is the Costas loop, which was invented by American engineer John Costas in 1956 (Costas, 1956; Costas, 1962).

The PLL-based circuits are widely used in radio engineering for signal demodulation, carrier frequency recovery, and frequency synthesis (see, e.g., (Best, 2007)). After the invention of integral circuits, PLL-based circuits have started to be applied to computer architecture, for example, for synchronization of multiprocessors' clocks (Smith, 1999; Gardner et al., 1993). At the present time there are lots of publications devoted to the study of PLL-based circuits.

One of the important problem, related to the study of PLL-based circuits, is to find a pull-in range – difference of reference and tunable oscillators' frequencies for which synchronization occurs for any initial state of the circuit. Two effective analytical approaches for the pull-in range estimation are known. The first one is based on the integration of the phase plane trajectories and the analysis of their behavior (Tricomi, 1933; Andronov et al., 1937). Using this approach, in (Viterbi, 1966) it is stated that the pull-in range of the classical PLL with sinusoidal characteristic of the phase detector is infinite (to complete rigorously explanations given in (Viterbi, 1966), one has to prove the nonexistence of heteroclitic trajectory and the first-order limit cycles). In a recent paper (not yet published) Roland E. Best formulated a similar statement as a conjecture for two-phase Costas loop. The second approach is based on the Lyapunov function (Lyapunov, 1892) construction and the use of global stability criteria for the cylindrical phase space (Yakubovich et al., 2004; Leonov and Kuznetsov, 2014).

In the present work rigorous analytical study of the pull-in range by both methods are discussed. Here the application of the method of phase plane analysis is demonstrated for the PLL-based circuits with sinusoidal phase detector (PD) characteristics and the method of Lyapunov function is applied to PD characteristics in general form.

2. MODEL OF PLL-BASED CIRCUITS IN SIGNAL'S PHASE SPACE

For the description of PLL-based circuits, a physical model in the signals space and a mathematical model in signal's phase space are used. The models of PLL-based circuits in signal's phase space were described in the works related to 60-s of XX century (Viterbi, 1966; Shakhgil'dyan and Lyakhovkin, 1966; Gardner, 1966). The main advantage of models in the signal's phase space is the nonexistence of high-frequency components. Thus, simulation in signal's phase space allows one to consider slow varying frequency only. By contrast, the simulation of PLL-based circuits in the signals space is complicated since one has to observe simultaneously both high-frequency (fast changing of phases) and low-frequency (relatively slow changing of frequencies) oscillations (Abramovitch, 2008).

The physical models of PLL-based circuits can be reduced to the models in signal's phase space (Leonov et al., 2012; Leonov and Kuznetsov, 2014) by the averaging methods (see, e.g., (Mitropolsky and Bogolubov, 1961; Samoilenko and Petryshyn, 2004)). In order to study models of PLL-based circuits in signal's phase space it

⋆ This work was supported by Saint-Petersburg State University (project 6.39.416.2014, s. 3-4; project 6.38.505.2014, s. 5.). and Russian Scientific Foundation (project 14-21-00041, s. 6).

Peer review under responsibility of International Federation of Automatic Control.
10.1016/j.ifacol.2015.09.274

is necessary to compute characteristic of a phase detector – nonlinear element of PLL-based circuits for matching tunable signals. The characteristic of a phase detector $\varphi(\theta_1(t)-\theta_2(t))$ (further it will be denoted $\theta_e(t)=\theta_1(t)-\theta_2(t)$) is a function with respect to the difference of phases of reference and tunable oscillators (for the model in the signals space the result of the work of phase detector $\varphi(t)$ depends on time t).

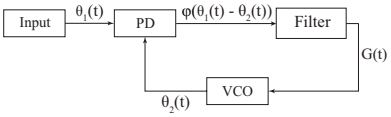

Figure 1. Model of PLL-based circuit in signal's phase space.

Let us describe a general model of PLL-based circuits in signal's phase space. A reference oscillator and a tunable oscillator generate phases $\theta_1(t)$ and $\theta_2(t)$ respectively. The frequency of carrier signal is constant and equals to ω_1:

$$\frac{d\theta_1(t)}{dt}=\omega_1. \tag{1}$$

The VCO free-running frequency is denoted by ω_{free}.

The phases $\theta_1(t)$ and $\theta_2(t)$ enter the inputs of a phase detector. A signal of phase detector output $\varphi(\theta_e(t))$ is filtered by Filter. In the context of considered conjecture the Filter is chosen to be proportionally-integrating with the transfer function $W(s)=\frac{b+as}{s}$, $a>0$, $b>0$. The Filter is described by the equation

$$\frac{dG(t)}{dt}=a\frac{d\varphi(\theta_e(t))}{dt}+b\varphi(\theta_e(t)). \tag{2}$$

The output of Filter $G(t)$ serves as a control signal for VCO:

$$\frac{d\theta_2(t)}{dt}=\omega_{free}+K_0G(t), \tag{3}$$

where $K_0>0$ is a VCO gain coefficient.

3. TWO-PHASE MODIFICATIONS OF PLL-BASED CIRCUITS

In this section two-phase PLL-based circuits: the two-phase PLL circuit and the two-phase Costas loop, are described.

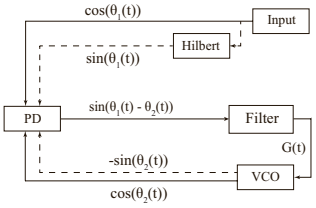

Figure 2. Two-phase PLL circuit.

A block diagram of the two-phase PLL circuit is shown in Fig. 2 (see also (Best et al., 2014)). The components of this circuit are the following: reference oscillator (Input), Hilbert converter (Hilbert), tunable oscillator (VCO), complex multiplier as a phase detector, and filter (Filter).

The reference oscillator Input generates a carrier signal $\cos(\theta_1(t))$. The carrier signal is transformed by the Hilbert converter in $\sin(\theta_1(t))$. The tunable oscillator VCO generates signals $cos(\theta_2(t))$ and $-\sin(\theta_2(t))$.

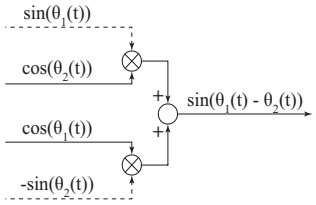

Figure 3. Complex multiplier of the two-phase PLL circuit.

To attain phase synchronization of frequency, the complex multiplier (see Fig. 3) is used. The signals, generated by Input and VCO, enter the input of the complex multiplier. Signal

$$\begin{aligned}\varphi(\theta_e(t))&=\sin(\theta_1(t))\cos(\theta_2(t))+\\&+\cos(\theta_1(t))(-\sin(\theta_2(t)))=\sin(\theta_e(t)),\end{aligned} \tag{4}$$

which is generated by a complex multiplier, enters the input of the Filter. The signal $G(t)$, obtained as a result of filtration $\varphi(\theta_e(t))$ serves as a control signal of VCO.

A physical model of the two-phase PLL circuit in the signals space is equivalent to a mathematical model in signal's phase space since the characteristic of the phase detector depends on $\theta_e(t)$.

By the given in Section 2 equations (1), (2), and (3), the work of the two-phase PLL circuit is described by the second order differential equation with respect to variable $\theta_e(t)$:

$$\ddot{\theta}_e(t)+aK_0\cos(\theta_e(t))\dot{\theta}_e(t)+bK_0\sin(\theta_e(t))=0. \tag{5}$$

A detailed study of equation (5) is given in Section 6.1.

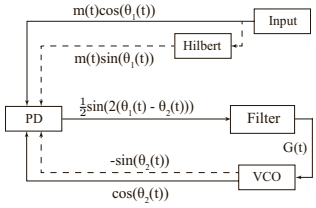

Figure 4. The two-phase Costas loop.

The device of the two-phase Costas loop (see Fig 4) is described in detail in (Tretter, 2007; Leonov and Kuznetsov, 2014; Best et al., 2014). The main difference between the two-phase Costas loop and the two-phase PLL circuit is a device of complex multiplier (see Fig. 5), which is used as a phase detector.

For the two-phase Costas loop, the characteristic of phase detector is as follows $\varphi(\theta_e(t))=\frac{1}{2}\sin(2\theta_e(t))$. As in the

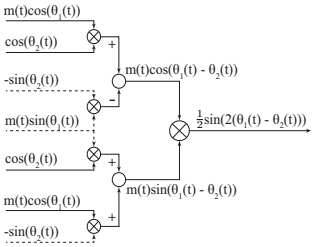

Figure 5. Complex multiplier of the two-phase Costas loop.

case of the two-phase PLL circuit, the two-phase Costas loop can be described by the second order differential equation

$$2\ddot{\theta}_e(t) + aK_0\cos(2\theta_e(t))2\dot{\theta}_e(t) + bK_0\sin(2\theta_e(t)) = 0. \quad (6)$$

Equation (6) is reduced to equation (5) by the change $\theta_e(t) \to \frac{1}{2}\theta_e(t)$.

4. DESCRIPTION OF THE PLL CIRCUIT

Consider a physical model of the PLL circuit in the signals space (see Fig. 6). The Input of reference oscillator

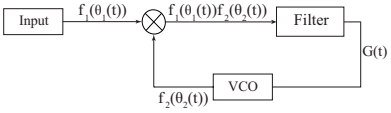

Figure 6. Model of the PLL circuit in signal's phase space.

generates a carrier signal $f_1(\theta_1(t))$ with the phase $\theta_1(t)$. The tunable oscillator VCO generates a signal $f_2(\theta_2(t))$ with the phase $\theta_2(t)$. A phase detector of the PLL circuit is a multiplier. The multiplier receives the signals of the reference and tunable oscillators and generates its product $f_1(\theta_1(t))f_2(\theta_2(t))$.

A phase detector characteristic of a mathematical model of the PLL circuit's depends on the form of signals of the reference and tunable oscillators. For the pairs of signals $f_1(\theta_1)$, $f_2(\theta_2)$, given in Table 1, the characteristics of phase detector are sinusoidal.

$f_1(\theta_1) = \sin(\theta_1)$ $f_2(\theta_2) = \sin(\theta_2)$	$\varphi(\theta_e) = \frac{1}{2}\cos(\theta_e)$
$f_1(\theta_1) = \sin(\theta_1)$ $f_2(\theta_2) = \mathrm{sgn}(\sin(\theta_2))$	$\varphi(\theta_e) = \frac{2}{\pi}\cos(\theta_e)$
$f_1(\theta_1) = \begin{cases} \frac{2}{\pi}\theta_1 + 1, \theta_1 \in [0;\pi], \\ 1 - \frac{2}{\pi}\theta_1, \theta_1 \in [\pi;2\pi] \end{cases}$ $f_2(\theta_2) = \sin(\theta_2)$	$\varphi(\theta_e) = \frac{4}{\pi^2}\sin(\theta_e)$

Table 1. Characteristic of PD $\varphi(\theta_e)$ of the PLL circuit.

Further a derivative with respect to θ_e will be denoted by φ'. From the given in Section 2 equations (1), (2), and (3) for the models of the PLL circuit in signal's phase space one obtains

$$\ddot{\theta}_e(t) + aK_0\varphi'(\theta_e(t))\dot{\theta}_e(t) + bK_0\varphi(\theta_e(t)) = 0. \quad (7)$$

$\varphi(\theta_e) = \frac{1}{2}\cos(\theta_e)$	$\theta_e \to \theta_e + \frac{\pi}{2}$ $K_0 \to 2K_0$
$\varphi(\theta_e) = \frac{2}{\pi}\cos(\theta_e)$	$\theta_e \to \theta_e + \frac{\pi}{2}$ $K_0 \to \frac{\pi}{2}K_0$
$\varphi(\theta_e) = \frac{4}{\pi^2}\sin(\theta_e)$	$K_0 \to \frac{\pi^2}{4}K_0$

Table 2. Reduction of equation (7) to equation (5).

For the characteristics of phase detector from Table 1, by the linear changes from Table 2 equation (7) can be reduced to equation (5).

5. DESCRIPTION OF THE COSTAS LOOP

Consider a model of electronic realization of the BPSK Costas loop (see Fig. 7). The components of the circuit

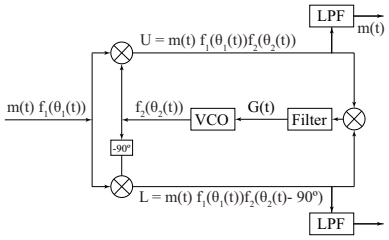

Figure 7. Realization of the BPSK Costas loop.

are the following: reference oscillator (Input), tunable oscillator (VCO), two multipliers, Hilbert converter, low-pass side filters (LPF), and filter (Filter).

The Input generates a signal $m(t)f_1(\theta_1(t))$, which is a product of a signal of data $m(t) = \pm 1$ and a carrier high-frequency signal $f_1(\theta_1(t))$. The VCO generates a signal $f_2(\theta_2(t))$.

In the lower branch of circuit the signal L is obtained by the Hilbert transformation of VCO signal and its multiplication by carrier signal. In the upper branch the signal U is obtained by the multiplication of carrier signal and bias-free signal of VCO. After a transient process, on the upper branch the demodulation process occurs. In this case the signals U and L pass the circuit's side filters (LPF).

The control signal $G(t)$ of tunable oscillator VCO is obtained after the passing through Filter of a signal, which arises as a result of multiplication (by the multiplier) of the signals U and L. Since $G(t)$ is independent on signal data $m(t)$, further one assumes that $m(t) \equiv 1$.

For sinusoidal signals $f_1(\theta_1(t)) = \sin(\theta_1(t))$ and $f_2(\theta_2(t)) = \sin(\theta_2(t))$ the characteristic of phase detector in signal's phase space is as follows

$$\varphi(\theta_e(t)) = -\frac{1}{8}\sin(\theta_1(t) - \theta_2(t)).$$

Similarly to the computations in Sections 3 and 4, a model of the Costas loop in signal's phase space can be described by the second order differential equation

$$\ddot{\theta_e}(t) - \frac{aK_0}{8}\cos(\theta_e(t))\dot{\theta_e}(t) - \frac{bK_0}{8}\sin(\theta_e(t)) = 0. \quad (8)$$

By the changes $\theta_e \to \theta_e + \pi$, $K_0 \to 8K_0$ equation (8) is reduced to equation (5).

6. ANALYTICAL APPROACHES TO PULL-IN RANGE ANALYSIS

6.1 Sinusoidal PD characteristic

Consider the conjecture on pull-in range of PLL-based circuits.

Assertion 1. The pull-in range for the considered PLL-based circuits with proportionally-integrating filter is infinite.

For equation (5), which describes the work of all considered circuits up to linear changes, Assertion 1 can be reformulated in the following way:

For arbitrary parameters of circuits $a > 0$, $b > 0$, and $K_0 > 0$ any solution of equation (5) tends to stationary set of system as $t \to +\infty$.

To prove Assertion 1, let us consider the classical analytical approach, based on the phase plane analysis. In (Viterbi, 1966), by the methods of phase plane analysis, it is explained that the pull-in range of the classical PLL with PI filter and sinusoidal characteristic of the phase detector is infinite. However to complete rigorously the explanations given in (Viterbi, 1966), one has to prove the nonexistence of a heteroclitic trajectory and first-order limit cycles.

The consideration of a filter Filter with small parameter allows one to integrate separatrices and demonstrate the nonexistence of heteroclinic cycles (Alexandrov et al., 2014).

Equation (5) with $a = \varepsilon$, where $0 < \varepsilon \ll 1$ is a small parameter, can be represented as the following equivalent system

$$\begin{cases} \dot{\theta_e}(t) = y(t), \\ \dot{y}(t) = -\varepsilon K_0 \cos(\theta_e(t)) y(t) - bK_0 \sin(\theta_e(t)). \end{cases} \tag{9}$$

Let us expand the separatrices of the upper half-plane of a phase plane $R(\theta_e, \varepsilon)$ and $S(\theta_e, \varepsilon)$ in a Taylor series in variable ε, and find a necessary number of terms of series for the conclusion about mutual disposition of the approximations of these separatrices. It is possible to show analytically that a mutual disposition of separatrices themselves on the phase plane coincides with a mutual disposition of their approximations by a Taylor series in variable $\varepsilon \ll 1$. A qualitative disposition of $R(\theta_e, \varepsilon)$ and $S(\theta_e, \varepsilon)$ is shown in Fig. 8.

Considered approach is also useful for the estimation of lock-in domain, which is bounded by the separatrices (Gardner, 1979). However, one of the problems of the phase plane analysis is that for any new type of PD characteristic one has to do a lot of new cumbersome integrations.

By contrast, the second approach, which is based on the Lyapunov function construction in the cylindrical phase space (Lyapunov, 1892), allows one to consider PD characteristic in general form. In (Bakaev, 1963) the following system

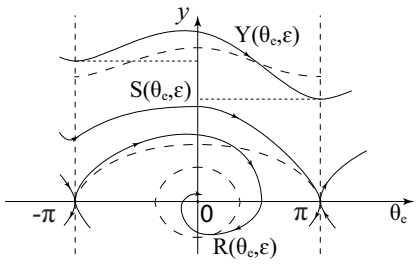

Figure 8. Phase portrait of system (9).

$$\begin{cases} \dot{x} = \sin\theta_e, \\ \dot{\theta}_e = -aK_0 \sin\theta_e - bK_0 x, \end{cases}$$

which is equivalent to (5), was consider and corresponding Lyapunov function was suggested:

$$V(x, \theta_e) = bK_0 \frac{x^2}{2} + 2\sin^2 \frac{\theta_e}{2}.$$

The required modifications of the classical global stability criteria for the cylindrical phase space have been developed in (Gelig et al., 1978; Leonov et al., 1992, 1996a,b; Yakubovich et al., 2004; Leonov and Kuznetsov, 2014).

6.2 PD characteristic in general form

Below we consider PLL with PD characteristic in general form, which is periodic with period Δ and continuous,

$$\begin{cases} \dot{z} = b\varphi(\theta_e), \\ \dot{\theta_e} = -K_0 z - aK_0 \varphi(\theta_e). \end{cases} \tag{10}$$

The following theorem is valid.

Theorem 1. Suppose

$$\int_0^{\Delta} \varphi(\theta_e) d\theta_e = 0;$$

$$\forall \theta_e^0 \in (-\infty, +\infty) \qquad \exists \delta > 0 :$$

$$\int_{\theta_e^0}^{\theta_e} \varphi(\theta_e) d\theta_e \neq 0, \qquad \forall \theta_e \in \left(\theta_e^0 - \delta, \theta_e^0 + \delta\right).$$

Then for $a > 0$, $b > 0$, and $K_0 > 0$ any solution of system (10) tends to the stationary set of the system as $t \to +\infty$.

The proof of the theorem is based on consideration of the following Lyapunov function:

$$V(z, \theta_e) = \frac{K_0}{2b} z^2 + \int_0^{\theta_e} \varphi(\theta_e) d\theta_e.$$

7. CONCLUSION

Two different analytical approaches for the pull-in range estimation are discussed. The first one is based on the integration of trajectories and can be applied to sinusoidal and piecewise linear PD characteristic (Alexandrov et al., 2014, 2015). The second one is based on Lyapunov function

constructions and allows one to study effectively PD characteristics in general form.

REFERENCES

Abramovitch, D. (2008). Efficient and flexible simulation of phase locked loops, part I: simulator design. In *American Control Conference*, 4672–4677. Seattle, WA.

Alexandrov, K.D., Kuznetsov, N.V., Leonov, G.A., Neittaanmäki, P., and Seledzhi, S.M. (2015). Pull-in range of the classical PLL with impulse signals. In *the 8th Vienna International Conference on Mathematical Modelling (MATHMOD 2015)*.

Alexandrov, K.D., Kuznetsov, N.V., Leonov, G.A., and Seledzhi, S.M. (2014). Best's conjecture on pull-in range of two-phase Costas loop. In *6th International Congress on Ultra Modern Telecommunications and Control Systems (ICUMT 2014)*, 78 – 82.

Andronov, A.A., Vitt, E.A., and Khaikin, S.E. (1937). *Theory of oscillations I.* ONTI NKTP SSSR, Moscow [in Russian].

Bakaev, Y.N. (1963). Stability and dynamical properties of astatic frequency synchronization system. *Radiotekhnika i Elektronika*, 8(3), 513–516.

Bellescize, H. (1932). La réception synchrone. *L'onde Électrique*, 11, 230–340.

Best, R.E., Kuznetsov, N.V., Leonov, G.A., Yuldashev, M.V., and Yuldashev, R.V. (2014). *Discontinuity and Complexity in Nonlinear Physical Systems*, volume 6, chapter Nonlinear analysis of phase-locked loop based circuits. Springer. doi:10.1007/978-3-319-01411-1_10.

Best, R. (2007). *Phase-Lock Loops: Design, Simulation and Application.* McGraw-Hill, 6th edition.

Costas, J.P. (1962). Receiver for communication system. US Patent 3,047,659.

Costas, J. (1956). Synchoronous communications. In *Proc. IRE*, volume 44, 1713–1718.

Gardner, F. (1966). *Phase-lock techniques.* John Wiley & Sons, New York.

Gardner, F. (1979). *Phase-lock techniques.* John Wiley & Sons, New York, 2nd edition.

Gardner, F., Erup, L., and Harris, R. (1993). Interpolation in digital modems - part II: Implementation and performance. *IEEE Electronics and Communication Engineering Journal*, 41(6), 998–1008.

Gelig, A., Leonov, G., and Yakubovich, V. (1978). *Stability of Nonlinear Systems with Nonunique Equilibrium (in Russian).* Nauka.

Leonov, G.A., Burkin, I.M., and Shepelyavy, A.I. (1996a). *Frequency Methods in Oscillation Theory.* Kluwer, Dordretch.

Leonov, G.A. and Kuznetsov, N.V. (2014). *Nonlinear Mathematical Models Of Phase-Locked Loops. Stability and Oscillations.* Cambridge Scientific Press.

Leonov, G.A., Kuznetsov, N.V., Yuldahsev, M.V., and Yuldashev, R.V. (2012). Analytical method for computation of phase-detector characteristic. *IEEE Transactions on Circuits and Systems - II: Express Briefs*, 59(10), 633–647. doi:10.1109/TCSII.2012.2213362.

Leonov, G.A., Ponomarenko, D.V., and Smirnova, V.B. (1996b). *Frequency-Domain Methods for Nonlinear Analysis. Theory and Applications.* World Scientific, Singapore.

Leonov, G.A., Reitmann, V., and Smirnova, V.B. (1992). *Nonlocal Methods for Pendulum-like Feedback Systems.* Teubner Verlagsgesselschaft, Stuttgart-Leipzig.

Lyapunov, A.M. (1892). *The General Problem of the Stability of Motion.* Kharkov.

Mitropolsky, Y. and Bogolubov, N. (1961). *Asymptotic Methods in the Theory of Non-Linear Oscillations.* Gordon and Breach, New York.

Samoilenko, A. and Petryshyn, R. (2004). *Multifrequency Oscillations of Nonlinear Systems.* Mathematics and Its Applications. Springer.

Shakhgil'dyan, V. and Lyakhovkin, A. (1966). *Fazovaya avtopodstroika chastoty (Phase Locked Systems).* Svyaz', Moscow [in Russian].

Smith, S.W. (1999). *The Scientist and Engineer's Guide to Digital Signal Processing.* California Technical Publishing, San Diego, California.

Tretter, S.A. (2007). *Communication System Design Using DSP Algorithms with Laboratory Experiments for the TMS320C6713TM DSK.* Springer.

Tricomi, F. (1933). Integrazione di unequazione differenziale presentatasi in elettrotechnica. *Annali della R. Shcuola Normale Superiore di Pisa*, 2(2), 1–20.

Viterbi, A. (1966). *Principles of coherent communications.* McGraw-Hill, New York.

Yakubovich, V.A., Leonov, G.A., and Gelig, A.K. (2004). *Stability of Stationary Sets in Control Systems with Discontinuous Nonlinearities.* World Scientific, Singapure.

PV

PULL-IN RANGE OF THE CLASSICAL PLL WITH IMPULSE SIGNALS

by

K. D. Aleksandrov, N. V. Kuznetsov, G. A. Leonov, P. Neittaanmäki,
S. M. Seledzhi 2015

IFAC-PapersOnLine, Vol. 48, No. 1, pp. 562 – 567

Available online at www.sciencedirect.com

ScienceDirect

IFAC-PapersOnLine 48-1 (2015) 562–567

IFAC Papers Online
CONFERENCE PAPER ARCHIVE

Pull-in range of the classical PLL with impulse signals

Konstantin D. Alexandrov ⋆ **Nikolay V. Kuznetsov** ⋆
Gennady A. Leonov ⋆ **Pekka Neittaanmäki** ⋆⋆
Svetlana M. Seledzhi ⋆

Saint-Petersburg State University, Universitetsky pr. 28, Saint-Petersburg, 198504, Russia
Dept. of Mathematical Information Technology, University of Jyväskylä, P.O. Box 35 (Agora), FIN-40014, Finland

Abstract In the present work the pull-in range of the classical PLL with impulse signals is studied. Numerical experiments in MatLab Simulink are presented and two analytical approaches are discussed.

Keywords: phase-locked loop, nonlinear analysis, PLL, Best's conjecture, hidden oscillations

1. INTRODUCTION

The PLL circuit has been invented by French engineer Henri de Bellescize in 1932 (Bellescize, 1932). Since that time, various modifications of PLL circuits (digital PLL, all-digital PLL, software PLL, neuronal PLL and so on) were developed and new circuits, based on PLL operation principles, were invented (e.g., Costas loop and PLL with squarer). PLL-based circuits are used for carrier recovery, demodulation, frequency synthesis in telecommunications. At present there are many books devoted to the design and analysis of PLL-based circuits (see, e.g., (Viterbi, 1966; Gardner, 1966; Best, 2007) and refs within).

Rigorous analysis of PLL-based circuits is a complicated problem since the consideration of these circuits leads to a system of nonautonomous differential equations (Gelig et al., 1978; Kudrewicz and Wasowicz, 2007; Leonov and Kuznetsov, 2014a). Numerical simulation of PLL-based circuits is also a challenging task since it is necessary to consider simultaneously both high-frequency and low-frequency oscillations.

An important problem in the study of PLL based circuits is to find a pull-in range. In a recent paper (not yet published) Roland E. Best (well-known expert on PLL-based circuits and the author of the bestseller on PLL-based circuits (Best, 2007)) states that the pull-in range of the two-phase Costas loop is infinite if the loop filter used as a PI filter (Best's conjecture).

There are two effective analytical approaches for the pull-in range estimation are developed. The first one is based on the integration of separatrices and the analysis of their behavior (see the pioneering works (Tricomi, 1933; Andronov, 1937; Gubar', 1961) and their further development, e.g., in (Stensby, 1997; Leonov and Kuznetsov, 2013)). The second approach is based on the frequency methods and Lyapunov function constructions (Lyapunov, 1892; Gelig et al., 1978; Leonov and Kuznetsov, 2014a).

In the present paper in order to study the pull-in range of PLL with triangular-characteristic phase detector and with proportionally-integrating filter a number of numerical experiments in MatLab Simulink has been made and analytical methods are discussed.

2. DESCRIPTION OF PLL MODELS IN THE SIGNAL SPACE AND SIGNAL'S PHASE SPACE

Consider a PLL model in the signal space. The components of this model (see Fig. 1) are the following: a reference oscillator (Input), a voltage-controlled oscillator (VCO), a multiplier, used as a phase detector (PD), and a filter (Filter).

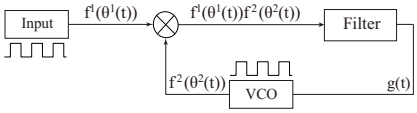

Figure 1. PLL model in the signal space.

A carrier signal $f^1(\theta^1(t)) = \mathrm{sgn}(\sin(\theta^1(t)))$ enters the Input. Carrier frequency ω^1 is a constant: $\frac{d\theta^1(t)}{dt} = \omega^1$.

The VCO with gain K_0 generates the signal $f^2(\theta^2(t)) = \mathrm{sgn}(\sin(\theta^2(t)))$. The VCO free-running frequency is equal to ω^2_{free}.

The signals $f^1(\theta^1(t))$ and $f^2(\theta^2(t))$ of reference and tunable oscillators enter the input of a multiplier, which is used as a phase detector, and at its output one has a product $f^1(\theta^1(t))f^2(\theta^2(t))$ of these signals. After filtration by Filter, this signal is used as a control signal $g(t)$ for VCO synchronization.

⋆ This work was supported by Saint-Petersburg State University (project 6.39.416.2014, s. 3-4; project 6.38.505.2014, s. 5.)
⋆⋆The author acknowledge the support of Russian Scientific Foundation (project 14-21-00041).

10.1016/j.ifacol.2015.05.090

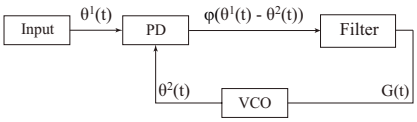

Figure 2. PLL model in signal's phase space.

Consider now the PLL model in signal's phase space (see Fig. 2).

For this model the phases $\theta^1(t)$ and $\theta^2(t)$, generated by reference and tunable oscillators, enter the input of phase detector, and the output of phase detector is a function with respect to phases difference: $\varphi(\theta^1(t)-\theta^2(t))$. It is known that for the considered impulse signals $f^1(\theta^1(t))$ and $f^2(\theta^2(t))$, the characteristic of phase detector is triangular (see, e.g., (Gardner, 1966; Leonov et al., 2012b)):

$$\varphi(\theta_e(t)) = \\ = \begin{cases} \frac{2}{\pi}\theta_e(t), & \text{if } -\frac{\pi}{2}+2\pi n < \theta_e(t) \le \frac{\pi}{2}+2\pi n; \\ -\frac{2}{\pi}\theta_e(t)+2, & \text{if } \frac{\pi}{2}+2\pi n < \theta_e(t) \le \frac{3\pi}{2}+2\pi n, \end{cases} \quad (1)$$

where $\theta_e(t) = \theta^1(t) - \theta^2(t)$. If the circuit achieves lock ($\theta^1(t) \equiv \theta^2(t) + \text{const}$), then $\varphi(\theta_e(t))$ is equal to a constant value.

The signal $\varphi(\theta_e(t))$, generated by phase detector PD, enters the input of filter Filter. At the output of Filter a signal $G(t)$ is generated and then it is used as a control signal for the VCO. One has

$$\frac{d\theta^2(t)}{dt} = \omega_{free}^2 + K_0 G(t).$$

In the considered case Filter is a proportionally-integrating filter with a transfer function $W(s) = \frac{\beta+as}{s}$, $a > 0$, $\beta > 0$ (Best, 2007). The relation between the input $\varphi(\theta_e)$ and the output $G(t)$ of Filter is as follows

$$\frac{dG(t)}{dt} = a\frac{d\varphi(\theta_e(t))}{dt} + \beta\varphi(\theta_e(t)).$$

A derivative with respect to time t is denoted by $\dot{\theta_e}$, and a derivative with respect to θ_e by φ'. The above equations yield the following relations:

$$\begin{cases} \dot{G}(\theta_e(t)) = a\varphi'(\theta_e(t))\dot{\theta}_e(t) + \beta\varphi(\theta_e(t)), \\ \dot{\theta_e}(t) = \omega^1 - \omega_{free}^2 - K_0 G(\theta_e(t)). \end{cases} \quad (2)$$

3. SIMULATION OF PLL WITH TRIANGULAR-CHARACTERISTIC PHASE DETECTOR

Simulation of the PLL model in the signal space is a very challenging task since it is required to consider simultaneously both very fast time scale signals and slow time scale phase differences between the signals. So, for the simulation, a small discretization step is used, what significantly increases time of simulations. To overcome these difficulties a Simulink model of PLL in signal's phase space (Fig. 3) is considered. It consists of four subsystems: reference oscillator (Input), voltage- controlled oscillator (VCO), phase detector (PD), and filter (Filter).

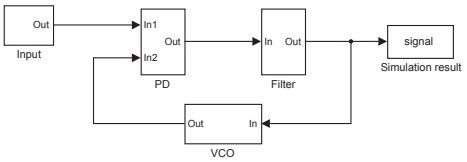

Figure 3. MatLab Simulink model of PLL in signal's phase space.

The block diagram of the reference oscillator is shown in Fig. 4. This block defines a phase as a function of time, which enters the input of the circuit.

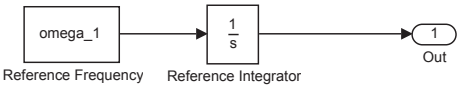

Figure 4. Reference oscillator of PLL model.

The block diagram of the voltage-controlled oscillator is shown in Fig. 5. VCO consists of six blocks: Simulink Constant block, which provides free-running frequency of VCO, Simulink Constant block, which provides initial phase shift of VCO, Gain block, integrator block, and two summation blocks. The phase detector (PD) is a

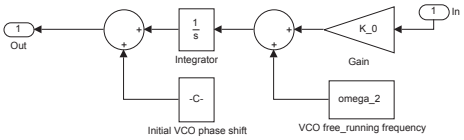

Figure 5. Voltage-controlled oscillator of PLL model.

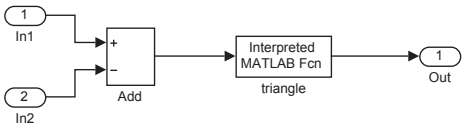

Figure 6. Triangular-characteristic phase detector of PLL model.

triangular-characteristic phase detector and can be defined by using MatLab standard functions.

In the considered case the filter subsystem (see Fig. 7) consists of one block of a filter transfer function. In the Simulink model a proportionally-integrating filter is used.

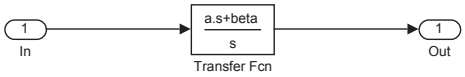

Figure 7. Proportionally-integrating filter of PLL model.

4. THE RESULTS OF SIMULATION.

For the Simulink model of the PLL with triangular-characteristic phase detector, which was described in Section 3, a number of simulations has been made. The simulations were made by standard Matlab solver ode15s, using the numerical Gear method with variable step. For ode15s the following parameters are taken: absolute tolerance error is equal to 10^{-12}, relative tolerance error is equal to 10^{-12}, initial time step is equal to 10^{-3}, and variable time step does not exceed 10^{-3}. All simulations for various values of parameters a, β, K_0, and $\Delta\omega = \omega^1 - \omega^2_{free}$ confirm that finally the Simulink model with PI filter achieves lock.

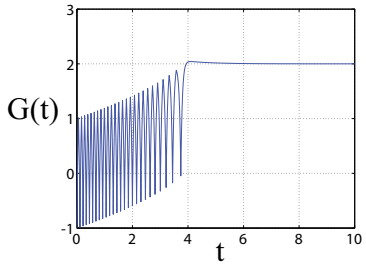

Figure 8. $a = 1$, $\beta = 1$, $K_0 = 10\pi$, $\Delta\omega = 20\pi$.

Consider the conjecture on the pull-in range of PLL with triangular-characteristic phase detector: *The pull-in range of PLL with triangular-characteristic phase detector and proportionally-integrating filter is infinite.* In other words, *for PLL with triangular-characteristic phase detector and proportionally-integrating filter, any solution of the corresponding system, described in Section 2, tends to a stationary set of system as* $t \to +\infty$.

Numerical simulations (see, e.g., Figs. 8, 9, 10) with the use of Simulink model from Section 3 confirms the conjecture.

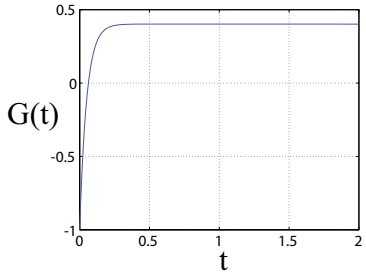

Figure 9. $a = 1$, $\beta = 0.1$, $K_0 = 10\pi$, $\Delta\omega = 4\pi$.

At the same time it can be remarked that the application of standard numerical analysis cannot guarantee the finding of undesired stable oscillations: see, e.g., examples of hidden oscillations and coexisting attractors in two-dimensional PLL-based models (Leonov and Kuznetsov, 2013).

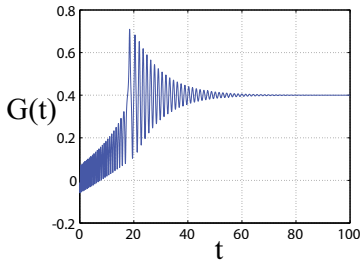

Figure 10. $a = 0.01$, $\beta = 1$, $K_0 = 10\pi$, $\Delta\omega = 4\pi$.

An oscillation in a dynamical system can be easily localized numerically if the initial conditions from its open neighborhood lead to long-time behavior that approaches the oscillation. Thus, from a computational point of view, it is natural to suggest the following classification of attractors, based on the simplicity of finding the basin of attraction in the phase space (Kuznetsov et al., 2010; Leonov et al., 2011, 2012a; Leonov and Kuznetsov, 2013): *An attractor is called a* hidden attractor *if its basin of attraction does not intersect with small neighborhoods of equilibria, otherwise it is called a* self-excited attractor.

For example, hidden attractors are attractors in the systems with no equilibria or with only one stable equilibrium (a special case of multistable systems and coexistence of attractors). Recent examples of hidden attractors can be found in (Zhusubaliyev and Mosekilde, 2014; Pham et al., 2014a,b; Wei et al., 2014b; Li and Sprott, 2014; Wei et al., 2014a; Kuznetsov et al., 2015; Burkin and Khien, 2014; Li et al., 2014; Zhao et al., 2014; Lao et al., 2014; Chaudhuri and Prasad, 2014).

In the next section one of the approach, based on trajectories integration, for an estimation of the pull-in range will be demonstrated. Some corresponding results can be also found in (Stensby, 1997, 2011; Alexandrov et al., 2014).

5. ANALYTICAL ESTIMATION OF THE PULL-IN RANGE

In the present section the system, corresponding to PLL circuit with triangle characteristic of phase detector, is considered. System (2), represented in Section 2, can be reduced to the following system of the second-order differential equations:

$$\dot{\theta_e} = y, \quad \dot{y} = -aK_0\varphi(\theta_e)'y - \beta K_0\varphi(\theta_e). \tag{3}$$

Theorem 1. For arbitrary $a > 0$, $\beta > 0$, and $K_0 > 0$ any solution of system (3) tends to stationary set of system as $t \to +\infty$.

For the proof it is sufficient to show the nonexistence of limit cycles on phase plane of system (3). Let us prove first the nonexistence of limit cycles of the second kind. Consider the upper semiplane of the phase plane. The calculations for the lower semiplane are the same.

On the interval $\theta_e \in \left[-\frac{\pi}{2}; \frac{\pi}{2}\right)$ by the changes $t \to t\sqrt{\frac{\pi}{2\beta K_0}}$, $y \to y\sqrt{\frac{2\beta K_0}{\pi}}$ system (3) takes the form

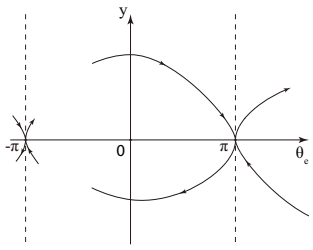

Figure 11. A qualitative phase portrait of system (3).

$$\frac{d\theta_e}{dt} = y, \quad \frac{dy}{dt} = -2h_1 y - \theta_e. \tag{4}$$

Here $h_1 = a\sqrt{\frac{K_0}{2\pi\beta}}$. In the considered interval there is one stationary point $(\theta_e, y) = (0;0)$. The point $(\theta_e, y) = (0;0)$ is a stable node, a degenerated node or a stable focus, which depends on the value h_1. Consider the case $h_1 > 1$ in detail. Other cases leads to the same qualitative results. Denote $\gamma_1 = \sqrt{h_1^2 - 1}$, $k_1 = \frac{h_1}{\gamma_1}$.

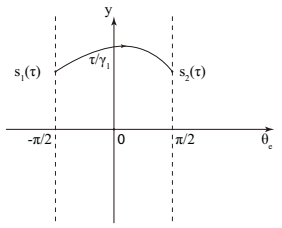

Figure 12. Transformation of the image point $\left(-\frac{\pi}{2}; s_1(\tau)\right)$ to the $\left(\frac{\pi}{2}; s_2(\tau)\right)$ on the phase plane.

Let us find a solution of system (4) such that on the considered interval a whole phase trajectory is located in the upper semiplane of the phase plane. A sought solution (see Fig. 12) moves the image point of the phase plane $\left(-\frac{\pi}{2}; s_1(\tau)\right)$ from the line $\theta_e = -\frac{\pi}{2}$ to the point of the phase plane $\left(\frac{\pi}{2}; s_2(\tau)\right)$ on the line $\theta_e = \frac{\pi}{2}$ in a time equal to $\frac{\tau}{\gamma_1}$, $\tau > 0$. The values of $s_1(\tau)$ and $s_2(\tau)$ can be found as the ordinates at instants of time $t = 0$ and $t = \frac{\tau}{\gamma_1}$, respectively (Andronov et al., 1966). Having found $s_1(\tau)$ and $s_2(\tau)$, one considers the function $s_1(s_2(\tau))$. The obtained expressions for $s_1(\tau)$, $s_2(\tau)$, $\frac{ds_1}{ds_2}(\tau)$, and $\frac{d^2 s_1}{ds_2^2}(\tau)$ are the following

$$s_1(\tau) = \frac{\pi}{2}\left(\frac{2\gamma_1 e^{k_1\tau}}{e^\tau - e^{-\tau}} + h_1 + \gamma_1 \frac{e^\tau + e^{-\tau}}{e^\tau - e^{-\tau}}\right); \tag{5}$$

$$s_2(\tau) = \frac{\pi}{2}\left(\frac{2\gamma_1 e^{-k_1\tau}}{e^\tau - e^{-\tau}} - h_1 + \gamma_1 \frac{e^\tau + e^{-\tau}}{e^\tau - e^{-\tau}}\right); \tag{6}$$

$$\frac{ds_1}{ds_2}(\tau) = e^{2k_1\tau}\frac{s_2}{s_1} > 0; \tag{7}$$

$$\frac{d^2 s_1}{ds_2^2}(\tau) = \frac{\pi^2}{4}\frac{e^{3k_1\tau}(e^\tau - e^{-\tau})}{2\gamma_1 s_1^3}(s_1 - s_2) > 0. \tag{8}$$

By relations (5), (6) it can be found an oblique asymptote of a graph of the function $s_1(s_2)$:

$$s_1(s_2) = s_2 + 2\pi h_1.$$

By relations (7), (8), the behavior of the curve $s_1(s_2)$ is conventionally shown in Fig. 13.

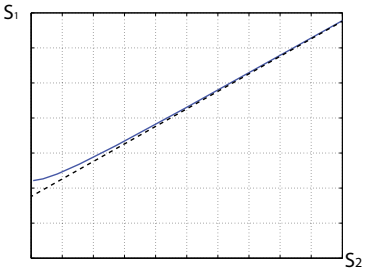

Figure 13. Behavior of function $s_1(s_2)$.

Similar reasonings are valid for system (3) on the interval $\theta_e \in \left[\frac{\pi}{2}; \frac{3\pi}{2}\right)$. In this interval a unique critical point $(\theta_e, y) = (\pi; 0)$ is a saddle.

On the interval $\theta_e \in \left[\frac{\pi}{2}; \frac{3\pi}{2}\right)$ by the changes $t \to t\sqrt{\frac{\pi}{2\beta K_0}}$, $y \to y\sqrt{\frac{2\beta K_0}{\pi}}$ the system can be represented as

$$\frac{d\theta_e}{dt} = y, \quad \frac{dy}{dt} = -2h_2 y + \theta_e - \pi. \tag{9}$$

Here $h_2 = -a\sqrt{\frac{K_0}{2\pi\beta}}$. Denote $\gamma_2 = \sqrt{h_2^2 + 1}$, $k_2 = \frac{h_2}{\gamma_2}$.

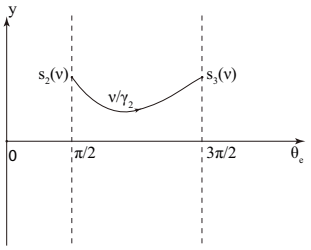

Figure 14. Transformation of the image point $\left(\frac{\pi}{2}; s_2(\nu)\right)$ to the $\left(\frac{3\pi}{2}; s_3(\nu)\right)$ on the phase plane.

Consider a solution of system (9) such that on the considered interval the phase trajectory is completely located in the upper semiplane of the phase plane. A sought solution (see Fig. 14) moves an image point of the phase plane $\left(\frac{\pi}{2}; s_2(\nu)\right)$ from the line $\theta_e = \frac{\pi}{2}$ to the point of phase plane $\left(\frac{3\pi}{2}; s_3(\nu)\right)$ on the line $\theta_e = \frac{3\pi}{2}$ in a time, equal to $\frac{\nu}{\gamma_2}$, $\nu > 0$. The values of $s_2(\nu)$ and $s_3(\nu)$ are the ordinates of image point at instants of time $t = 0$ and $t = \frac{\nu}{\gamma_2}$, respectively. Consider a function $s_3(s_2(\nu))$. The expressions for $s_2(\nu)$, $s_3(\nu)$, $\frac{ds_3}{ds_2}(\nu)$, and $\frac{d^2 s_3}{ds_2^2}(\nu)$ are the following

$$s_2(\nu) = \frac{\pi}{2}\left(\frac{2\gamma_2 e^{k_2\nu}}{e^\nu - e^{-\nu}} + h_2 + \gamma_2 \frac{e^\nu + e^{-\nu}}{e^\nu - e^{-\nu}}\right); \tag{10}$$

$$s_3(\nu) = \frac{\pi}{2}\left(\frac{2\gamma_2 e^{-k_2\nu}}{e^{\nu}-e^{-\nu}} - h_2 + \gamma_2\frac{e^{\nu}+e^{-\nu}}{e^{\nu}-e^{-\nu}}\right); \quad (11)$$

$$\frac{ds_3}{ds_2} = e^{-2k_2\nu}\frac{s_2}{s_3} > 0; \quad (12)$$

$$\frac{d^2 s_3}{ds_2^2} = \frac{\pi^2}{4}\frac{e^{3k_2\nu}(e^{\nu}-e^{-\nu})}{2\gamma_2 s_2^3}(s_2 - s_3) < 0. \quad (13)$$

By relations (10), (11) one can find an oblique asymptote of a graph of the function $s_3(s_2)$: $s_3(s_2) = s_2 - 2\pi h_2$. By relations (12), (13) a behavior of the curve $s_3(s_2)$ is conventionally shown in Fig. 15.

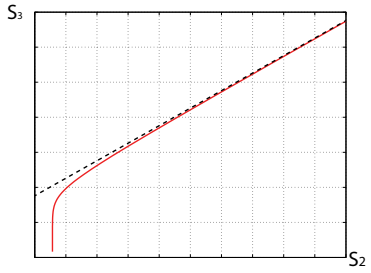

Figure 15. Behavior of the function $s_3(s_2)$.

In the considered case $h_1 = -h_2$. It means that the curves $s_1(s_2)$, $s_3(s_2)$ as functions with respect to s_2 have the same oblique asymptote. Besides, the obtained relations for $\frac{ds_1}{ds_2}$, $\frac{ds_3}{ds_2}$, $\frac{d^2 s_1}{ds_2^2}$, and $\frac{d^2 s_3}{ds_2^2}$ justify the fact that $s_1(s_2)$, $s_3(s_2)$ do not intersect oblique asymptote and, therefore, do not intersect. The mutual disposition of $s_1(s_2)$ and $s_3(s_2)$ is shown in Fig. 16. The obtained result shows the

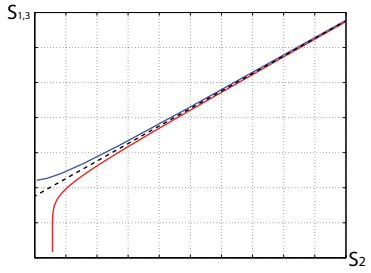

Figure 16. Mutual disposition of functions $s_1(s_2)$ and $s_3(s_2)$.

nonexistence of limit cycles of the second kind in the upper semiplane of system (3). The existence of limit cycle of the second kind implies the intersection of $s_1(s_2)$ and $s_3(s_2)$. By the same reasonings it is proved the nonexistence of the second kind limit cycles in the lower semiplane of system (3).

Thus, to finalize the proof, one need only to prove the nonexistence of the first kind limit cycles. To reduce the consideration, instead of integration of trajectories and their analysis similar to that presented above, here we refer to the dichotomy criterion, described in detail in (Leonov and Kuznetsov, 2014a).

Thus, one can prove that the phase plane of system (3) does not contain any limit cycles and all solutions of system (3) tend to the set of stationary points as $t \to +\infty$. In other words, the PLL circuit will achieve lock for any initial difference of frequencies ω^1 and ω^2_{free} of reference oscillator and VCO.

6. CONCLUSION.

In the present paper the problem of the pull-in range estimation is discussed. Numerical method and two effective analytical approaches for the pull-in range estimations are presented. One of the analytical approaches is based on the integration of separatrices and the analysis of their behavior, while the other approach is based on the frequency methods and Lyapunov function constructions. One of the problems of the first method is that for any new PD characteristic one has to perform many new tedious integrations (as it was demonstrated above). Another problem is that while this approach is useful for the two-dimensional models, its generalization for a multidimensional models is a challenging task. The advantage of this approach is that it allows one to estimate also the lock-in range corresponding to a domain of the phase space, where the loop achieves a lock without cycle slips. If the aim is to study the pull-in range only then to avoid cumbersome integrations one can use the approach based on Lyapunov function construction for the cylindrical phase space. For the model considered in this paper it is possible to construct Lyapunov function of the type "quadratic form plus the integral of nonlinearity" (see, e.g., (Gelig et al., 1978; Leonov and Kuznetsov, 2014b)). The advantage of this approach is that it allows to consider various PD characteristics at once.

REFERENCES

Alexandrov, K., Kuznetsov, N., Leonov, G., and Seledzhi, S. (2014). Best's conjecture on pull-in range of two-phase Costas loop. In *Ultra Modern Telecommunications and Control Systems and Workshops (ICUMT), 2014 6th International Congress on*, 78–82. IEEE. doi: 10.1109/ICUMT.2014.7002082.

Andronov, A.A. (1937). *Oscillations.*

Andronov, A.A., Vitt, E.A., and Khaikin, S.E. (1966). *Theory of Oscillators.* Pergamon Press, Oxford.

Bellescize, H. (1932). La réception synchrone. *L'onde Électrique*, 11, 230–340.

Best, R.E. (2007). *Phase-Lock Loops: Design, Simulation and Application.* McGraw-Hill.

Burkin, I. and Khien, N. (2014). Analytical-numerical methods of finding hidden oscillations in multidimensional dynamical systems. *Differential Equations*, 50(13), 1695–1717.

Chaudhuri, U. and Prasad, A. (2014). Complicated basins and the phenomenon of amplitude death in coupled hidden attractors. *Physics Letters, Section A: General, Atomic and Solid State Physics*, 378(9), 713–718.

Gardner, F. (1966). *Phase–lock techniques.* John Wiley.

Gelig, A., Leonov, G., and Yakubovich, V. (1978). *Stability of Nonlinear Systems with Nonunique Equilibrium (in Russian).* Nauka.

Gubar', N.A. (1961). Investigation of a piecewise linear dynamical system with three parameters. *J. Appl. Math. Mech.*, 25(6), 1011–1023.

Kudrewicz, J. and Wasowicz, S. (2007). *Equations of Phase-Locked Loops: Dynamics on the Circle, Torus and Cylinder*, volume 59. World Scientific.

Kuznetsov, A., Kuznetsov, S., Mosekilde, E., and Stankevich, N. (2015). Co-existing hidden attractors in a radio-physical oscillator system. *Journal of Physics A: Mathematical and Theoretical*. Accepted.

Kuznetsov, N.V., Leonov, G.A., and Vagaitsev, V.I. (2010). Analytical-numerical method for attractor localization of generalized Chua's system. *IFAC Proceedings Volumes (IFAC-PapersOnline)*, 4(1), 29–33. doi: 10.3182/20100826-3-TR-4016.00009.

Lao, S.K., Shekofteh, Y., Jafari, S., and Sprott, J. (2014). Cost function based on Gaussian mixture model for parameter estimation of a chaotic circuit with a hidden attractor. *International Journal of Bifurcation and Chaos*, 24(1).

Leonov, G.A. and Kuznetsov, N.V. (2013). Hidden attractors in dynamical systems. From hidden oscillations in Hilbert-Kolmogorov, Aizerman, and Kalman problems to hidden chaotic attractors in Chua circuits. *International Journal of Bifurcation and Chaos*, 23(1). doi: 10.1142/S0218127413300024. art. no. 1330002.

Leonov, G.A. and Kuznetsov, N.V. (2014a). *Nonlinear Mathematical Models Of Phase-Locked Loops. Stability and Oscillations*. Cambridge Scientific Press.

Leonov, G.A. and Kuznetsov, N.V. (2014b). *Nonlinear Mathematical Models of Phase-Locked Loops. Stability and Oscillations*. Cambridge Scientific Publisher.

Leonov, G.A., Kuznetsov, N.V., and Vagaitsev, V.I. (2011). Localization of hidden Chua's attractors. *Physics Letters A*, 375(23), 2230–2233. doi: 10.1016/j.physleta.2011.04.037.

Leonov, G.A., Kuznetsov, N.V., and Vagaitsev, V.I. (2012a). Hidden attractor in smooth Chua systems. *Physica D: Nonlinear Phenomena*, 241(18), 1482–1486. doi:10.1016/j.physd.2012.05.016.

Leonov, G.A., Kuznetsov, N.V., Yuldahsev, M.V., and Yuldashev, R.V. (2012b). Analytical method for computation of phase-detector characteristic. *IEEE Transactions on Circuits and Systems – II: Express Briefs*, 59(10), 633–647. doi:10.1109/TCSII.2012.2213362.

Li, C. and Sprott, J.C. (2014). Coexisting hidden attractors in a 4-D simplified Lorenz system. *International Journal of Bifurcation and Chaos*, 24(03). doi: 10.1142/S0218127414500345. Art. num. 1450034.

Li, Q., Zeng, H., and Yang, X.S. (2014). On hidden twin attractors and bifurcation in the Chua's circuit. *Nonlinear Dynamics*, 77(1-2), 255–266.

Lyapunov, A.M. (1892). *The General Problem of the Stability of Motion*. Kharkov.

Pham, V.T., Jafari, S., Volos, C., Wang, X., and Golpayegani, S. (2014a). Is that really hidden? The presence of complex fixed-points in chaotic flows with no equilibria. *International Journal of Bifurcation and Chaos*, 24(11). doi:10.1142/S0218127414501466. Art. num. 1450146.

Pham, V.T., Rahma, F., Frasca, M., and Fortuna, L. (2014b). Dynamics and synchronization of a novel hyperchaotic system without equilibrium. *International Journal of Bifurcation and Chaos*, 24(06). Art. num. 1450087.

Stensby, J. (1997). *Phase-Locked Loops: Theory and Applications*. Phase-locked Loops: Theory and Applications. Taylor & Francis.

Stensby, J. (2011). An exact formula for the half-plane pull-in range of a PLL. *Journal of the Franklin Institute*, 348(4), 671–684.

Tricomi, F. (1933). Integrazione di unequazione differenziale presentatasi in elettrotechnica. *Annali della R. Shcuola Normale Superiore di Pisa*, 2(2), 1–20.

Viterbi, A. (1966). *Principles of coherent communications*. McGraw-Hill, New York.

Wei, Z., Moroz, I., and Liu, A. (2014a). Degenerate Hopf bifurcations, hidden attractors and control in the extended Sprott E system with only one stable equilibrium. *Turkish Journal of Mathematics*, 38(4), 672–687.

Wei, Z., Wang, R., and Liu, A. (2014b). A new finding of the existence of hidden hyperchaotic attractors with no equilibria. *Mathematics and Computers in Simulation*, 100, 13–23.

Zhao, H., Lin, Y., and Dai, Y. (2014). Hidden attractors and dynamics of a general autonomous van der Pol-Duffing oscillator. *International Journal of Bifurcation and Chaos*, 24(06). doi:10.1142/S0218127414500801. Art. num. 1450080.

Zhusubaliyev, Z. and Mosekilde, E. (2014). Multistability and hidden attractors in a multilevel DC/DC converter. *Mathematics and Computers in Simulation*. Doi:10.1016/j.matcom.2014.08.001.

PVI

BEST'S CONJECTURE ON PULL-IN RANGE OF TWO-PHASE COSTAS LOOP

by

K. D. Aleksandrov, N. V. Kuznetsov, G. A. Leonov, S. M. Seledzhi 2014

IEEE 6th International Congress on Ultra Modern Telecommunications and Control Systems (ICUMT 2014), pp. 78 – 82

2014 6th International Congress on Ultra Modern Telecommunications and Control Systems and Workshops (ICUMT)

Best's conjecture on pull-in range of two-phase Costas loop

Alexandrov K. D.*, Kuznetsov N. V.*†, Leonov G. A.*, Seledzhi S. M.*
*Saint-Petersburg State University, Universitetsky pr. 28, Saint-Petersburg, 198504, Russia
†Dept. of Mathematical Information Technology, University of Jyväskylä, P.O. Box 35 (Agora), FIN-40014, Finland
Email: nkuznetsov239@gmail.com

***Abstract*—In the present work for checking conjecture on pull-in range of two-phase Costas loop, a number of numerical experiments in MatLab Simulink has been made. In addition, the analytical approach to the proof of the conjecture is presented.**

I. INTRODUCTION

The Costas loop was suggested by American engineer John Costas in 1956 [1], [2] and is widely used now in the control circuits for carrier phase recovery [3], [4], [5]. A detailed mathematical description of Costas loop can be found, e.g., in [6], [7], [8], [9]. At the present time there are a great number of modifications, for example, QPSK realization, BPSK realization, two-phase Costas loop. Various modifications of Costas loop are widely used in wireless receivers [10]. With a mathematical point of view the investigation of Costas loops and its modifications is a complicated problem since the description of this circuit leads to the analysis of nonautonomous differential equation [11], [12], [13], the right-hand side of which involves both high-frequency and low-frequency components [14]. In such problems the consideration of simplified mathematical models (for example, the linear one), which are more convenient for investigation, can lead to incorrect conclusions [15], [16].

In this paper the two-phase Costas loop as suggested by Tretter [17] is considered. The advantage of two-phase Costas loop in comparison to the original circuit of 50s of XX century is elimination of high-frequency oscillations by using the complex multiplier. One of the main problem, connected with investigation of Costas loops, is the finding of pull-in range –maximal initial difference of frequencies of reference and voltage-controlled oscillators, over which the loop can achieve lock. In a recent paper (not yet published) Roland E. Best (well-known expert in PLL-based circuits and the author of the bestseller on PLL-based circuits [3]) states that the pull-in range of the two-phase Costas loop is infinite if the loop filter used is a PI filter (Best's conjecture).

In this paper a number of numerical experiments in MatLab Simulink has been made and the analytical approach to the proof of Best's conjecture is presented.

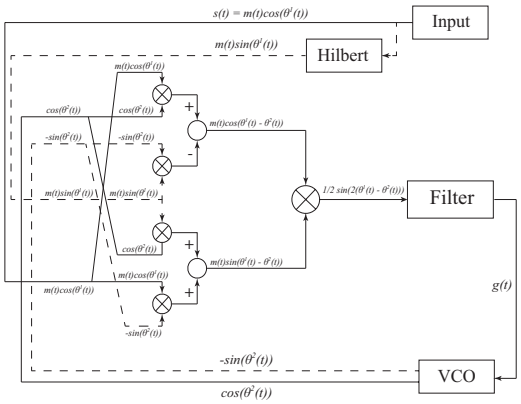

Figure 1: Two-phase Costas loop modification.

II. DESCRIPTION OF TWO-PHASE COSTAS LOOP

Consider the two-phase Costas loop modification (see Fig. 1). The components of this circuit are reference oscillator (Input), filter (Filter), complex multiplier as a phase detector, and voltage-controlled oscillator (VCO).

A carrier signal $m(t)\cos(\theta^1(t))$ enters the input, where $m(t) = \pm 1$ is a slowly varying data signal. A carrier frequency is equal to ω^1:

$$\dot{\theta^1}(t) = \omega^1.$$

A carrier signal is transformed by Hilbert transformation into $m(t)\sin(\theta^1(t))$. Two input and two VCO signals enter the complex multiplier, which is used to compare phases of the signals.

The relations, describing the operation of complex multiplier, take the form

$$m(t)\cos(\theta^1(t))\cos(\theta^2(t)) - m(t)\sin(\theta^1(t))(-\sin(\theta^2(t))) = \quad (1)$$
$$= m(t)\cos(\theta^1(t) - \theta^2(t)),$$

$$m(t)\sin(\theta^1(t))\cos(\theta^2(t)) + m(t)\cos(\theta^1(t))(-\sin(\theta^2(t))) = \quad (2)$$
$$= m(t)\sin(\theta^1(t) - \theta^2(t)).$$

If the loop achieves lock (for example, $\theta^1(t) = \theta^2(t)$), then the signal (2) is equal to zero. At once the signal (1) is equal to $m(t)$, i.e., a demodulation is realized.

The multiplication of signals (1) and (2):

$$u(t) = \varphi(\theta^1(t) - \theta^2(t)) = m(t)\cos(\theta^1(t) - \theta^2(t)) \cdot$$
$$\cdot m(t)\sin(\theta^1(t) - \theta^2(t)) = \frac{1}{2}\sin(2(\theta^1(t) - \theta^2(t)))$$

after additional filtration (by the Filter) is used as a control signal for VCO.

In the considered case Filter is a proportionally-integrating filter with transfer function $W(s) = \frac{\beta + as}{s}$, $a > 0$, $\beta > 0$.

The relation between input $u(t)$ and output $g(t)$ of Filter has the form

$$\dot{g}(t) = a\dot{u}(t) + \beta u(t).$$

It should be noted that in the case of Filter absence the circuit can also achieve lock, but only in the range $|\omega^1 - \omega^2|$.

The control signal $g(t)$ is used to adjust the VCO frequency to the frequency of input carrier signal

$$\dot{\theta^2}(t) = \omega^2 + K_0 g(t),$$

where VCO gain is $K_0 > 0$ and VCO output signals are $\cos(\theta^2(t))$ and $-\sin(\theta^2(t))$.

III. SIMULATION OF TWO-PHASE COSTAS LOOP

Simulation of two-phase Costas loop in signal space is highly difficult problem, since it is required to consider simultaneously both very fast time scale of signals and slow time scale of phase difference between the signals. Therefore, the analysis and simulation are mostly performed in signal's phase space (Fig. 2) [1], [18], [5], [3], [8], [19].

The model in signal's phase space consists of four subsystems – reference oscillator, phase detector (PD), filter (Filter), and voltage-controlled oscillator (VCO).

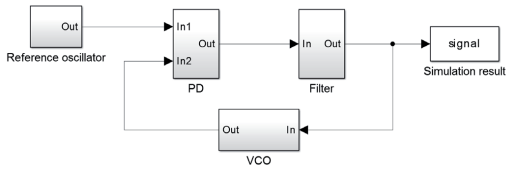

Figure 2: MatLab Simulink model of two-phase Costas loop.

The device of a subsystem of reference oscillator is shown in Fig. 3. This block determines a phase, as a function of time, which enters the input of the circuit.

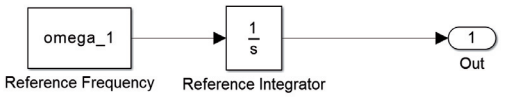

Figure 3: Reference oscillator of two-phase Costas loop.

The device of a subsystem of voltage-controlled oscillator is shown in Fig. 4. The VCO consists of six blocks: two blocks Simulink Constant, which provides eigenfrequency and initial phase shift of the VCO, two summation blocks, Gain block and integrator block.

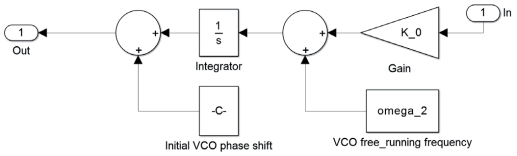

Figure 4: Voltage-controlled oscillator.

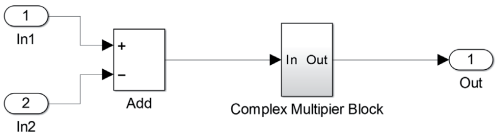

Figure 5: Phase detector (PD) in two-phase Costas loop.

The phase detector (PD) in Simulink model consists of the difference block and complex multiplier subsystem, shown in Fig. 6, which simulates the operation of complex multiplier.

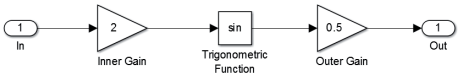

Figure 6: Complex multiplier of two-phase Costas loop.

In the considered case the filter subsystem (see Fig. 7) consists of one block of a transfer function of filter.

IV. THE RESULTS OF SIMULATION AND BEST'S CONJECTURE

Best's conjecture on the the pull-in range of two-phase Costas loop is formulated in the following way:

Assertion 1. *The pull-in range of two-phase Costas loop with proportionally-integrating filter is infinite.*

Figure 7: Filter of two-phase Costas loop.

In other words:

Assertion 2. *For two-phase Costas loop with a transfer function of filter* $W(s) = \frac{\beta + as}{s}$, $a > 0$, $\beta > 0$, *any solution of the corresponding system, described in section II, tends to a stationary set of system as* $t \to +\infty$.

For numerical check of Best's conjecture a number of simulations have been made with the use of above Simulink model of two-phase Costas loop. The simulation was made by a standard MatLab solver ode15s, by using the numerical Gear method with variable step. For ode15s the following parameters are taken: an absolute tolerance error is equal to 10^{-12}, a relative tolerance error is equal to 10^{-12}, the initial step is equal to 10^{-3}, and a variable step does not exceed 10^{-3}.

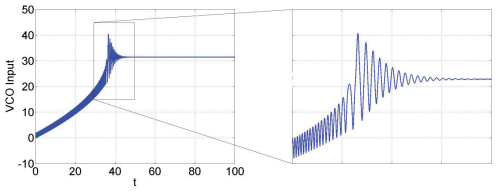

Figure 8: $a = 0.1$, $\beta = 0.1$, $K_0 = 10$, $\omega^1 = 100$, $\omega^2 = 97$.

All the simulations for the different values of parameters a, β, K_0, and the different frequencies θ^1 and θ^2 confirm that two-phase Costas loop achieves lock state (see the examples in Fig. 8, 9, 10).

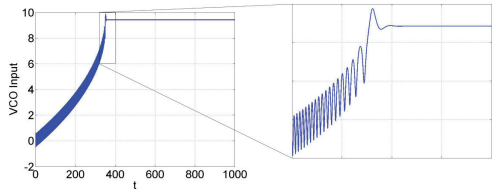

Figure 9: $a = 0.1$, $\beta = 10$, $K_0 = 10$, $\omega^1 = 100$, $\omega^2 = 90$.

V. INVESTIGATION OF SYSTEM STABILITY FOR SMALL VALUE OF FILTER PARAMETER

Consider the analytical approach to the verification of Best's conjecture. Denote $\theta_e = \theta^1 - \theta^2$. The equations from

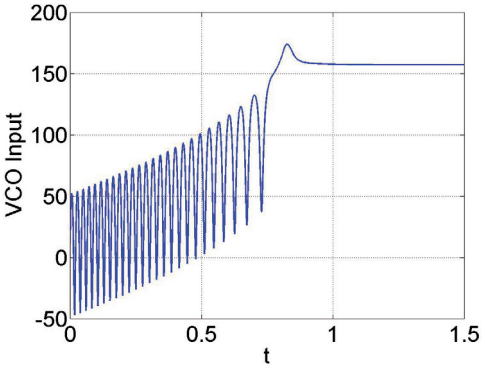

Figure 10: $a = 10$, $\beta = 50$, $K_0 = 10$, $\omega^1 = 100$, $\omega^2 = 50$.

section II imply the following relations[1]

$$\begin{cases} \dot{g}(\theta_e) = a\varphi'(\theta_e)\dot{\theta}_e + \beta\varphi(\theta_e), \\ \dot{\theta}_e = \omega^1 - \omega^2_{free} - K_0 g(\theta_e). \end{cases} \tag{3}$$

System (3) describes the operation of two-phase Costas loop. It can be reduced to the following differential equation of second order with respect to $x = 2\theta_e$

$$\ddot{x} + aK_0\cos(x)\dot{x} + \beta K_0 \sin(x) = 0. \tag{4}$$

Relation (4) can be represented by the following equivalent system

$$\begin{cases} \dot{x} = y, \\ \dot{y} = -aK_0\cos(x)y - \beta K_0\sin(x). \end{cases} \tag{5}$$

One can investigate only the behavior of system (5) in the range $-\pi < x \leq \pi$ since the right-hand side of system is 2π-periodic. Equating the right-hand side of system (5) to zero, one obtains that in the considered range there are two critical points $(x, y) = (0; 0)$ and $(x, y) = (\pi; 0)$. It can be checked that the point $(0; 0)$ on the phase plane is a stable node or stable focus and $(\pi; 0)$ is a saddle. Besides, taking into account periodicity, the critical point $(-\pi; 0)$ is also a saddle.

Theorem 1. *For small value of parameter* $a = \varepsilon$, $0 < \varepsilon \ll 1$, *any solution of system (5) as* $t \to +\infty$ *tends to a stationary set of system (5).*

The main idea of the proof is the following. For the proof it is necessary to make the analysis of the behavior of separatrices of saddle points. Their behavior defines a qualitative picture of a phase portrait of system (5). Consider equation equivalent to (5)

$$y'(x) = -\frac{aK_0\cos(x)y(x) + \beta K_0\sin(x)}{y(x)}. \tag{6}$$

[1]A derivative with time t is denoted by $\dot{\theta}_e$, and a derivative with respect to x is denoted by y'.

The right-hand side of (6) discontinues on $y = 0$. This line is an isocline of vertical inclinations of phase portrait of system (6) [20]. Further are considered the separatrices of upper semiplane of the phase space. The reasoning for the lower semiplane is similar.

Consider the case $a = \varepsilon$, $1 \ll \varepsilon \neq 0$. The following separatrices of equation (6) are considered, namely a separatrix $R(x,\varepsilon)$, which leaves the saddle point $(-\pi;0)$ and is situated in its first quadrant, and the separatrix $S(x,\varepsilon)$, which tends to the saddle point $(\pi;0)$ and is placed in its second quadrant. By expanding of separatrices $R(x,\varepsilon)$ and $S(x,\varepsilon)$ in Taylor series in variable ε it is possible to determine a mutual disposition of these separatrices approximations. In addition it is possible to show that a mutual disposition of separatrices on a phase plane coincides with a mutual disposition of their approximations, obtained by Taylor series, taking into account $\varepsilon \ll 1$. A qualitative disposition of $R(x,\varepsilon)$ and $S(x,\varepsilon)$ is shown in Fig. 11. Then it is necessary

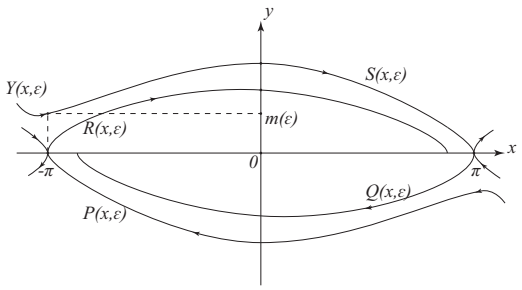

Figure 11: Phase portrait of system (5).

to show that on the phase plane of system (5) there are no any limit cycles of the second order. Consider an arbitrary phase trajectory $Y(x,\varepsilon)$ such that $Y(-\pi,\varepsilon) = M$, where $M \geq m(\varepsilon) = S(-\pi,\epsilon)$ is a fixed constant. By a similar approximation, obtained by Taylor series, it can be proved that $Y(-\pi,\varepsilon) > Y(\pi,\varepsilon)\ \forall M \geq m(\varepsilon)$. This means that on the upper semiplane of phase plane (6) there are no any limit cycles of second kind.

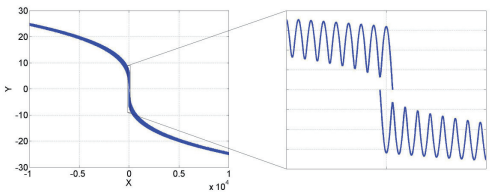

Figure 12: Separatrices on a phase plane of system (6).

Similarly, considering a behavior of separatrix $P(x,\varepsilon)$, which leaves the saddle point $(-\pi;0)$ in its fourth quadrant, and $Q(x,\varepsilon)$, which tends to the saddle point $(\pi;0)$ in its third quadrant, and using the Taylor series expansion of phase trajectories in parameter a, it is possible to show that in the lower semiplane there are also no any limit cycles of second kind. Fig. 12 shows the real behavior of separatrices on a phase plane.

The theorem is proved.

VI. CONCLUSION

In the present work for checking Roland E. Best conjecture on the pull-in range of two-phase Costas loop, a number of numerical experiments is MatLab Simulink has been made. The analytical approach to the proof of this conjecture is suggested.

ACKNOWLEDGEMENTS

This work was supported by Saint-Petersburg State University projects 6.39.416.2014 (sections I-IV) and 6.38.505.2014 (section V).

References

[1] J. Costas, "Synchoronous communications," in *Proc. IRE*, vol. 44, 1956, pp. 1713–1718.

[2] J. P. Costas, "Receiver for communication system," Jul. 1962, US Patent 3,047,659.

[3] R. E. Best, *Phase-Lock Loops: Design, Simulation and Application.* McGraw-Hill, 2007.

[4] L. Couch, *Digital and Analog Communication Systems*, 7th ed. Pearson/Prentice Hall, 2007.

[5] W. Lindsey, *Synchronization systems in communication and control.* New Jersey: Prentice-Hall, 1972.

[6] N. V. Kuznetsov, G. A. Leonov, and S. M. Seledzhi, "Nonlinear analysis of the Costas loop and phase-locked loop with squarer," in *Proceedings of the IASTED International Conference on Signal and Image Processing, SIP 2009*, 2009, pp. 1–7.

[7] G. A. Leonov, "Computation of phase detector characteristics in phase-locked loops for clock synchronization," *Doklady Mathematics*, vol. 78, no. 1, pp. 643–645, 2008.

[8] G. A. Leonov and N. V. Kuznetsov, *Nonlinear Mathematical Models Of Phase-Locked Loops. Stability and Oscillations.* Cambridge Scientific Press, 2014.

[9] G. A. Leonov, N. V. Kuznetsov, M. V. Yuldashev, and R. V. Yuldashev, "Nonlinear dynamical model of Costas loop and an approach to the analysis of its stability in the large," *Signal processing*, 2014, submitted.

[10] R. D. Stephens, *Phase-Locked Loops for Wireless Communications: Digital, Analog and Optical Implementations.* Springer, 2002.

[11] G. A. Leonov, "Phase-locked loops. theory and application," *Automation and Remote Control*, vol. 10, pp. 47–55, 2006.

[12] J. Kudrewicz and S. Wasowicz, *Equations of Phase-Locked Loops: Dynamics on the Circle, Torus and Cylinder.* World Scientific, 2007, vol. 59.

[13] G. A. Leonov, N. V. Kuznetsov, and S. M. Seledzhi, *Automation control - Theory and Practice.* In-Tech, 2009, ch. Nonlinear Analysis and Design of Phase-Locked Loops, pp. 89–114.

[14] D. Abramovitch, "Phase-locked loops: A control centric tutorial," in *Proceedings of the American Control Conference*, vol. 1, 2002, pp. 1–15.

[15] G. A. Leonov, N. V. Kuznetsov, M. V. Yuldahsev, and R. V. Yuldashev, "Analytical method for computation of phase-detector characteristic," *IEEE Transactions on Circuits and Systems – II: Express Briefs*, vol. 59, no. 10, pp. 633–647, 2012.

[16] G. A. Leonov and N. V. Kuznetsov, "Hidden attractors in dynamical systems. From hidden oscillations in Hilbert-Kolmogorov, Aizerman, and Kalman problems to hidden chaotic attractors in Chua circuits," *International Journal of Bifurcation and Chaos*, vol. 23, no. 1, 2013, art. no. 1330002.

[17] S. A. Tretter, *Communication System Design Using DSP Algorithms with Laboratory Experiments for the TMS320C6713TM DSK*. Springer, 2007.
[18] F. Gardner, *Phase–lock techniques*. New York: John Wiley, 1966.
[19] R. E. Best, N. V. Kuznetsov, G. A. Leonov, M. V. Yuldashev, and R. V. Yuldashev, "Simulation of analog Costas loop circuits," *International Journal of Automation and Computing*, 2014, accepted.
[20] E. A. Barbashin and V. A. Tabueva, *Dynamical systems with cylindrical phase space*. Nauka, Moscow, 1969.

PVII

VISUALIZATION OF FOUR LIMIT CYCLES OF TWO-DIMENSIONAL QUADRATIC SYSTEMS IN THE PARAMETER SPACE

by

G. A. Leonov, I. G. Burova, K. D. Aleksandrov 2013

Differential Equations, Vol. 49, No. 13, pp. 1675 – 1703